Therapeutic potential of the endocannabinoid system

in a novel mouse model of Huntington's Disease

Jessica K. Cao

A dissertation

submitted in partial fulfillment of the

requirement for the degree of

Doctor of Philosophy

University of Washington

2018

Reading Committee:

Nephi Stella, *chair*

Edith Wang, *member*

John Neumaier, *member*

Program Authorized to Offer Degree:

Pharmacology

University of Washington

Abstract

Therapeutic potential of the endocannabinoid system

in a novel mouse model of Huntington's Disease

Jessica K. Cao

Chair of the Supervisory Committee:

Nephi Stella

Department of Pharmacology

Huntington's Disease is a fatal, inherited neurodegenerative disease characterized by profound disturbances of the basal ganglia and gradual deterioration of motor and cognitive functions with development of psychiatric deficits. Early impairment of the endogenous cannabinoid signaling system is thought to be one of many hallmarks of this neurodegenerative disease and a possible molecular event that drives disease pathogenesis. Reduction of this system suggests absence of its many neuroprotective qualities and that this may contribute to the neuropathology in Huntington's Disease. The purpose of this thesis is to characterize novel lines of the HdhQ mouse model that accurately recapitulate Huntington's Disease and to use that model to explore the therapeutic potential of the endogenous cannabinoid signaling system in delaying or preventing disease development. In this thesis, I report that the HdhQ350/+ model, the HdhQ line expressing 350 polyglutamines, exhibits both sex-dependent behavioral impairments and

neuropathology despite males and females expressing equal mutant huntingtin protein levels, suggesting a sex-dependent effect of expanded polyglutamines in mouse models. Additionally, I report that the HdhQ200/200 mouse, the line homozygous for 200 polyglutamines, more accurately replicates Huntington's Disease, both behaviorally and pathologically. Short-term pharmacological enhancement of endogenous cannabinoids in this mouse model through ABHD6 inhibition shows potential in rescuing select behavioral impairments. Together, this doctoral thesis puts forth efforts to understand the impact of polyglutamine expansions in mouse models and to uncover a novel therapeutic in the treatment of Huntington's Disease by exploring the promising domain of the endocannabinoid signaling system.

Acknowledgements

First and foremost, I would like to thank Nephi Stella for guiding and mentoring me through the years on this project. He has provided me with a rich environment in which I have been able to flourish as both a student and a scientist. I am grateful for the opportunity to work in his lab and for all of our scientific discussions that have broadened my thinking and understanding. I would also like to thank my thesis committee, Drs. Gwenn Garden, John Neumaier, Edith Wang, Dirk Keene, and Rich Gardner. Their continued interest and support in my project has helped excelled my graduate journey.

I would like to thank all of my fellow lab members, past and present, for their everyday support and in particular Katie and Sofia for their assistance on this project throughout the years.

I am grateful for the many friends and colleagues whom I have met over my years at the University of Washington; these lasting relationships have helped me through the many challenges of this project while also allowing me to enjoy the journey. I am grateful for Julian and his unfailing enthusiasm, support and love, and for Matt, who has always been by my side. And lastly, I am especially grateful for the love and encouragement of my parents, Toa and Kien, and my brother, Anthony. I would not be the person I am today without them. Thank you.

List of Abbreviations

Abbreviation	Full name
2-AG	2-arachidonoylglycerol
ABHD12	α/β-serine hydrolase domain 12
ABHD6	α/β-serine hydrolase domain 6
ABPP	activity-based protein profiling
AEA	anandamide
AF	aggregation foci
BDNF	brain-derived neurotrophic factor
BMP	lysobisphosphatidic acid
CB_1	cannabinoid type 1 receptor
CB_2	cannabinoid type 2 receptor
CBP	CREB-binding protein
CNR1	cannabinoid type 1 receptor gene
CNR2	cannabinoid type 2 receptor gene
D1R	dopamine type 1 receptor
D2R	dopamine type 2 receptor
DAGL	diacylglycerol lipase
DARPP-32	dopamine- and cAMP-regulated neuronal phosphoprotein

eCB	endogenous cannabinoid
exNMDA	extrasynaptic NMDA receptor
FAAH	fatty acid amide hydrolase
FP-Rh	fluorophosphonaterhodamine
HD	Huntington's Disease
Hdh	mouse gene homolog to HTT
HTT	Huntingtin gene
Htt	Huntingtin protein
MAGL	monoacyglycerol lipase
mHtt	mutant Huntingtin protein
miRNA	micro RNA
MSN	medium spiny neuron
NAPE	N-arachidonoylphosphatidylethanolamide
NAPE-PLD	NAPE-specific phospholipase D
NII	intranuclear inclusion
PKA	cAMP-dependent protein kinase
PLC	phospholipase C
polyQ	polyglutamine

PSD-95	postsynaptic density protein 95
REST	RE-1 silencing transcription factor
SDDAGE	semi-denaturing detergent agarose gel electrophoresis
sqIHC	semi-quantitative immunohistochemistry
TBI	traumatic brain injury
THC	Δ^9-tetrahydrocannabinol

Thesis Overview

The research described in this doctoral thesis can be generalized as a study of Huntington's Disease (HD) and the therapeutic potential of the endogenous cannabinoid (eCB) system. Chapter I outlines the rationale for the research and begins with background information on HD, including pathophysiology, clinical features and mouse models. The second part reviews eCB signaling and culminates into a more specific discussion regarding the current state of eCB signaling in HD.

Chapter II describes a study on a novel genetic mouse model of HD, the HdhQ350/+ mouse line. The goal of this study was to characterize the disease profile of this mouse line, behaviorally and pathologically, and to observe the impact of elevated polyglutamine repeats on disease progression. This study showed that there was a sex-dependent effect of elevated polyglutamines repeats on both behavioral symptoms and pathology in the HdhQ350/+ mouse line.

Chapter III describes a study on the HdhQ200/200 mouse line and the therapeutic potential of targeting eCB signaling in HD. The goal of this study was to establish a more accurate mouse model of HD and to test the hypothesis that short-term ABHD6 inhibition could prevent or delay HD pathology and symptomatology in a more accurate mouse model of HD. This study showed that the HdhQ200/200 mouse line better replicated HD behavioral and pathological development compared to previously established models and that short-term ABHD6 inhibition has promise of alleviating behavioral HD disease progression.

Table of Contents

Chapter I: General Introduction

1.1 Huntington's Disease: clinical, genetic and pathological features

Huntington's Disease (HD) is a fatal, autosomal dominant neurodegenerative disease characterized by progressive impairments where patients show deterioration of motor, cognitive and psychiatric control. HD was first described in 1872 by the young physician, George Huntington, who would later provide the namesake of the disease. Dr. Huntington noted that the disease's "most marked and characteristic feature is a clonic spasm affecting the voluntary muscles." Patients, however, do not lose sense of consciousness, as he eloquently expresses, "the will is there, but its power to perform is deficient" (Huntington, 2003). Symptoms manifest during middle-age and the disease begins with subtle changes in personality, cognition and motor control. This can include irritability, disinhibition, loss of reliability, forgetfulness, restlessness, and incoordination (Walker, 2007). Eventually, symptoms will progress into distinct chorea, motor impersistence, slowed saccadic eye movements, speech deterioration, attention deficits, cognitive slowing, depression, mania, and psychosis (Peavy et al., 2010; Ross & Tabrizi, 2011; Roze et al., 2011; Walker, 2007). Other symptoms include weight loss, sleep and circadian rhythm disturbances, apathy, and loss of executive function (Roos, 2010). As the disease progresses, the choreic movements are replaced by akineto-rigid parkinsonism with dystonic postures (Roze et al., 2011). The typical latency to death is 15-20 years after diagnosis, often due to complications from falls, inanition, dysphagia, or aspiration. Unfortunately, there are no current treatments to alter the course of HD, only a limited number of symptomatic therapies.

HD shows a prevalence of about 5 affected individuals per 100,000 worldwide but 10-13 per 100,000 in Caucasian populations (Raymond, 2017). Although physicians have noted its genetic inheritance since the middle ages, it was not until 1993 that the gene for HD (*HTT*) was

identified (MacDonald et al., 1993). This breakthrough discovery allowed for an actual target to explore HD pathology research, therapeutics and for a possible cure. In HD, an expanded sequence of the nucleotides CAG is repeated at the 5' terminal, exon 1 of a novel gene, IT15, on chromosome 4 of diseased families. The trinucleotide encodes for the amino acid, glutamine, and the repeated section is identified as a polyglutamine, or polyQ, tract. PolyQ repeats between 36-40 result in incomplete penetrance and repeats above 40 are fully penetrant, causing full neurodegenerative syndromes to develop. There is an inverse relationship between polyQ repeat length and age of disease onset, although not with rate of progression (Andrew et al., 1993; Rosenblatt et al., 2006). PolyQ repeats above 28 show instability during DNA replication, with most leading to expansion (73%) instead of contraction (23%) (Walker, 2007). Instability is common during spermatogenesis and somatic instability, and mosaicism also occurs in HD. This leads to propagation and increased severity of the disease through heritage.

Huntingtin protein (Htt) is a highly conserved, 348kDa multi-domain protein ubiquitously expressed throughout the mammalian body but highly concentrated in the brain and testes (Landles & Bates, 2004; Walker, 2007). Although the complete function of Htt is unknown and has little sequence homology to other proteins, Htt knockdown leads to cellular apoptosis and its absence is embryonically lethal in mice (Dragatsis, Efstratiadis, & Zeitlin, 1998; Duyao et al., 1995; Nasir et al., 1995; Tong et al., 2011; Zeitlin, Liu, Chapman, Papaioannou, & Efstratiadis, 1995). The gene contains a GC-rich promoter region, indicative of a housekeeping gene, and is essential for gastrulation, neurogenesis, neuronal survival, vesicle trafficking, vesicle membranes, and microtubule trafficking (Holzmann, Schmidt, Thiel, brain, & 2001, 2001; Zuccato, Valenza, & Cattaneo, 2010). Htt is localized to many subcellular compartments, including the nucleus, cell body, dendrites, nerve terminal, golgi apparatus,

endoplasmic reticulum and mitochondria. Curiously, it also contains both a nuclear import and export sequence. Htt is cleaved by caspases, calpains and aspartyl proteases. Its cleavage by caspase 6 in particular is required for the neuronal dysfunction and degeneration in HD (Graham et al., 2006). Htt's interaction with caspase 3 inhibits caspase 3's apoptosis activity and its interaction with calpain regulates intracellular calcium levels. Htt is also directly involved with a vast number of binding partners; some include IP_3 (calcium signaling), CIP4 (CDC42-dependent signaling), CtBP (transcription factor), FIP2 (cell morphogenesis), Grb2 (growth factor receptor binding protein), PACSIN1 (endocytosis, actin cytoskeleton), PSD-95 (synaptic scaffolding protein), RasGAP, SH3GL3 (endocytosis), SIN3A (transcriptional repressor) (Cha, 2000; Landles & Bates, 2004; Luthi-Carter & Cha, 2003). This diversity of binding partners highlights the multitude of cell processes in which Htt is involved in.

HD is a result of both a loss of function of the normal protein and a gain of function of the mutant protein (mHtt). Constant production of mHtt is required for the disease and critically contributes to disease progression by sequestering the transcription factors for thousands of genes, interfering with protein-protein interactions and inhibiting enzymes. Most notably, mHtt aggregates into neuronal intranuclear inclusions (NIIs) and cytoplasmic aggregation foci (AF) and into both soluble and insoluble fragments. Longer polyQ lengths induce conformational changes, forming aggregates that have β-sheet structures characteristic of amyloids and are composed of toxic NH_2-terminal fragments (Landles & Bates, 2004; Ross & Tabrizi, 2011). These truncated fragments translocate to the nucleus and are a pathogenic signature of HD, as the nuclear export sequence is typically more active than the nuclear import sequence on the normal protein. mHtt aggregation is primarily found in nuclei, but can also be found elsewhere in the cell, including the cytoplasm, axon terminals and dendrites. Recent studies have shown that

mHtt's ability to enter and stay in the nucleus is attributed to a defective nucleocytoplasmic transport due to aggregation in nuclear pore complexes (Grima et al., 2017). This toxicity is intensified by the impairment of the UPS system in HD; proteasomes are irreversibly sequestered into aggregates induced by mHtt, leading to ubiquitin- and proteasome-depletion in the cell (Schipper-Krom, Juenemann, & Reits, 2012). In addition, post-translational modifications influence toxicity of mHtt through conformational changes, aggregation propensity, cellular localization, and clearance (Ross & Tabrizi, 2011). The multitude of disruptions caused by mHtt on cellular function, through hijacking normal protein expression and interactions, as well as its difficulty for cells to clear, makes HD an especially challenging disease to isolate a target.

The high concentration of Htt, and consequently mHtt, in the striatum of the brain leads it to be a highly susceptible target in HD, although the selectivity of Htt expression in this region is not entirely understood. Striatal atrophy begins as early as 15 years prior to symptom onset, with degeneration of up to 95% of GABAergic medium spiny neurons (MSNs) by death. Larger interneurons are spared, however (Ross & Tabrizi, 2011; Roze et al., 2011). Degeneration of MSNs occur in a dorso-ventral, medio-lateral gradient, and those in the indirect pathway that express dopamine D2 receptors (D2R) and enkephalin and project to the globus pallidus exterior, are lost first. This is in line with the initiation of symptoms, as the indirect pathway is a key mediator of suppressing unwanted movements; loss of this system results in chorea (Shepherd, 2013). Later stages see atrophy in the

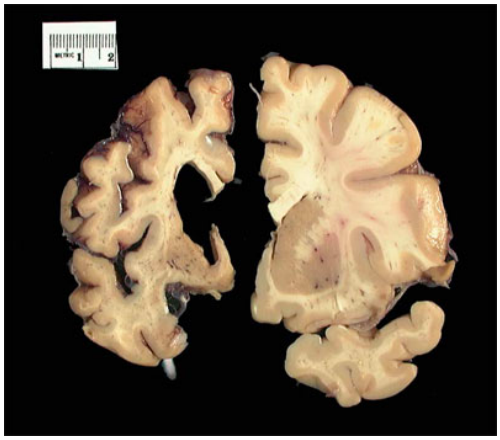

Figure 1.1. Coronal slice of Huntington's brain (left) versus normal brain (right) showing severe atrophy (Harvard Brain Tissue Resource Center).

cerebral cortex, subcortical white matter, thalamus, select hypothalamic nuclei, and upon death, brain weights are roughly 30% reduced due to atrophy (Figure 1.1).

There are numerous pathways implicated in HD that contribute to the widespread cell dysfunction and death of the striatum due to the ubiquitous role of Htt. One major pathway is due to impaired anterograde transport of the brain-derived neurotrophic factor (BDNF) from the cortex to the striatum. BDNF is normally produced in the cortex and transported to the striatum, providing neuronal support and stimulating morphological differentiation amongst other things. Htt colocalizes with microtubules and directly interacts with β-tubulin (via HAP1, p150), forming part of the dynactin complex required for anterograde transport. mHtt has impaired interactions with the complex, resulting in reduced BDNF transport to the striatum (Landles & Bates, 2004). Recent evidence also shows that mHtt decreases BDNF secretion from astrocytes via inhibiting Rab3a, disrupting BDNF vesicle docking on the plasma membrane for exocytosis and further diminishing BDNF supplies to the striatum (Hong, Zhao, Li, & Li, 2016). In addition, mHtt impairs transcription of BDNF in the cortex. Htt normally sequesters RE-1 silencing transcription factor (REST) in the cytoplasm but mHtt is unable to efficiently bind to REST, releasing it into the nucleus, and REST consequently inhibits transcription of a number of genes, including BDNF (Roze et al., 2011). mHtt not only releases transcriptional repressors, but it also sequesters transcription factors, including CREB-related genes involved in cell viability. Interactions between mHtt and CREB-binding protein (CBP) downregulates CREB-related genes. For instance, disruption of Sp1 reduces transcription of D2R and repression of PGC-1α reduces genes required for mitochondrial biogenesis and respiration (Landles & Bates, 2004; Roze et al., 2011). A number of other genes are also downregulated, such as DARPP-32 (marker for MSNs), cannabinoid type 1 (CB_1) receptor, and synaptophysin (presynaptic marker) (Glass,

Faull, & Dragunow, 1993; Goto & Hirano, 1990; Van Dellen et al., 2000). mHtt has increased binding to p53 than Htt, up-regulating proapoptotic targets (Apostol, 2005). Other cell death pathways initiated by mHtt include activation of JNK/caspase 3 cascade and autophagy induction via mTOR sequestration (Apostol, 2005; Landles & Bates, 2004).

Excitotoxicity is another major contributor to cellular dysfunction and death in HD. Increased spontaneous glutamate transmission from the cortex into the striatum characterizes the early stages of HD. Animal models have shown accelerated release of vesicles from pre-synaptic cortical terminals and increased post-synaptic AMPA-evoked whole-cell currents. During late stages of HD, excitatory transmission is drastically reduced, paralleling a loss of dendritic complexity, reduced length and spine density, and reduced expression of postsynaptic structural proteins in MSNs (Raymond, 2017).

The shift in glutamatergic signaling from cortical neurons to MSNs plays a role in HD through NMDA receptor signaling. These receptors are involved in synaptic plasticity as well as balancing cell survival and cell death pathways. GluN2B-containing NMDA receptors are highly expressed on MSNs and mHtt further increases this surface expression, possibly through a PSD-95-dependent mechanism (Miller & Bezprozvanny, 2010). This subunit is of particular importance, as GluN2B-containing NMDA receptors show a higher affinity for glutamate, augmenting excitotoxicity seen in HD (Papouin & Oliet, 2014). Interestingly, synaptic NMDA receptor expression remains the same in HD while extrasynaptic NMDA receptor (exNMDAR) expression, specifically those containing GluN2B, is increased. Activation of exNMDARs result in inhibition of cell survival and plasticity, enhanced cell death signaling via increases in the stress signals p38, MAPK and calpain, reduced ERK-1/2 and CREB signaling, induced mitochondrial dysfunction, activated pro-death molecules, and increased long-term potentiation

(Gouix, Léveillé, Nicole, Cellular, & 2009; Hardingham, Fukunaga, & Bading, 2002; Kaufman et al., 2012; Léveillé et al., 2010; Raymond, 2017). Activation of these receptors come from glutamate spill-over from synapses, partially due to HD-related impairment of glutamate clearance by astrocytes (Ehrlich, 2012). These mechanisms are illustrated in Figure 1.2.

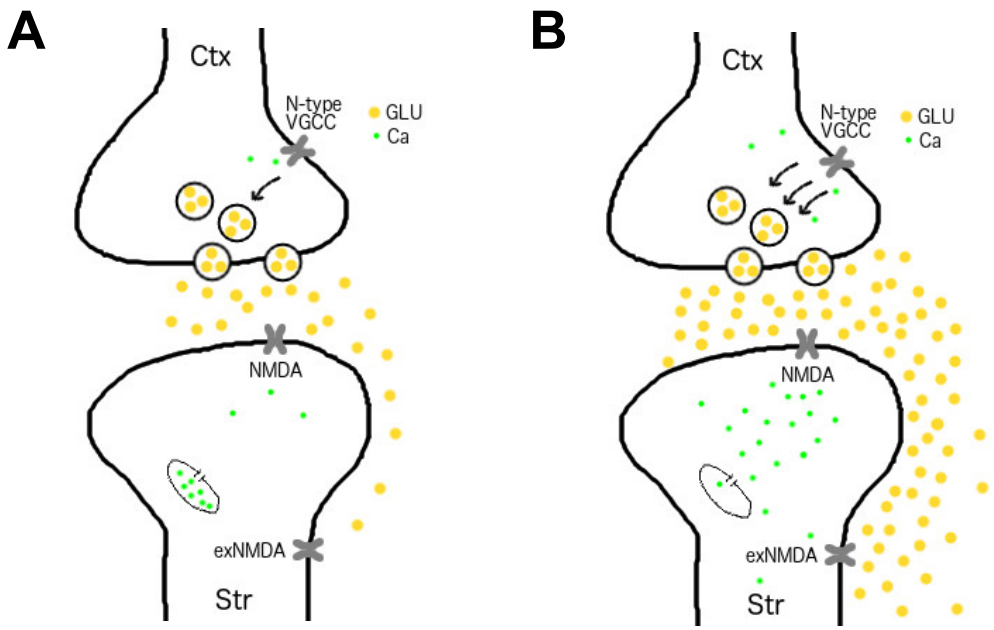

Figure 1.2. Schematic of glutamate transmission and intracellular calcium levels in the corticostriatal connection of (A) healthy and (B) HD synapses. Increased glutamate transmission from the cortex to the striatum, due to increased activity of N-type voltage-gated calcium channels for example, results in excitoxicity through various mechanisms, such as activation of exNMDA receptors. There is also release of calcium from intracellular stores due to protein-interactions by mHtt, contributing to cell death.

Maintaining low intracellular calcium concentrations is essential for cell homeostasis. Research has shown that there is increased intracellular calcium response to glutamate challenges. This aberrant calcium signaling in HD occurs through a variety of calcium-sensitive channels, receptors, intracellular stores, calcium-buffering proteins, and plasma membrane transporters. It has been shown that mHtt reduces the ability of mitochondria to sequester

calcium, enhancing the sensitivity to calcium-induced mitochondrial membrane depolarization, and through interactions with PGC-1α, as described above (Raymond, 2017). mHtt also increases sensitivity to IP3, enhancing calcium release from intracellular stores (Tang et al., 2003). It was recently shown that excessive calcium leak and reduced calcium stores are also linked to aberrant function of ryanodine receptors (Suzuki, Nagai, Wada, & Koike, 2012). N-type calcium channels also have increased calcium influx caused by disrupted interactions with syntaxin1A due to mHtt, possibly contributing to the accelerated release of glutamate-containing vesicles in cortical terminals (Swayne et al., 2005). Altogether, this short-term increase in calcium shifts the threshold for cellular plasticity, survival and growth, contributing to overall cellular dysfunction and death in HD.

1.2 Huntington's Disease: animal models

Due to HD's known underlying genetic etiology, many animal models have attempted to replicate HD but creating a valid model to fully reproduce the disease has proven difficult. The first mouse models were neurotoxin-mediated striatal lesioning models. The neurotoxins quinolinic and kainic acid replicated excitotoxicity, while the 3-NP and malonate models disrupted the mitochondria through cellular energy depletion by targeting the electron transport chain (Borlongan, Koutouzis, & Sanberg, 1997; Coyle & Schwarcz, 1976; Ferrante, 2009; Mary Y Heng, Detloff, & Albin, 2008; Kalonia, Kumar, & Kumar, 2010; Pouladi, Morton, & Hayden, 2013; Sanberg, Calderon, Giordano, & Tew, 1989). Although some of these models spared interneurons and specifically targeted MSNs, disease progression occurred quickly, in contrast to the slow pace of HD development in patients. This reduced the validity of these models and

better models were needed to simulate the proper time course of the disease and corresponding symptoms. Therefore, genetic models were explored.

The first genetic animal model to carry polyQ expansions was the R6 mouse model; exon 1 of the human *HTT* was inserted in the R6/1 mouse line, carrying roughly 115 CAGs, and the R6/2 mouse line, carrying 150 CAGs (Mangiarini et al., 1996). Because it contained a non-neuronal specific promoter, there was evidence of mHtt aggregation accumulation and generalized atrophy in several CNS organs not afflicted in HD. The large number of studies performed with R6/1 and R6/2 mice also show that these lines do not recapitulate behavioral HD characteristics of the disease. For example, R6/2 mice exhibit an extremely aggressive and rapid disease progression detected as early as 4-6 weeks of age, a 12-16 week life-span and widespread nuclear mHtt inclusions in brain areas typically absent in HD (Pouladi et al., 2013). R6/2 mice also suffer from a high incidence of symptoms that do not develop in HD, including seizures, diabetes and neuromuscular junction abnormalities (Mary Y Heng et al., 2008). Remarkably, studies performed on subsequent R6/2 mouse lines expressing greater than 300 CAG repeats do not exhibit such a rapid disease progression and survive longer than those expressing 115-150 CAG repeats (Morton et al., 2009). This may be due to a delayed onset of neuronal mHtt aggregate formation, alteration of accessibility to the nucleus or decreased expression of mRNA. Other N-terminal fragment models include the N171-82Q mouse model, which contain a human *HTT* cDNA with 82 CAGs run off a mouse prion promoter, which restricts expression to neurons (Schilling et al., 2007). Although there is increased apoptosis in striatal and cortical neurons, motor impairments starting at 12 weeks of age and a shortened lifespan, there is no pronounced striatal neuronal inclusions (Mary Y Heng et al., 2008; Pouladi et al., 2013). In the N-terminal fragment models, mHtt aggregation is observed at birth, which contrasts with HD. In full-length

mouse models, aggregation is observed in an age-dependent manner. These models are either knock-in models expressing the exon 1 or the full-length *HTT* on an endogenous mouse promoter. They include the CAG140 model, zQ175 model and the HdhQ model (Mary Y Heng et al., 2008; Pouladi et al., 2013). In contrast to the N-terminal fragment models, these mice have higher levels of mHtt expression although a delayed motor symptom development. Specifically, the CAG140 model display increased locomotor activity at 1 month of age but then hypoactivity at 4 months, followed by gait anomalies at 1 year of age. Curiously, behavioral symptoms precede neuropathological abnormalities (Menalled & Brunner, 2014). The zQ175 model exhibits early reduced motor coordination and grip strength, as well as a slight reduction in survival of approximately 100 weeks of age (Menalled & Brunner, 2014; Peng et al., 2016). Several mouse lines have been generated from the HdhQ mouse model, expressing 150 to 315 CAGs. These lines have demonstrated a variety of behavioral phenotypes and varying pathology that differ from line to line and provide a helpful look into the effects of varying CAG tracts on disease development (M Y Heng et al., 2010; Kumar et al., 2016; Lin et al., 2001). In addition, excitotoxicity is seen only in the full-length models. It is also noted that there is a more severe behavioral and pathological phenotype in animals run on a human promoter compared to the knock-in models.

A last group of rodent models are the YAC/BAC HD models, which utilize either yeast or bacterial artificial chromosomes to insert full-length human *HTT* transgenes, which includes all introns and exons to ensure appropriate regulation and tissue-specific expression (Hodgson et al., 1999; Yu-Taeger et al., 2012). Although of these models display select progressive motor, cognitive and psychiatric phenotypes, they did not show signs of neuronal loss or a reduced lifespan. A complete list of mouse models mentioned is summarized in Table 1.1.

Neurotoxin-mediated striatal lesioning models		Molecular target/transgene product	Promoter	CAG repeat length	Behavioral phenotype	Neuropathology	Survival
Quinolinic acid		Excitotoxicity			Hyperkinetic, weight loss	Lesions	
Kainic acid		Excitotoxicity			Motor impairment	Neurodegeneration	
3-NP		Inhibit mitchondrial citric acid cycle			Hyperkinetic then hypokinetic	Lesions	
Malonate		Inhibit succinate dehydrogenase			Weight loss, motor impairment, locomotor deficits	Lesions	
N-terminal fragment models							
R6 series		67 amino acids of human HTT	human HTT				
	R6/1			116	Weight loss, motor impairment	Brain atrophy, aggregates	12+ months
	R6/2			144	Weight loss, motor impairment, clasping, grip sternth loss, various cognitive deficits, seizures, diabete, NMJ and cardiac dysfunction	Brain atrophy, aggregation, reactive astrogliosis, nuclear inclusions, decrease of various receptor expression	12-16 weeks
N171-82Q		171 amino acids of human HTT cDNA	mouse Prp	82	Weight loss, tremor, clasping, motor impairment	Nuclear inclusions, reactive astrogliosis, neurodegeneration	20-24 weeks
Full-length models							
CAG140		chimeric human HTT exon 1:mouse Hdh	mouse Hdh	140	Hyperkinetic then hypokinetic, gait deficits	Aggregation, nuclear inclusions	
zQ175					Motor impairment, grip strength loss, weight loss, locomotor deficits, balance deficits	Aggregation, nuclear inclusions, brain atrophy, neurodegeneration	100 weeks
HdhQ series		mouse Hdh	mouse Hdh				
	HdhQ150/+			150	Motor impairment, balace deficits tremor, ataxic	Aggregation, nuclear inclusions, reactive astrogliosis, decreased D1/D2 receptors	normal
	HdhQ200/+			200	Grip strength loss, gait deficits, balance deficits, motor impairment	Nuclear inclusions, aggregation, reactive astrogliosis	normal
	HdhQ315/+			315	Motor imapairment, grip strength loss, locomotor deficits	Aggregation, decreased D1/D2 binding, brain atrophy	normal
YAC128		human HTT	human HTT	128	Hyperkinetic then hypokinetic, motor impairment, cognitive deficits	Brain atrophy, aggregation, increased NMDA/AMPA/mGluR1/mGluR2 binding	normal
BAC		human HTT	human HTT	97	Weight gain, small motor impairment	General brain atrophy, neurodegeneration, aggregation	normal

Table 1.1. Summary of common mouse models of HD and corresponding characteristics.

A number of other model organisms have been used to study HD pathogenesis. *D. melanogaster* displays expanded polyQ-dependent disease development with a delayed onset. *C. elegans* has been a great tool to screen for drugs and to study protein aggregation dynamics (Nussbaum-Krammer & Morimoto, 2014). Curiously, the window of polyglutamine toxicity in *C elegans* mirrors what occurs in humans. Recent work has looked at sheep and miniature pig models (Pouladi et al., 2013). The sheep model contains a full-length *HTT* cDNA with 73 CAGs, run on a human *HTT* promoter, but has yet to show an overt phenotype at 18 months. The miniature pig model expresses an N-terminal fragment but also has yet to show a phenotype at 16 months despite evidence of reduced DARPP-32 expression. Rhesus macaque models expressing the human exon 1 have shown promise; this model thus far shows progressive motor function impairment and cognitive decline (Pouladi et al., 2013).

The diverse variety of animal models illustrates the difficulty in reproducing HD *in vivo*. These many different strategies all have their limitations, between fully depicting behavioral symptoms to replicating molecular and cellular pathology. The complexity of human HD, as it affects multiple signaling pathways, and the temporal nature of protein aggregation causes HD to be difficult to model. Therefore, more accurate models are needed to further HD research, including exploring different signaling systems for novel therapeutics.

1.3 Endogenous cannabinoid signaling system

The endogenous cannabinoid (eCB) signaling system was first inferred from the

psychoactive effects of Δ^9-tetrahydrocannabinol (THC) (Elphick, 2012). It consists of two identified and cloned receptors, CB_1 and CB_2. CB_1 was first identified in 1988 and cloned in 1990 (Little, Compton, Johnson, & Melvin, 1988; Matsuda, Lolait, Brownstein, Young, & Bonner, 1990). Encoded by the CNR1 gene on chromosome 6, it is a $G_{i/o}$-protein coupled receptor. Of the G_i-protein, the α subunit mainly inhibits adenylyl cyclase activity, leading to downstream inhibition of L-, N- and P/Q-type voltage-gated calcium channels which prevent action potential-dependent vesicular neurotransmitter release. The α subunit can also activate potassium channels and stimulate various MAPK pathways, which hyperpolarize the pre-synaptic membrane. Additionally, β/γ subunits activate phospholipase C (PLC) and PI3K pathways, whose actions together with the α subunit, reduce neurotransmitter release from the presynaptic neuron (Stella, 2004). This is known as the canonical pathway of CB_1 and referred to as retrograde signaling. The prolonged, repeated activation of CB_1 can also regulate gene transcription of other proteins.

CB_1 is primarily found on neurons, at the axons and axon terminals, as identified by radio-ligand binding, lesion studies and *in situ* hybridization (Elphick, 2012). The isolation of CB_1 receptors onto the presynaptic membrane is part of the defining retrograde signaling mechanism employed by the eCB system. CB_1 is also found on cells outside of the CNS, but at much lower levels.

In contrast to CB_1's substantial expression in the brain, CB_2 is primarily expressed by immune cells and only in the brain by activated microglia. CB_2 is encoded by the CNR2 gene on chromosome 1, and cloned in 1993, it has only 44% amino acid sequence homology to CB_1, which may explain the different expression pattern and function (Munro, Thomas, & Abu-Shaar, 1993; Stella, 2004). It is also a $G_{i/o}$-coupled receptor whose primary role is to reduce

inflammation through the induction of apoptosis of immune cells and inhibition of macrophage ability to process antigens and prime helper T-cells (Mackie & Stella, 2006; Stella, 2004). Agonists of CB_2 induce cell migration, reduce cytotoxin release and increase the rate of cell proliferation (Stella, 2004). There are two additional cannabinoid receptors, CB-vanilloid and abnormal-cannabidiol receptor, yet to be identified and cloned (Stella, 2004).

There are two known eCB ligands, anandamide (AEA) and 2-arachidonoylglycerol (2-AG). AEA was discovered in 1992 and is a partial agonist of CB_1 (Stella, 2004). In fact, *in vivo* administration of AEA mimics many effects of THC. AEA production is tonically low, through a multi-step enzymatic pathway that generates N-arachidonoylphosphatidylethanolamide (NAPE), which is converted to NAPE-specific phospholipase D (NAPE-PLD) and then into AEA and phosphatidic acid (Elphick, 2012). A rise in intracellular calcium is required to increase the conversion of NAPE (Stella, 2004). 2-AG was identified in 1995 and is 200 times more abundant than AEA in the brain (Stella, 2004). It is a full agonist of CB_1 and CB_2 and is released in a transient, stimulated manner (Elphick, 2012). 2-AG production requires a sustained increase in intracellular calcium due to cellular depolarization to activate diacylglycerol lipase (DAGL) to cleave arachidonic acid into 2-AG (Stella, 2004).

eCB signaling is terminated through three mechanisms: 1) desensitization, 2) internalization of CB receptors and 3) clearance of eCBs, or enzymatic hydrolysis. Desensitization of CB_1 receptors occurs via β-arrestin binding, signaling the receptor for phosphorylation by GRKs and leading to internalization from the presynaptic membrane (Turu & Hunyady, 2010). The mechanism of clearance of eCBs via transporters is less elucidated. There is evidence that suggests fatty acid binding proteins play a large role in intracellular shuttling of eCBs from the synaptic cleft across the plasma membrane; however not much else has been

discovered (Kaczocha, Glaser, & Deutsch, 2009). The mechanism of enzymatic hydrolysis of eCBs, on the other hand, is better understood. AEA is hydrolyzed by the integral membrane enzyme fatty acid amide hydrolase (FAAH), which converts AEA to arachidonic acid and ethanolamine (Mackie & Stella, 2006). 2-AG is hydrolyzed 85% by monoacyglycerol lipase (MAGL) and the remaining 15% by α/β-serine hydrolase domain 6 (ABHD6) and 12 (ABHD12) into arachidonic acid and glycerol (Blankman, Simon, & Cravatt, 2007; Marrs et al., 2010). Despite its smaller contribution to eCB enzymatic degradation, ABHD6 has become a promising therapeutic target for the treatment of diseases with etiologies involving eCB deficits.

1.4 ABHD6

ABHD6 was discovered in the microglial cell line, BV2, as BV2 cells lack MAGL but are still able to hydrolyze 2-AG. Identified through activity-based protein profiling (ABPP) using multi-dimensional protein identification analysis, ABHD6 is a highly conserved protein and mainly expressed on the cell soma and dendrites (Blankman et al., 2007; Marrs et al., 2010). It is primarily found on principal glutamatergic neurons, with some expression on GABA interneurons and astrocytes. In contrast to MAGL, which is found in the presynaptic cytosol, ABHD6 is a 30kDa integral membrane enzyme on the postsynaptic dendrite, with the catalytic domain facing the cytoplasm. ABHD12 is also found on the postsynaptic neuron but faces the extracellular side (Blankman et al., 2007; Marrs et al., 2010; Navia-Paldanius, Savinainen, & Laitinen, 2012; Straiker et al., 2009). This allows ABHD6 both spatial and temporal control of 2-AG, as it lays on the same cellular side as DAGL and effecting 2-AG levels as it is synthesized (Figure 1.3). Recent ABPP analysis on brain tissue found highest expression in the cerebellum, hippocampus, frontal cortex and striatum at much higher levels than MAGL and ABHD12

(Baggelaar et al., 2017). ABHD6 is not just a specific enzyme for 2-AG. It was also found to degrade BMP, or lysobisphosphatidic acid, in late endosomes and lysosomes, accounting for 90% of BMP hydrolase in the liver, indicating a major role of ABHD6 in lipid metabolism (Pribasnig et al., 2015).

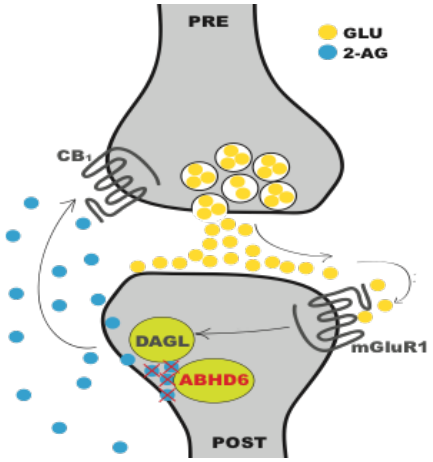

Figure 1.3. Schematic of ABHD6 action on eCBs (Marrs, W).

ABHD6 and ABHD12 are serine hydrolases, one of the largest protein superfamilies. Although members contain the canonical hydrolase fold of an 8-stranded parallel α/β structure with a nucleophile-his-acid catalytic triad, members are very diverse in sequence, substrate and catalytic activity (Li, Fei, Xu, & Ji, 2008). In fact, ABHD6 and ABHD12 share only about 20% sequence homology (Blankman et al., 2007). ABHD6 is encoded on chromosome 3p14.3 and the catalytic triad was postulated at amino acid sites S148-D278-H306 (Li et al., 2008; Navia-Paldanius et al., 2012). Its expression is abnormally regulated in cancer and disease, especially in certain tumor cell lines as well as in systemic lupus erythematosus (Li et al., 2008; Max, Hesse, Volkmer, & Staege, 2009; Oparina et al., 2014). Recently, high-resolution proteomics on brain tissue revealed that ABHD6 can be a bound component to native AMPA receptor complexes and extensive work has found that overexpression of ABHD6 *in vitro* reduces excitatory neurotransmission mediated by AMPA receptors. It reduced glutamate-mediated current and surface expression of the subunit GluA1 in HEK293T cells expressing stargazin, a protein that plays a critical role in AMPA receptor transport to the plasma membrane (Wei et al., 2016). In fact, it was found that the C-terminal tail of GluA1 was required for binding between ABHD6 and GluA1, although later research found that ABHD6 also binds to

GluA2 and GluA3 (Wei et al., 2017). This suggests an additional role for ABHD6 in AMPA receptor transport, which is independent to ABHD6's enzymatic function (Wei et al., 2017).

The most studied role of ABHD6 is its place in the eCB signaling system. As mentioned above, ABHD6 was found to hydrolyze 2-AG, accounting for roughly 4% of total 2-AG hydrolysis (Blankman et al., 2007)). ABHD6 mRNA is abundant in neurons and low in microglia, and inhibition of ABHD6 induces robust long-term depression that is mediated through CB_1 receptors (Marrs et al., 2010).

A number of carbamates have been identified to inhibit ABHD6, specifically through a covalent modification of the catalytic Ser148 (Bowman & Makriyannis, 2012). Various ABHD6 inhibitors have been developed over recent years, some exhibiting non-specific activity. UCM710 inhibits both ABHD6 and FAAH, but not MAGL (Marrs et al., 2011). WWL70 was recently found to inhibit PGE_2 synthesis and PGE_2-G production independent of CB_1, CB_2 or ABHD6 in microglia after LPS-induced inflammation, and this was blocked by COX-2 inhibition (Alhouayek, Masquelier, Cani, Lambert, & Muccioli, 2013; Tanaka et al., 2017). A next-generation line of inhibitors has emerged with higher potency, selectivity and *in vivo* activity through the addition of polar substituents (Hsu et al., 2013). These inhibitors have IC_{50}s of 1nm and can target systemic (KT-182) or peripheral (KT-203) ABHD6 or are available orally (KT-185). Remarkably, ABHD6 inhibition avoids CB_1-mediated analgesia and hypomotility commonly seen with MAGL inhibitors (Marrs et al., 2010; Naydenov, Horne, et al., 2014). Thus, the reduced side-effect profile makes this target a promising therapeutic strategy for modulating eCB signaling in disease.

Inhibition of ABHD6 has recently been explored as a powerful pharmacological target for a number of biological diseases. ABHD6 inhibition was first explored in the treatment of

traumatic brain injury (TBI) (Tchantchou & Zhang, 2013). In TBI, after an initial insult, secondary injury is associated with excitotoxicity, inflammation, oxidative stress, and neuronal death. Although 2-AG is increased immediately after injury, its rapid hydrolysis may reduce its protective effects. This further supports the need to target eCB hydrolyzing enzymes. In a mouse model of TBI, post-injury treatment of chronic ABHD6 inhibition improved motor coordination and working memory performance, although did not improve spatial learning or memory. This may be due to the abundance of ABHD6 in the prefrontal cortex and striatum, therefore rescuing corresponding behavioral impairments over hippocampal-related behaviors. Pathologically, ABHD6 inhibition reduced lesion volume (mediated through CB_1), reduced neuronal degradation (mediated by both CB_1 and CB_2), suppressed expression of ICAM-1, a marker of inflammation and blood-brain-barrier dysfunction, and attenuated the increase in iNOS and COX-2 expression (Tchantchou & Zhang, 2013). ABHD6 inhibition has also been used to treat neuroinflammation in a mouse model of multiple sclerosis (Wen, Ribeiro, Tanaka, & Zhang, 2015). Chronic treatment with WWL70 ameliorated clinical signs and reduced mRNA levels of the inflammatory markers TNF-α, iNOS and IL-1b. It also reduced the number of CD4+ T-cell infiltrates and TNF-α+ cells, which was blocked by the CB_2 receptor antagonist, AM630, and lost in the CB_2-/- mice. Although recent evidence has emerged regarding additional targets to WWL70, research into ABHD6 inhibition in inflammation should consider the COX-2 and PGE pathways (Tanaka et al., 2017; Wen et al., 2018). Taken together, this shows that some of the therapeutic benefits of ABHD6 inhibition are mediated through CB_1 and CB_2 receptors, depending on the type of injury and primary outcome measures of interest.

ABHD6 is also a highly promising target in the treatment of seizures. Work by the Stella laboratory has shown that inhibition of ABHD6 through acute WWL123 treatment is able to

decrease pentylenetetrazole-induced generalized tonic-clonic and myoclonic seizure incidence and severity (Naydenov, Horne, et al., 2014). It reduced seizure-related mortality and, curiously, this was mediated through $GABA_A$ receptors and not CB_1 or CB_2. Additionally, both chronic treatment of WWL123 for 6 weeks and acute treatment of WWL123 was able to completely block spontaneous seizures found in the R6/2 mouse model of HD. In addition, although treatment with SR141716, a CB_1 antagonist, worsened seizures, it did not antagonize the effect of WWL123 when co-administered together. Therefore, the combination of 2-AG's actions, via ABHD6 inhibition, on CB_1 and $GABA_A$ receptors make it a powerful therapeutic tool to dampen excess excitatory transmission in seizures.

Lastly, ABHD6 inhibition has been an emerging topic for the potential treatment of obesity, due to its role in lipid metabolism. Antisense oligonucleotide-treatment to reduce ABHD6 levels in the liver was able to protect against body weight and fat mass gain, increase physical activity and energy expenditure and improve glucose and insulin tolerance in mice fed a high-fat diet (Thomas et al., 2013). Global ABHD6-/- mice also had similar results (Zhao et al., 2015). Further research has found that in β cells, ABHD6 negatively regulated glucose-stimulated insulin secretion by hydrolyzing various monoacylglycerols (Zhao et al., 2016). To further elucidate the role of ABHD6 in obesity, mice with genetic deletion of ABHD6 specifically in the ventromedial hypothalamus had blunted fasting-induced feeding and reduced food intake, energy expenditure and adaptive thermogenesis in response to metabolic challenges, suggesting that ABHD6 plays a major role in regulating counter-regulatory responses to major metabolic shifts (Fisette et al., 2016). All together, these results show the broad therapeutic potential of targeting ABHD6 in the treatment of various diseases.

1.5 Huntington's Disease and eCBs

The eCB signaling system and CB_1 have been extensively studied in HD. CB_1 was first found to be reduced on MSN terminals in postmortem tissue of HD patients (Glass et al., 1993). PET scans can detect downregulation of CB_1 receptors in early-stage HD patients (Van Laere et al., 2010), and this downregulation is reliably measured presymptomatically in numerous HD mouse models, including the R6/1, R6/2, YAC128, and HdhQ150 models (Dowie et al., 2009; Horne et al., 2012; Pouladi et al., 2012; Woodman et al., 2007). This expression reduction precedes the loss of other synaptic markers, including dopamine D1 and D2 receptors (Glass et al., 1993). Additional subtypes of striatal interneurons lose CB_1 expression in the R6/2 mouse, such as NPY interneurons (Horne et al., 2012). The molecular details of this downregulation have been elucidated; mHtt indirectly represses transcription of *Cnr1* to decrease CB_1 expression through release of REST in R6/2 mice (Blazquez et al., 2010). Considering that CB_1 signaling controls the expression of various neuroprotectants (such as BDNF, which is reduced in HD) and reduces glutamate release in response to excitotoxicity (which has been implicated in MSN dysfunction and degeneration), it is likely that loss of CB_1 may be involved in HD pathogenesis (Chiodi et al., 2012; Marsicano et al., 2003). As few FDA-approved HD treatments exist and are only for symptom management, this presents a major gap in treatment and healthcare for HD patients, illustrating a need for more effective options. The reduction in CB_1 expression early in HD pathogenesis suggests that targeting the eCB system may be a promising therapeutic approach.

There have been several studies investigating the role of the eCB system in HD. A number of studies have generated CB_1-knockout mice on N171-82Q and R6/2 mice and found that CB_1 knockout worsened HD-related motor impairments (Blazquez et al., 2010; Mievis,

Blum, & Ledent, 2011). R6/2:CB_1-/- mice also displayed a decrease in GAD67 (a GABA marker), synaptophysin and PSD-95 and there was a decrease in striatal volume. Curiously, there was only an effect on BDNF levels in R6/2:CB_1-/-, but not N171-82Q:CB_1-/- mice. Because those mice were universal CB_1-knockouts, a more recent study in 2014 explored which population of CB_1 receptors was vital for neuroprotection (Chiarlone et al., 2014). Glu-CB_1-/- and GABA-CB_1-/- mice were injected with quinolinic acid in the striatum to imitate HD and found that the former group was more sensitive to damage in loss of DARPP-32 expression and motor impairments, suggesting that CB_1 receptors on glutamatergic neurons are most vital for protection against HD. Although this population is smaller than those found on GABAergic neurons, loss of CB_1 receptors on glutamatergic neurons from the cortex input into the striatum would enhance glutamate transmission and serve as an important pathway to excitotoxicity in HD. To further support this, a recent study published by the Stella lab showed that genetic rescue of CB_1 receptors in the MSNs of R6/2 mice prevented the loss of excitatory striatal synaptic proteins and dendritic spine number and density, as well as restored striatal synaptic function through the rescue of spontaneous excitatory postsynaptic currents in MSNs (Naydenov, Sepers, et al., 2014). This data suggests a key role of CB_1 in the pathogenesis of HD.

Although eliminating the eCB system on a HD background causes broad behavioral impairments, studies utilizing cannabinoids to treat HD models have yielded ambiguous results. One of the earliest studies in 2010 found that neither short-term treatments of CB_1 agonists (synthetic and phyto-derived) or a FAAH inhibitor were able to improve behavioral impairments in the R6/1 mouse (Dowie et al., 2010). However, two studies in later years found that a different synthetic agonist and the same phyto-derived agonist at a lower dose were able to rescue pathology and motor impairments in R6/1 and R6/2 mice (Blazquez et al., 2010; Pietropaolo et

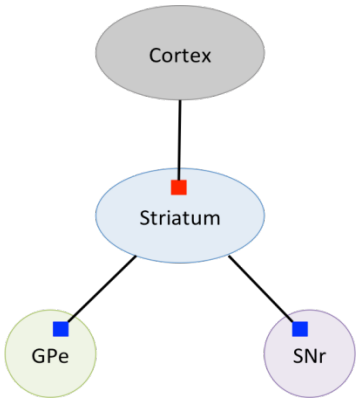

Figure 1.4. Diagram of differential CB_1 receptor subpopulations in the basal ganglia. Low doses of THC target CB_1 receptors on glutamatergic afferents (red) and high doses target CB_1 receptors on GABAergic afferents (blue).

(Blazquez et al., 2010; Pietropaolo et al., 2014). There are several explanations to these seemingly conflicting results. First, different doses of THC target specific subpopulations of CB_1 receptors (Figure 1.4); low doses of THC affect CB_1 receptors on glutamatergic neurons whereas high doses target CB_1 receptors on GABAergic neurons (Bellocchio et al., 2010; Rey, Purrio, Viveros, & Lutz, 2012). Because both studies targeted different subpopulations of CB_1 receptors that have opposing effects, this would confound interpretations on the role of CB_1 receptors. Second, short-term treatment with high doses of cannabinoids leads to CB_1 receptor desensitization, resulting in an overall decrease in receptors and number of therapeutic targets. Therefore, there is a strong need to investigate CB treatments that both minimizes receptor desensitization and targets CB_1 receptors in the appropriate subpopulation.

Although there have been many landmark discoveries into the pathology of HD, there still remains many unknowns, as effective treatments or a cure have yet to be discovered. Many deficiencies are due to the lack of an adequate *in vivo* model that fully replicates HD, behaviorally and pathologically. This thesis aims to establish a more accurate mouse model of HD and to use that model to investigate if modulating the eCB system is effective in alleviating or delaying the onset of HD symptoms and pathology.

Chapter II: Sex-Dependent Behavioral Impairments in the HdhQ350/+ Mouse Line

2.1 Overview and rationale

The HdhQ mouse model was developed using gene targeting technology whereby elevated CAG repeats were inserted into the *Hdh* gene, the mouse homolog to the human HTT gene (Lin et al., 2001). Thus, in contrast to previous HD mouse models, the HdhQ model lacks human DNA, contains a purely murine genome, expresses only 2 copies of HTT or *Hdh,* and the mutant protein is regulated the same way as normal Htt. Natural germline alterations in repeat lengths in the HdhQ150 line were leveraged to create several allelic lines with repeats up to 315 CAGs in length. These lines represent powerful genetic tools to study how changes in the number of CAG repeats affect the pathological process and behavioral impairments in mice and whether they reliably model human HD (Pouladi et al., 2013). The heterozygous 200 CAG line (HdhQ200/+) reliably recapitulates key aspects of HD pathology and motor dysfunction, including the accumulation of neuronal mHtt intranuclear inclusions in both the striatum and cortex, as well as mHtt aggregation foci in the cytoplasm after 40 weeks of age. By 80 weeks of age, HdhQ200/+ mice have reduced grip strength and abnormal gait, both of which represent symptoms thought to parallel human HD symptoms (M Y Heng et al., 2010). However, HdhQ200/+ mice still live a normal lifespan of approximately 2 years and thus do not mimic the reduced lifespan known to occur in human adult-onset HD. A recent study found that HdhQ315/+ mice had a more aggressive phenotype than the HdhQ200/+ line (Kumar et al., 2016). HdhQ315/+ mice showed deficits in motor coordination, open field and grip strength as early as 30 weeks of age. Pathologically, HdhQ315/+ mice had striatal aggregates at 70 weeks of age despite not exhibiting neuronal loss. Thus, the HdhQ mouse model represents a valuable genetic tool to study the effects of expanded polyglutamine repeats on disease progression.

Given the altered pathogenesis occurring in the R6 allelic series with elevated CAG repeat lengths, it is still unclear whether HdhQ lines expressing CAGs above 315 repeats will recapitulate the behavioral impairments and neuropathological indices commonly measured in other HD mouse models. Here, we studied a newly developed line of the HdhQ allelic series, mice expressing 350 CAGs, by performing a longitudinal study of behavioral and neuropathological indices commonly measured in other HD mouse models. We found evidence of sex-dependent variances in behavioral impairments with sex-dependent changes in select HD neuropathological indices despite equal expression and aggregation of mHtt in relevant brain areas in animals of each sex.

2.2 Results

2.2.1 General phenotype of Hdh350/+ mice: Life span, weight and grip strength

Breeding of HdhQ350/+ by HdhQ350/+ mice produced average litter sizes of 4.6 pups. Of 101 mice from this cross, 0 were HdhQ350/350, 44 were HdhQ350/+ and 57 were HdhQ+/+, or wild-type, a result which deviates significantly from the expected 1:2:1 Mendelian ratio (χ^2 (2, N=3)=64.16, $p<0.0001$). Note that we did not observe any cannibalism after birth and thus the most likely is that homozygote mice died in utero, and heterozygous HdhQ350 mice show reduced viability.

Prior to 70 weeks of age, mice did not exhibit overt signs of tremor, hunching, unsteady movements or staggering gait. We also did not observe any spontaneous or handling-induced seizures. However, by 70 weeks of age, HdhQ350/+ mice of both sexes had significantly reduced weight. Figure 2.1A shows that HdhQ350/+ males had 9.4% reduced body weight by 40 weeks of age compared to male wild-type littermates, and Figure 2.1B shows that female HdhQ350/+

mice had 9.2% reduced body weight by 30 weeks of age compared to wild-type littermate females. In addition, post-hoc analyses revealed significant loss as early as 30 weeks of age in female HdhQ350/+ mice. Thus HdhQ350/+ mice of both sexes failed to gain weight as typically seen in wild-type mice. Although there was a significant effect of genotype in both groups (male:

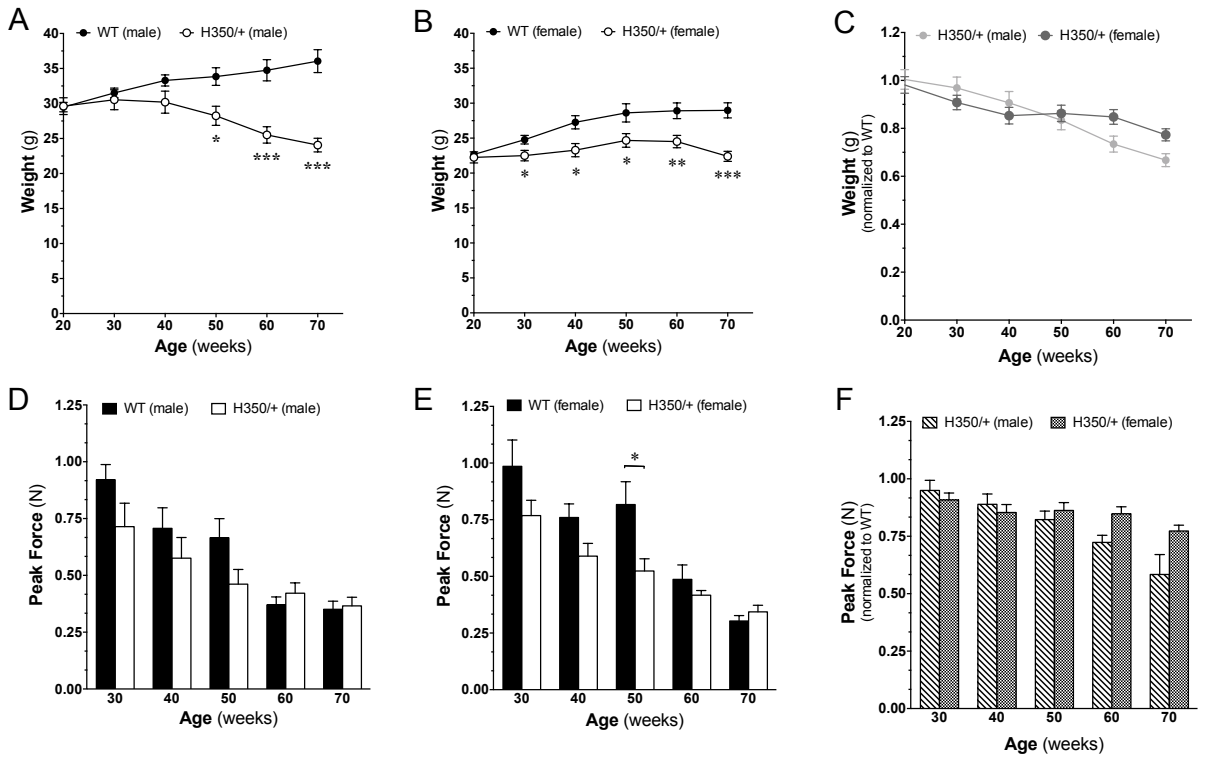

Figure 2.1. General phenotype of HdhQ350/+ male and female mice compared to wild-type littermates. (A) Male and (B) female HdhQ350/+ mice showed reduced weight compared to their respective wild-type littermates. (C) When normalized to their respective wild-type littermates, both male and female HdhQ350/+ had similar reductions in weight. (D) Male and (E) female HdhQ350/+ mice showed reduced grip strength, starting at 30 weeks of age. (F) When normalized to their respective wild-type littermates, both sexes had similar reductions in grip strength. N=7-8 for all groups. Error bars represent S.E.M. and *p<0.05, **p<0.01, ***p<0.001 with two-way ANOVA with Bonferroni post-hoc test.

$F_{(1, 13)}$=11.23, p=0.005; female: $F_{(1, 14)}$=9.72, p=0.008) (Figure 2.1A, B), there was no overall effect of sex on weight loss in HdhQ350/+ mice when normalizing weights to wild-type

littermates (to assess for progressive weight loss) (Figure 2.1C). These results show that both male and female HdhQ350/+ mice equally failed to gain weight over time.

Lack of increase in body weight might be due to loss in muscle mass and strength. We used a grip strength meter to measure forelimb grip strength and found that both male and female HdhQ350/+ mice exhibited significantly reduced grip strength compared to respective wild-type littermates when analyzed by two-way ANOVA (male: $F_{(1, 12)}=7.89$, $p=0.016$; female: $F_{(1, 14)}=18.39$, $p=0.001$) (Figure 2.1D, E). Bonferroni post-hoc analysis showed a significant decrease in grip strength in HdhQ350/+ females at 50 weeks of age. Statistical analysis of the reduction in grip strength relative to wild-type mice revealed no sex-dependent loss in HdhQ350/+ mice (Figure 2.1F). These results suggest that a portion of the reduced body weight mass measured in both male and female HdhQ350/+ mice might be linked to loss of muscle mass.

2.2.2 Locomotor activity of Hdh350/+ mice: Dark and light phase activities

Several HD mouse models exhibit circadian disturbances typified by increased activity during the night (when mice are active) and decreased activity during the day (when mice are less active) (Morton, 2013; Pouladi et al., 2013). We used the Noldus PhenoTyper, a home-cage monitoring system, to measure daily patterns of locomotion, hiding, feeding, and drinking over 72-hour time periods. We found that both HdhQ350/+ males and females exhibited an overall decrease in spontaneous locomotion during the active dark phase (male: $F_{(1,61)}=8.51$, $p=0.005$; female: $F_{(1, 64)}=45.37$, $p<0.0001$) (Figure 2.2A, B). Post-hoc analysis indicated that HdhQ350/+ females exhibited a significant decrease in spontaneous activity during the dark phase at 50 weeks of age (Figure 2.2B). Further analyses between male and female HdhQ350/+ mice when normalized to their respective wild-type littermates to assess for a sex-dependent reduction in dark phase activity revealed an overall significant effect of sex ($F_{(1, 60)}=15.67$, $p=0.0002$),

indicating that female HdhQ350/+ mice were more severely affected by the mutation in the dark phase activity (Figure 2.2C). Post-hoc analysis revealed a significant difference at 70 weeks of age. By sharp contrast, we found no significant differences in spontaneous activity measured during the light phase between HdhQ350/+ mice and their respective wild-type littermates (Figure 2.2D, E), and thus, there was no sex-dependent difference in light phase activity in HdhQ350/+ mice (Figure 2.2F). These results suggest that HdhQ350/+ mice of both sexes exhibited a decrease in spontaneous activity during the dark phase, with females exhibiting a more severe deficit.

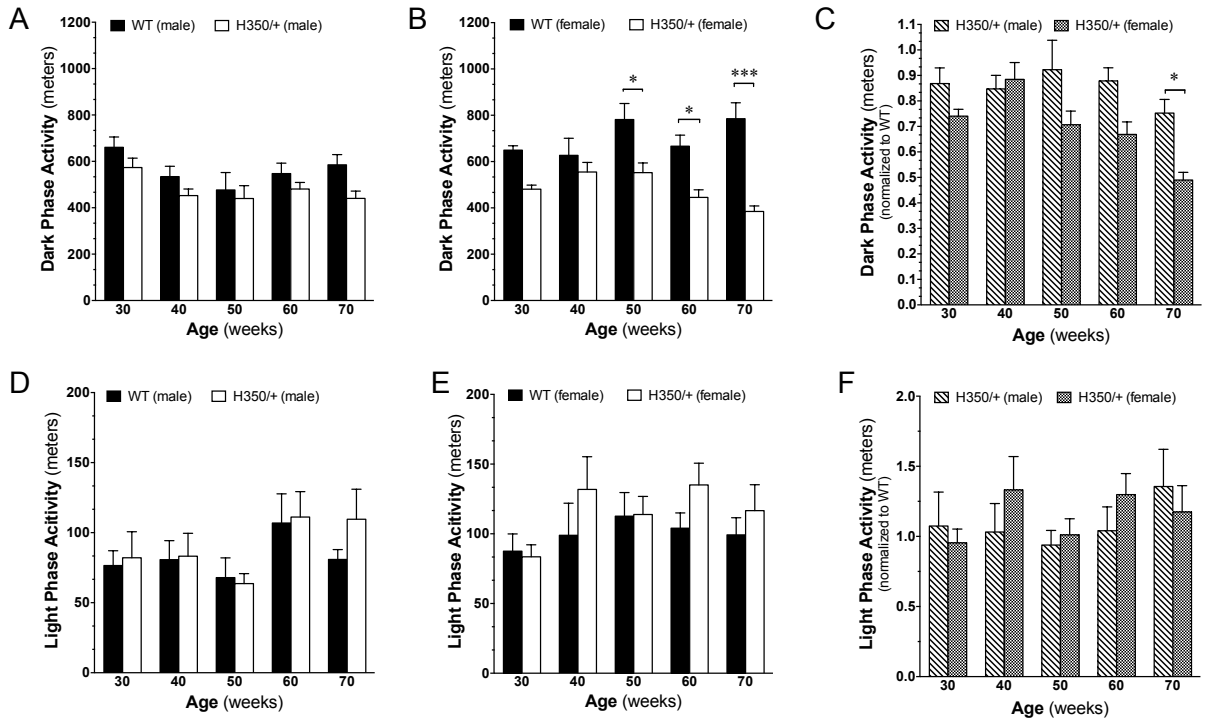

Figure 2.2. Spontaneous locomotor activity is affected in the dark, but not light, phase. (A) Male and (B) female HdhQ350/+ mice traveled less during the dark phase compared to their respective wild-type littermates. (C) Female HdhQ350/+ mice showed a sex-dependent decline in locomotor activity during the dark phase when normalized to their respective wild-type littermates. (D) Male and (E) female HdhQ350/+ mice traveled similarly to their respective wild-type littermates during the light phase. (F) There was no sex-dependent difference in locomotor activity during the light phase when normalized to their respective wild-type littermates. N=7-8 for all groups. Error bars represent S.E.M. and *p<0.05, ***p<0.001 with two-way ANOVA with Bonferroni post-hoc test.

To extend these results, we measured the time spent in various zones within the PhenoTyper chamber (i.e. focusing on the time spent along the walls, in the hidden zone and in the feeding zone during the dark phase). Because HdhQ350/+ males and females weighed less and were less active than their wild-type counterparts, we were curious on other habitual behaviors and if HdhQ350/+ animals were eating less, despite being less active. We found that HdhQ350/+ mice of both sexes spent similar amounts of time in the hidden and feeding zone compared to their respective wild-type littermates (Supplementary Figure 2.1A-D). Female HdhQ350/+ mice spent significantly more time along the walls than wild-type female mice, suggesting increased thigmotaxis (tendency for rodents to remain close to vertical surfaces) and possible anxiety ($F_{(1,\ 60)}$=4.96, p=0.030) (Supplementary Figure 2.2A, B). In addition, only HdhQ350/+ females spent more time with their bodies contracted, or hunched, at nearly all ages, suggesting possible discomfort and illness ($F_{(1,\ 60)}$=8.09, p=0.006) (Supplementary Figure 2.2C, D) (Horn, Henry, Meyers, & Magnusson, 2011).

These results demonstrate sex-dependent reduction of nocturnal activity and signs of sickness in HdhQ350/+ mice with overall more pronounced symptoms measured in HdhQ350/+ females. Based on these results, we focused our analysis on 40- and 60-week-old animals, which reflect disease onset and progression in the HdhQ350/+ line, respectively.

2.2.3 Motor behavior of HdhQ350/+ mice: Motor coordination, motor learning and gait

Motor impairment represents a classical symptom measured in many HD mouse models (Pouladi et al., 2013; Walker, 2007). Here we determined if HdhQ350/+ mice show deficits in both motor coordination and motor learning as assessed by the accelerating rotarod over 3 days of 7 trials per day (Costa, Cohen, & Nicolelis, 2004). Motor coordination was measured by comparing daily averages of an animal's latency to fall. Figure 2.3A and C show that at 40

weeks of age, both male and female HdhQ350/+ mice did not differ from wild-type controls in their motor coordination over 3 days of testing. However, at 60 weeks of age, HdhQ350/+ males showed a significant reduction in motor coordination on the second and third days of testing (day 2: $F_{(1, 14)}$=9.64, p=0.008; day 3: $F_{(1, 13)}$=6.5, p=0.024), whereas HdhQ350/+ females showed no significant reduction in motor coordination (Figure 2.3A and C). Accordingly, analysis of each

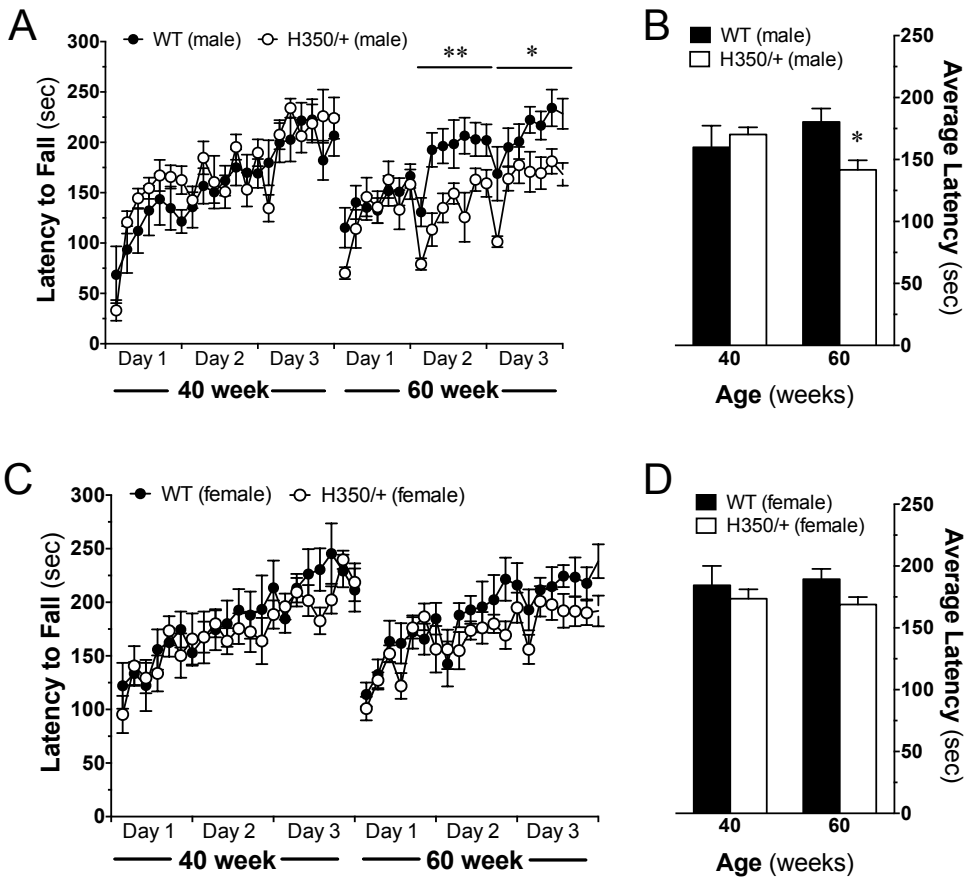

Figure 2.3. Motor coordination is affected in male, but not female, HdhQ350/+ mice. Mice were tested over 3 days on an accelerating rotarod at various ages. (A) Male HdhQ350/+ mice showed reduced motor coordination on the second and third trial days at 60 weeks of age. (B) Male HdhQ350/+ mice had a lower average latency to fall at 60 weeks of age. (C) Female HdhQ350/+ mice had similar motor coordination on all trial days, compared to female wild-type littermates. (D) Female HdhQ350/+ mice had similar average latencies to fall at 40 and 60 weeks of age. N=7-8 for all groups. Error bars represent S.E.M. and *p<0.05, **p<0.01 with two-way ANOVA with Bonferroni post-hoc test.

group's average latency to fall per age reached significance only in HdhQ350/+ males, especially at 60 weeks of age ($F_{(1,\ 14)}$=8.54, p=0.011) (Figure 2.3B, D). These results show that only HdhQ350/+ males reliably recapitulate the common impairment in motor coordination measured in other HD mouse models and that this symptom develops between 40 and 60 weeks of age in the HdhQ350/+ line.

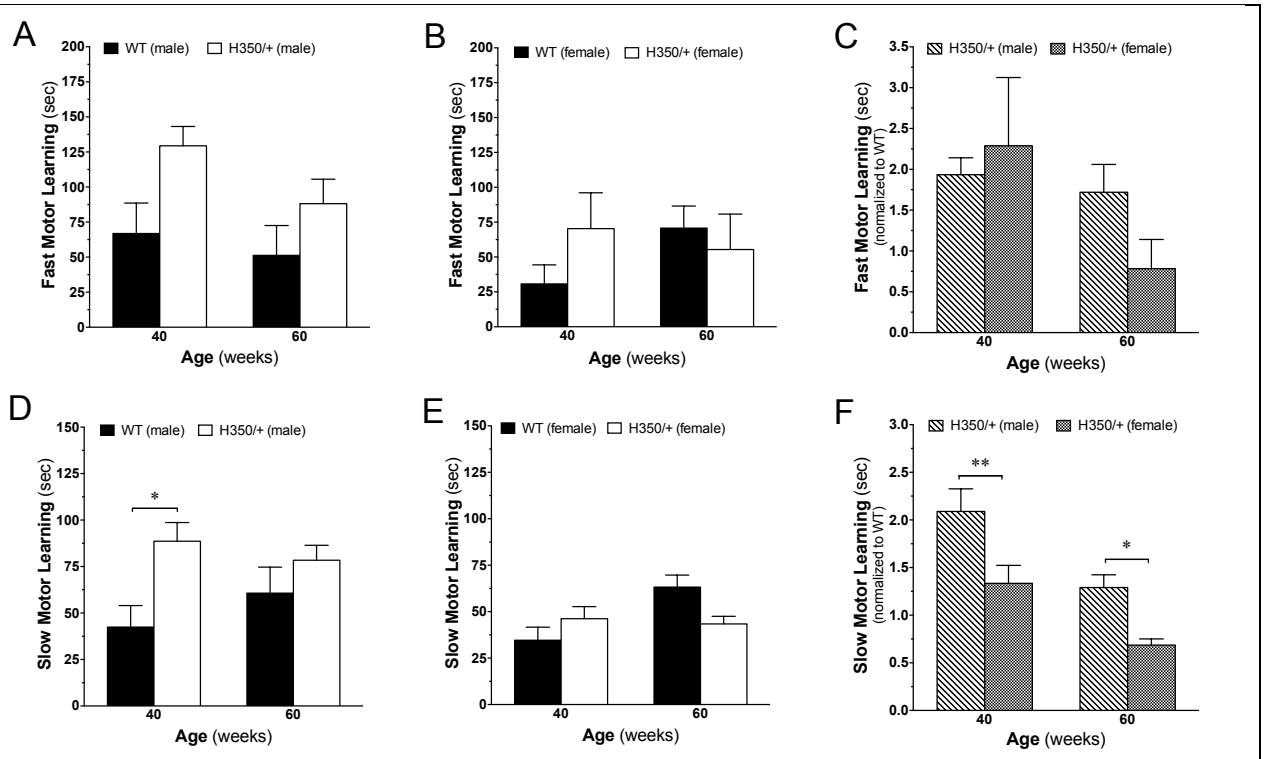

Figure 2.4. Motor learning is affected in male, but not female, HdhQ350/+ mice. Fast motor learning was calculated by improved performance between the first and last trial on day 1. Slow motor learning was calculated by cumulative improved performance over all 3 days (See Materials and Methods). (A) HdhQ350/+ males showed significantly enhanced fast motor learning while (B) HdhQ350/+ females did not. (C) Comparison of male HdhQ350/+ mice to female HdhQ350/+ mice when normalized to their respective wild-type littermates in fast motor learning revealed no difference between sexes. (D) HdhQ350/+ males showed significantly enhanced slow motor learning while (E) HdhQ350/+ females did not differ from their respective wild-type littermates. (F) Comparison of male HdhQ350/+ mice to female HdhQ350/+ mice when normalized to their respective wild-type littermates revealed a significant difference in slow motor learning between sexes. N=8 for all groups. Error bars represent S.E.M. and *p<0.05, **p<0.01, with two-way ANOVA with Bonferroni post-hoc test.

Impaired motor learning is thought to result from dysfunction of the corticostriatal loop involved in the acquisition of new motor skills (Walker, 2007). To determine the effect of the HdhQ350/+ mutation on motor learning involving the corticostriatal circuitry, we adopted a method in which *fast* motor learning is determined by measuring improvement in motor performance on the rotarod within the first training session (day 1) and *slow* motor learning is determined by measuring improvement across all 3 testing days (Costa et al., 2004). Figure 2.4A shows that HdhQ350/+ males exhibited enhanced fast motor learning compared to corresponding wild-type littermates when analyzing data gathered at 40 and 60 weeks of age using a two-way ANOVA ($F_{(1,\ 14)}$=0.73, p=0.041). Figure 2.4B shows that HdhQ350/+ females were not significantly different from wild-type females. Analysis between male and female HdhQ350/+ mice normalized to their respective wild-type littermates showed no significant differences between sexes in regard to fast motor learning (Figure 2.4C). In regards to slow motor learning, we found enhanced slow motor learning in HdhQ350/+ males compared to wild-type males when analyzing data gathered at both 40 and 60 weeks of age ($F_{(1,\ 14)}$=6.72, p=0.021) (Figure 2.4D) and again, no difference in females (Figure 2.4E). Here, post-hoc analysis showed that enhanced slow motor learning reached significance at 40 weeks for HdhQ350/+ males. Further analysis revealed a significant difference between male and female HdhQ350/+ mice in their slow motor learning when normalized to their respective wild-type littermates ($F_{(1,\ 14)}$=15.11, p=0.0001) (Figure 2.4F). These results suggest that only HdhQ350/+ male mice exhibit enhanced improvement of motor learning over multiple days of rotarod testing.

Gait abnormalities represent hallmarks of HD symptoms (Walker, 2007). To complement our measures of motor coordination and learning, we utilized the Noldus CatWalk XT System that allows for unbiased, automated gait analysis. We found a significant reduction in hind paw

step cycle (a measurement of the time it takes for a paw to lift and place back down) in female HdhQ350/+ mice ($F_{(1, 40)}$=5.74, p=0.021) but not males (Figure 2.5A, B). We measured a significant increase in front paw stride length in HdhQ350/+ males ($F_{(1, 42)}$=4.59, p=0.038) but not in HdhQ350/+ females when compared to their respective wild-type littermates (Figure 2.5C, D) and no differences in front paw or hind paw swing speed for either sex (Supplementary Figure 2.3A-D). There was a significant difference in front paw base of support in HdhQ350/+ males but not females, as these mice had a reduced base of support, indicative of

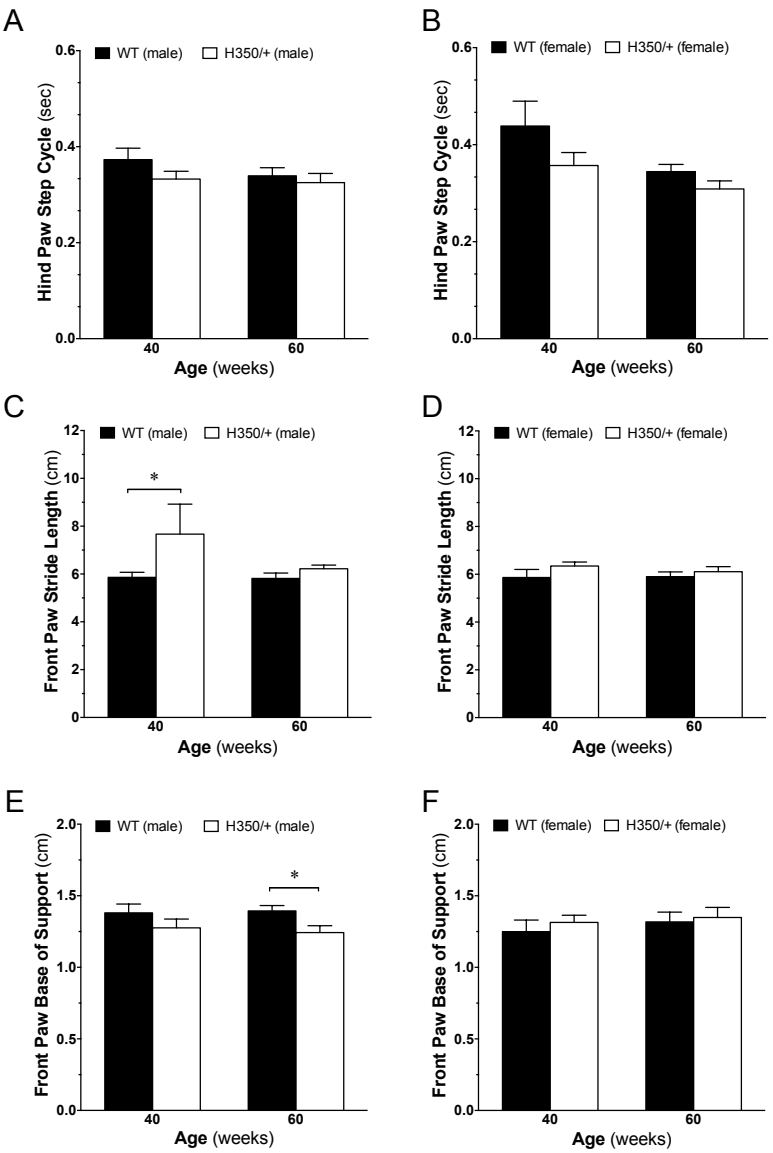

Figure 2.5. HdhQ350/+ males and females show deficits in gait. (A) Male HdhQ350/+ mice do not have altered hind paw step cycle but (B) female HdhQ350/+ show increased hind paw step cycle at 40 and 60 weeks of age. (C) Male HdhQ350/+ mice have increased front paw stride length at 40 and 60 weeks of age but (D) female HdhQ350/+ mice do not. (E) Male HdhQ350/+ mice have reduced front paw base of support but (F) female HdhQ350/+ mice do not. N=6-8 for all groups. Error bars represent S.E.M. and *p<0.05, with two-way ANOVA with Bonferroni post-hoc test.

reduced stability through movement ($F_{(1, 19)}$=5.35, p=0.032) (Figure 2.5E, F). Bonferroni post-hoc tests reached significance at 60 weeks of age in HdhQ350/+ males (Figure 2.5E). Together, these results suggest that HdhQ350/+ mice, especially males, show clear gait abnormalities and that part of the changes in their motor performance as measured by the spontaneous locomotion and motor coordination and learning could be accounted for by changes in gait.

2.2.4 Psychiatric and cognitive function of HdhQ350/+ mice: Anxiety and exploration

HD patients exhibit a spectrum of psychiatric symptoms that range from irritability to psychosis and include anxiety and loss of interest (Pouladi et al., 2013; Walker, 2007). Indices of anxiety can be measured in mice with the elevated plus maze and when coupled to measures of novel environment exploration, provide an initial assessment of psychiatric and cognitive dysfunction. Analysis of anxiety using the elevated plus maze confirmed that male and female wild-type mice spent more time in the closed arms than the open arms of the maze (Figure 2.6A-D). When comparing HdhQ350/+ to wild-type mice, we found no significant differences in the time spent in the closed or open arms irrespective of age or sex (Figure 2.6A-D). Furthermore, we found no change in the frequency to enter the closed arms for either sex but did find a significant difference in the frequency to enter open arms for female HdhQ350/+ mice ($F_{(1, 13)}$=5.78, p=0.032), but not for male mice (Supplementary Figure 2.4A-D). These results show that HdhQ350/+ mice do not exhibit overt changes in anxiety-like behavior.

Activity in the first hour of being placed in the PhenoTyper chamber was used to assess the mouse's interest and exploratory behavior of a novel environment. As expected, male and female wild-type mice showed high levels of exploratory activity during the initial hour, covering approximately 100 meters/hour compared to approximately 10 meters/hour when

measured 24 hours later (Figure 2.6E, F and Supplementary Figure 2.5A, B). There was no difference between male and female HdhQ350/+ and wild-type littermates in their exploratory

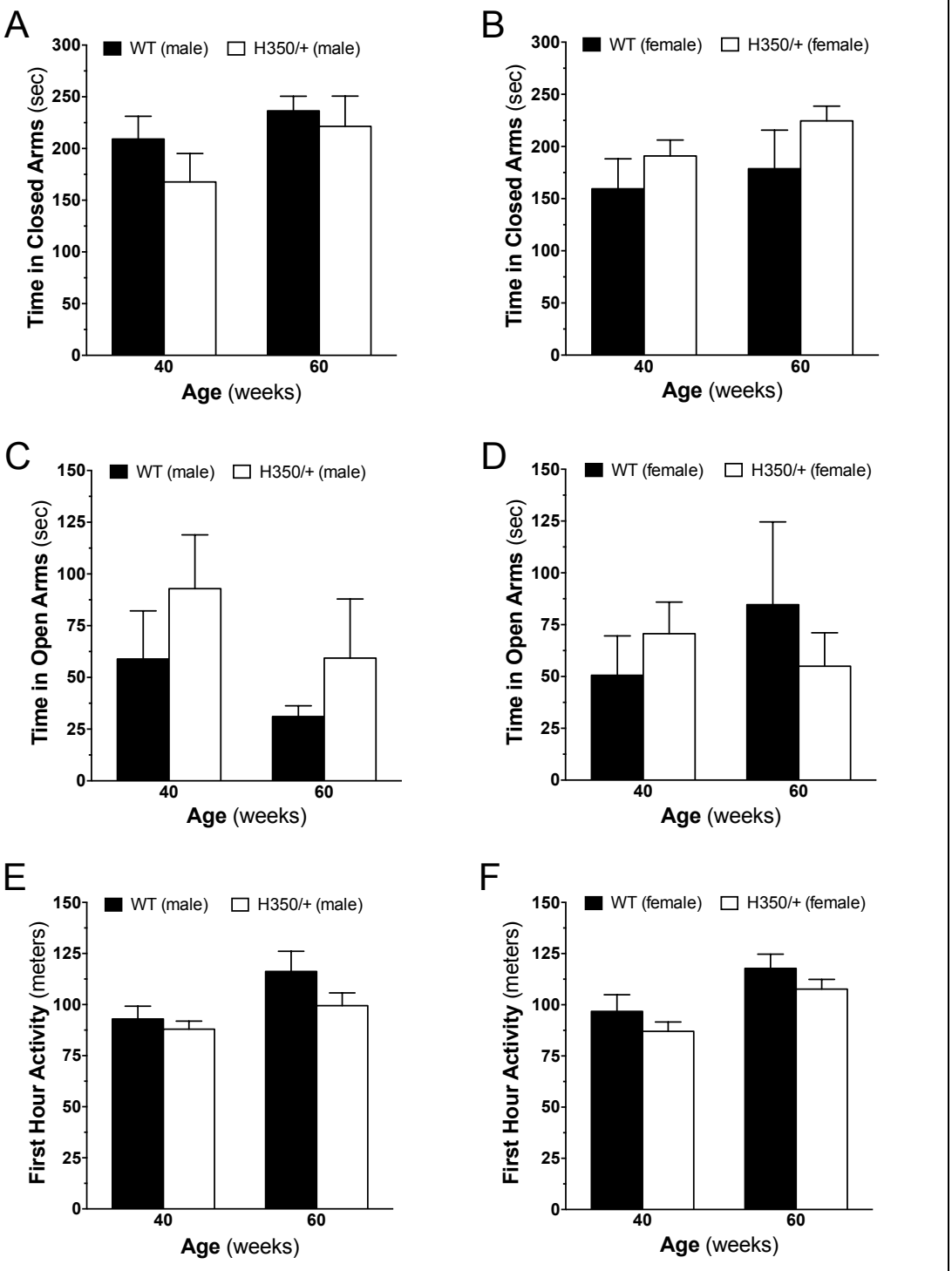

Figure 2.6. Psychiatric and cognitive functions are unaffected in HdhQ350/+ males and females. On the elevated plus maze, HdhQ350/+ (A) males and (B)

females generally spent similar amounts of time in the closed arms than their respective wild-type littermates. HdhQ350/+ (C) males and (D) females spent similar amounts of time in the open arms than their respective wild-type littermates. Exploration was measured by the distance mice traveled within the first hour of being placed into the PhenoTyper chamber. (E) Male HdhQ350/+ mice and (F) female HdhQ350/+ mice covered similar distances than their respective wild-type littermates at 40 and 60 weeks of age. N=7-8 for all groups. Error bars represent S.E.M., with two-way ANOVA with Bonferroni post-hoc test.

activity during this initial hour when measured at 40 or 60 weeks of age (Figure 2.6E, F). Expectedly, we found no difference in activity 24 hours later between HdhQ350/+ and wild-type male mice (Supplementary Figure 2.5A). Curiously, we found a significant increase in activity 24 hours later in HdhQ350/+ females over wild-type females, especially at 60 weeks of age ($F_{(1, 27)}$=6.77, p=0.015) (Supplementary Figure 2.5B). Taken together, these results suggest no striking anxiety or reduction in exploratory behavior exhibited by the HdhQ350/+ mouse line.

2.2.5 mHtt expression in HdhQ350/+ brains: Protein expression and aggregation

A portion of HD pathogenesis is linked to mHtt aggregates accumulating in the striatum (Labbadia & Morimoto, 2013; Walker, 2007). To verify that mHtt protein is expressed and aggregates in HdhQ350/+ striatum, we measured mHtt expression in this tissue by western blot using an antibody that recognizes polyglutamine expansions over 37 CAGs (Trottier et al., 1995). Supplementary Figure 2.6A and B show that mHtt protein is expressed in the striatum of both male and female HdhQ350/+ mice and as expected, aggregates were detected in the stacking gel. Aggregated Htt was not observed in wild-type littermates. Furthermore, semi-quantitative analysis of mHtt band intensity indicated no significant difference in expression levels between sexes at 40 or 60 weeks of age (Figure 2.7A). Analyses of mHtt expression between 40 and 60 weeks revealed no significant differences for either sex (data not shown).

These results show that mHtt protein is expressed at similar levels in both male and female HdhQ350/+ striatum.

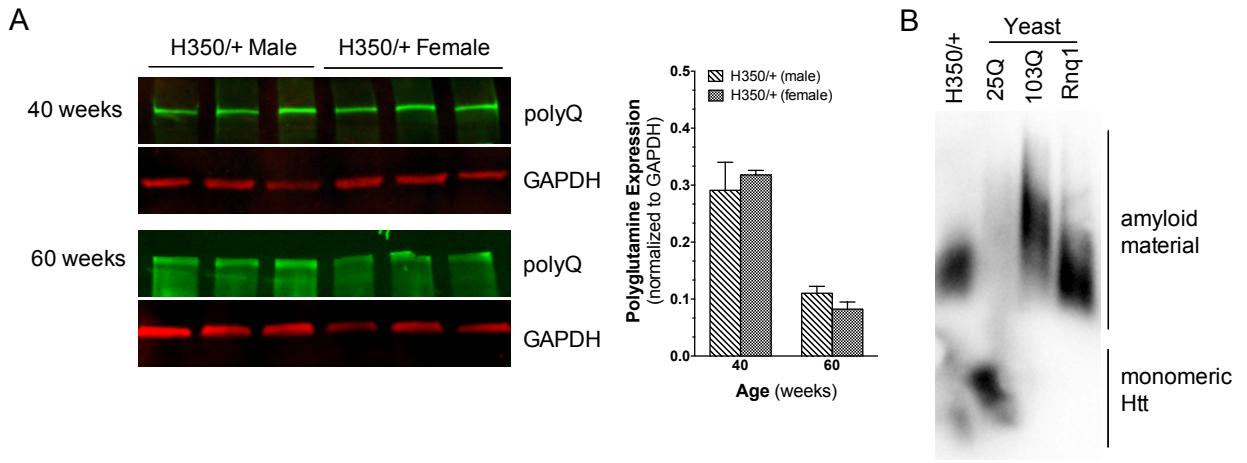

Figure 2.7. mHtt expression and aggregation in striatal tissue of HdhQ350/+ males and females. Western blot of polyglutamine expansion at 40 and 60 weeks of age in (A) male and female HdhQ350/+ mice. Quantification of mHtt between male and female HdhQ350/+ mice showed no difference in protein expression levels. (B) SDDAGE blot comparing SDS solubility of striatal H350/+ tissue to yeast strains of 25 polyglutamines, 103 polyglutamines and prion Rnq1. Error bars represent S.E.M., with two-way ANOVA with Bonferroni post-hoc test.

To extend these results, we used semi-denaturing detergent agarose gel electrophoresis (SDDAGE) to detect large polymers formed by mHtt proteins (Halfmann & Lindquist, 2008). This approach has been successfully used to study the aggregation of proteins with elevated polyglutamine repeats. Accordingly, we validated this method using stringent standards of the field: a yeast model expressing 25 polyglutamines as a negative control and a yeast model expressing 103 polyglutamines and Rnq1, a yeast prion known to also form amyloid aggregates, as positive controls (Konopka). Thus, under low SDS conditions and blotting with an antibody that recognizes large polyglutamine tracts, we found a clear signal indicating aggregates in striatal HdhQ350/+ tissue (Figure 2.7B). Together, these results demonstrate the equal

expression and aggregation of HdhQ350 protein in the striatum of male and female HdhQ350/+ mice.

2.2.6 Neuropathology of HdhQ350/+ brains: Medium spiny neurons and neuronal markers

To investigate whether motor behavior impairments measured in the HdhQ350/+ model might be correlated with known neuropathological markers of HD pathogenesis, we used western blots and semi-quantitative immunohistochemistry (sqIHC) to assess for the expression of DARPP-32, synaptophysin and CB_1 receptors in the striatum as previously described by our laboratory (Horne et al., 2012). We first measured the expression of DARPP-32, a dopamine- and cAMP-regulated neuronal phosphoprotein in medium spiny neurons (MSNs) known to be down-regulated in mouse models of HD (Roze et al., 2011), and found a significant reduction in its expression in female HdhQ350/+ mice at 40 and 60 weeks when compared to female wild-type littermates ($F_{(1, 4)}$=47.38, p=0.002) and no change in HdhQ350/+ males compared to male wild-type littermates (Figure 2.8A, B). To investigate if this difference was due to a reduction of DARPP-32-specific protein expression or general cell loss, we used sqIHC analysis on brain slices that focused on the dorsal lateral striatum. We assessed for cell loss by measuring the size of DARPP-32-positive cells and found no significant difference between genotypes in either sex (Figure 2.8C, D). Analyzing the number of DAPI-positive cells further validated this result, as we found no differences between genotypes, irrespective of sex (Figure 2.8E, F). These results suggest that only female HdhQ350/+ mice show a reduction in striatal DARPP-32 expression with no evidence of cell loss.

Loss in the expression of both synaptophysin, a key component of presynaptic machinery for neurotransmitter release, and the cannabinoid CB_1 receptor, a presynaptic G protein-coupled receptor that regulates neurotransmitter release, represent neuropathological hallmarks of early

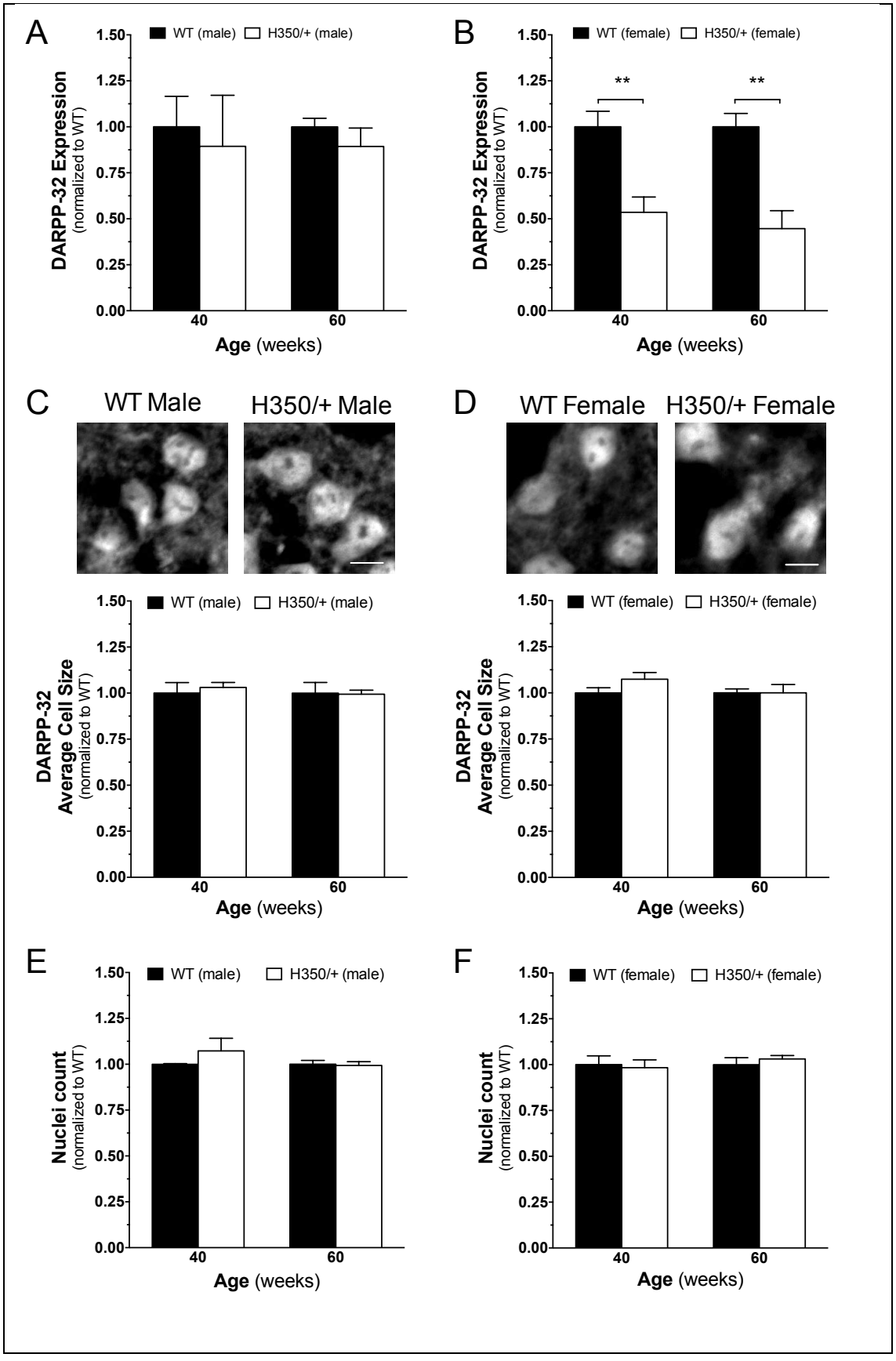
A
WT (male)
H350/+ (male)
DARPP-32 Expression
(normalized to WT)
1.50
1.25
1.00
0.75
0.50
0.25
0.00
40
60
Age (weeks)
B
WT (female)
H350/+ (female)
**
**
DARPP-32 Expression
(normalized to WT)
Age (weeks)
C
WT Male
H350/+ Male
DARPP-32
Average Cell Size
(normalized to WT)
D
WT Female
H350/+ Female
E
Nuclei count
(normalized to WT)
F

Figure 2.8. HdhQ350/+ females, but not males, exhibit typical HD protein loss in the striatum. (A) Male HdhQ350/+ mice did not show changes in DARPP-32 protein expression at 40 or 60 weeks when compared to male wild-type littermates. (B) Female HdhQ350/+ mice showed significant reductions in DARPP-32 protein expression at 40 and 60 weeks of age. (C) Male HdhQ350/+ and (D) female HdhQ350/+ mice had no significant differences in average size of DARPP-32-positive cells compared to respective wild-type littermates. Representative images are cropped and captured at 40x. Scale bar denotes 10um. DAPI-positive cells quantified in the dorsolateral striatum showed no difference in (E) male HdhQ350/+ and (F) female HdhQ350/+ mice when compared to their respective wild-type littermates. N=3 for all groups. Error bars represent S.E.M. and **p<0.01, with two-way ANOVA with Bonferroni post-hoc test.

HD pathogenesis (Glass et al., 1993; Goto & Hirano, 1990). Western blot analysis of striatal tissue showed no difference in synaptophysin expression between male or female HdhQ350/+ mice and wild-type littermates, irrespective of age (Supplementary Figure 2.7A, B). Reduction of CB_1 receptor expression is known to occur in MSNs of several HD mouse models (Denovan-Wright & Robertson, 2000; Horne et al., 2012; McCaw et al., 2004; Naydenov, Sepers, et al., 2014). Interestingly, we found no significant changes in CB_1 receptor expression in the striatum with this mouse model (Supplementary Figure 2.7C, D). Using sqIHC, we then investigated CB_1 expression on the MSN terminals projecting into the globus pallidus by co-staining with enkephalin and also found no changes in CB_1 expression on the axon terminals (Supplementary Figure 2.8A, B). Combined, these results show that the expression of certain neuropathological markers of HD pathogenesis (DARPP-32) is reduced in the HdhQ350/+ mouse model in a sex-dependent manner.

2.3 Discussion

We report a longitudinal study of the HdhQ350/+ mouse line that focuses on behavioral indices commonly measured in other mouse models of HD. We provide evidence for sex-dependent alterations of motor performance as measured by several readouts and no evidence of anxiety or decreases in exploratory behavior. HdhQ350/+ mice had reduced weight and grip strength independent of sex. While we demonstrate that the HdhQ350 protein is expressed and aggregated in the brain, we only found a significant decrease in DARPP-32 expression in female HdhQ350/+ mice, with no significant changes in the expression of two other neuropathological markers commonly measured in HD research. Our study indicates that the HdhQ350/+ mouse line recapitulates select physical and behavioral impairments commonly measured in other HD mouse models but not equal loss of common neuropathological markers. In addition, our results suggest that polyglutamine expansions and expression of mHtt protein may affect disease progression and severity in a sex-dependent manner, indicating an importance to study both sexes with other HD and polyglutamine animal models.

The HdhQ350/+ mouse line was generated through selective breeding of the HdhQ mouse model. Here we report that, unlike the HdhQ150 and HdhQ200 lines, homozygous HdhQ350/350 mice were most likely embryonic lethal (M Y Heng et al., 2010; M Y Heng, Tallaksen-Greene, Detloff, & Albin, 2007; Lin et al., 2001). This has been previously noted to occur in the HdhQ315/+ line (Kumar et al., 2016). In addition, we found a significant reduction in heterozygote viability. The HdhQ350/+ line does reproduce several key physical symptoms known to occur in other HD mouse models. We show that HdhQ350/+ males and females exhibit significant weight loss as early as 30 weeks of age, whereas it has been published that only female HdhQ200/+ mice lose weight after 50 weeks of age and only HdhQ150/150, but not HdhQ150/+, mice display any weight deficits (M Y Heng et al., 2010; M Y Heng et al., 2007;

Lin et al., 2001). Because mice spent normal amounts of time at the feeding area of the PhenoTyper cage and no overt deficits in feeding behavior were observed by researchers or animal technicians, this weight loss is likely due to a physiological impairment that remains to be identified. Interestingly, the early loss in weight is paralleled by a reduction in grip strength; both male and female HdhQ350/+ mice exhibit reduced forelimb grip strength at 30 weeks of age. This result contrasts with what has been measured in HdhQ200/+ mice, which do not exhibit this phenotype until 80 weeks of age (M Y Heng et al., 2010). While early reduction in grip strength suggests that the HdhQ350/+ mice may have a defect in muscle development, a study of muscle tissue is needed to better understand this HdhQ350/+ associated impairment.

We found significant changes in dark phase spontaneous activity in both HdhQ350/+ males and females and no changes in light phase activity. Remarkably, we found a more severe phenotype in female HdhQ350/+ mice, especially at 70 weeks of age. A study on circadian patterns with the R6/2 model showed shifted circadian patterns and there has been evidence of phase-delayed circadian rhythm in HD patients (Morton, 2013; Morton et al., 2005). Together, these results suggest that HdhQ350/+ mice exhibit similar activity disturbances to other mouse models of HD.

Analysis of motor coordination using the rotarod revealed significant deficits at 60 weeks of age in male HdhQ350/+ mice. Both HdhQ150/+ and HdhQ200/+ mice do not exhibit motor deficits on the rotarod and even HdhQ150/150 mice do not show a deficit until 100 weeks of age (M Y Heng et al., 2010; M Y Heng et al., 2007). In line with our results, a study on BACHD mice revealed that male BACHD mice exhibit poorer motor coordination than female BACHD mice (Kuljis et al., 2016). In addition, a study on a transgenic HD rat model showed motor impairments in only males and a study on R6/2 mice showed that males exhibited earlier

symptoms of other motor impairments, including hanging, rearing and climbing (Bode et al., 2008; Zarringhalam et al., 2012). Analysis of wheel-running, another measurement of motor activity, on R6/1 mice also showed a decrease only in males (Zajac et al., 2010). Furthermore, we found striking differences in motor learning with male HdhQ350/+ mice, suggesting disruptions or adaptations in the corticostriatal loop in this mouse line. The corticostriatal loop is involved in action selection, motor control, sequence learning, and habit formation (Shepherd, 2013). However, we also note that our results may be due to the initial poorer starting performance of the HdhQ350/+ mice and/or impairment of learning retention between days, either of which would result in a poorer initial performance of the first trial for HdhQ350/+ animals in the rotarod assay. In any case, this represents a novel finding, as motor learning has not been explored in-depth in previous HD mouse models.

Earlier studies have reported gait instability in the HdhQ150/150, HdhQ150/+, HdhQ200/+, and HdhQ315/+ lines, as measured by different paradigms than those used in our study. Specifically, 70-week-old HdhQ150/150 and 50-week-old HdhQ200/+ mice are significantly unstable when traversing a balance beam (M Y Heng et al., 2010; M Y Heng et al., 2007). In addition, HdhQ315/+ animals show a slower latency to traverse a ladder starting at 40 weeks of age as well (Kumar et al., 2016). The Noldus CatWalk XT System used in our study is an automated, highly sensitive tool that detected slight alterations mainly in male HdhQ350/+ mice. Specifically, we saw increases in the length of stride of their front paws and decreases in their front base of support. Thus, sex-dependent gait instability occurs in the HdhQ350/+ line.

Psychiatric deficits and cognitive dysfunction as measured by indices of anxiety and exploration have not been studied in previous HdhQ lines, and our study uncovered no significant impairments in these behavioral readouts. Whereas we saw initial indication of

anxiety through thigmotaxis in the PhenoTyper chamber in female HdhQ350/+ mice, this impairment was not confirmed with the elevated plus maze. Note that studies have shown that only female R6/1 mice exhibit depressive-like phenotypes, as measured with the sucrose preference test, forced swim test, tail-suspension test, and novelty-suppressed feeding test (Pouladi et al., 2013), which may be linked to a disruption in the hypothalamic-pituitary-adrenal axis (Du et al., 2012). These mice also have disrupted short-term memory acquisition due to stress, suggesting sex-dependent cognitive deficits (Mo, Renoir, Pang, & Hannan, 2013). By contrast, R6/2 and BACHD mice exhibit decreased anxiety as measured by the elevated plus maze, and a study on R6/2 and HdhQ mice carrying increasing CAG repeats showed a nonlinear profile of depression through the forced swim test (Adjeroud et al., 2015; Bissonnette, Vaillancourt, Hébert, Drolet, & Samadi, 2013; Ciamei, Detloff, & Morton, 2015). It is important to emphasize that psychiatric deficits may depend on the behavioral paradigm and readout, as select HD mouse models exhibit differing results with the open field test, elevated Z maze, fear conditioning, and forced swim test (Pouladi et al., 2013). Based on this evidence, we conclude that there may be sex-dependent psychiatric deficits that are detected using certain behavioral paradigms.

One of the most interesting findings of our analyses is a sex difference in the disease progression occurring in the HdhQ350/+ line. Few studies on other HD mouse models have separately analyzed male and female cohorts and previous studies on HdhQ150/150, HdhQ150/+, HdhQ200/+ and HdhQ315/+ lines did not identify any overt sex-differences (M Y Heng et al., 2010; M Y Heng et al., 2007; Kumar et al., 2016; Lin et al., 2001). We found a more severe general phenotype in HdhQ350/+ females with an earlier onset of weight loss, increased body contractions indicating distress, increased thigmotaxis and a more severe loss of dark-phase

locomotor activity. Conversely, we measured a more severe impairment in motor coordination and learning, as well as gait in HdhQ350/+ males. Taken together, our results suggest possible sex-dependent behavioral deficits due to the HdhQ350/+ mutation.

We show that the HdhQ350 line also models a sex-dependent reduction of striatal DARPP-32 expression only in HdhQ350/+ females. Interestingly, heterozygous and homozygous HdhQ150 mice of both sexes show significant reduction in the number of MSNs by 100 weeks of age whereas this does not occur in HdhQ200/+, HdhQ315/+ or in our HdhQ350/+ mice. These previous studies did not report any sex differences. Combined with our results, this suggests that the elevated CAG repeats may differentially affect sexes in mouse models (M Y Heng et al., 2010; M Y Heng et al., 2007; Kumar et al., 2016; Lin et al., 2001). Our results propose that the behavioral symptoms we measured in the HdhQ350/+ line results from dysfunction rather than loss of striatal neurons. Remarkably, we did not detect a down-regulation of synaptophysin or CB_1 receptor expression, common markers of HD pathogenesis. While down-regulation of these two markers has been demonstrated in most HD mouse models, no evidence exists for their direct involvement in disease development (Blazquez et al., 2010; Dowie et al., 2009; Horne et al., 2012; Naydenov, Sepers, et al., 2014). In fact, our laboratory showed that despite genetically restoring expression of CB_1 receptors in MSNs of R6/2 mice, motor impairments were not rescued (Naydenov, Sepers, et al., 2014). Thus, further investigation into other synaptic markers would be needed to identify the neuronal dysfunctions occurring in the HdhQ350/+ model.

R6/2 mice carrying over 200 CAG repeats show a delayed onset of symptoms and prolonged survival than those expressing under 200 CAG repeats (Morton et al., 2009). Importantly, this incidence does not parallel what is observed in human HD patients, where disease severity strongly correlates with the number of CAG repeats in a patient's gene (Andrew

et al., 1993). When assessing disease onset and progression in the HdhQ150/+, HdhQ200/+, HdhQ315/+ and our current study on the HdhQ350/+ mouse lines (M Y Heng et al., 2010; M Y Heng et al., 2007; Kumar et al., 2016; Lin et al., 2001), it appears that increasing the number of CAG repeats to 350 may elicit molecular mechanisms of neuronal dysfunction that differ from previously developed mouse models of HD (Duzdevich et al., 2011) and may recapitulate only a portion of human HD.

In summary, we show that the HdhQ350/+ mouse line expresses mHtt proteins that aggregate. We expected parallel declines in behavioral measurements and neuropathology indices in both male and female HdhQ350/+ mice, hypothesizing that key HD markers would decline prior to symptom onset. However, the discrepancies between our neuropathological and behavioral measures revealed a clear disassociation between the development of pathology and behavior in this mouse line. In addition, we found differences in disease onset and severity between males and females. We conclude that elevated CAG repeats trigger sex-dependent pathological processes that remain to be identified, indicating an importance of considering sex when studying HD animal models.

2.4 Supplementary figures

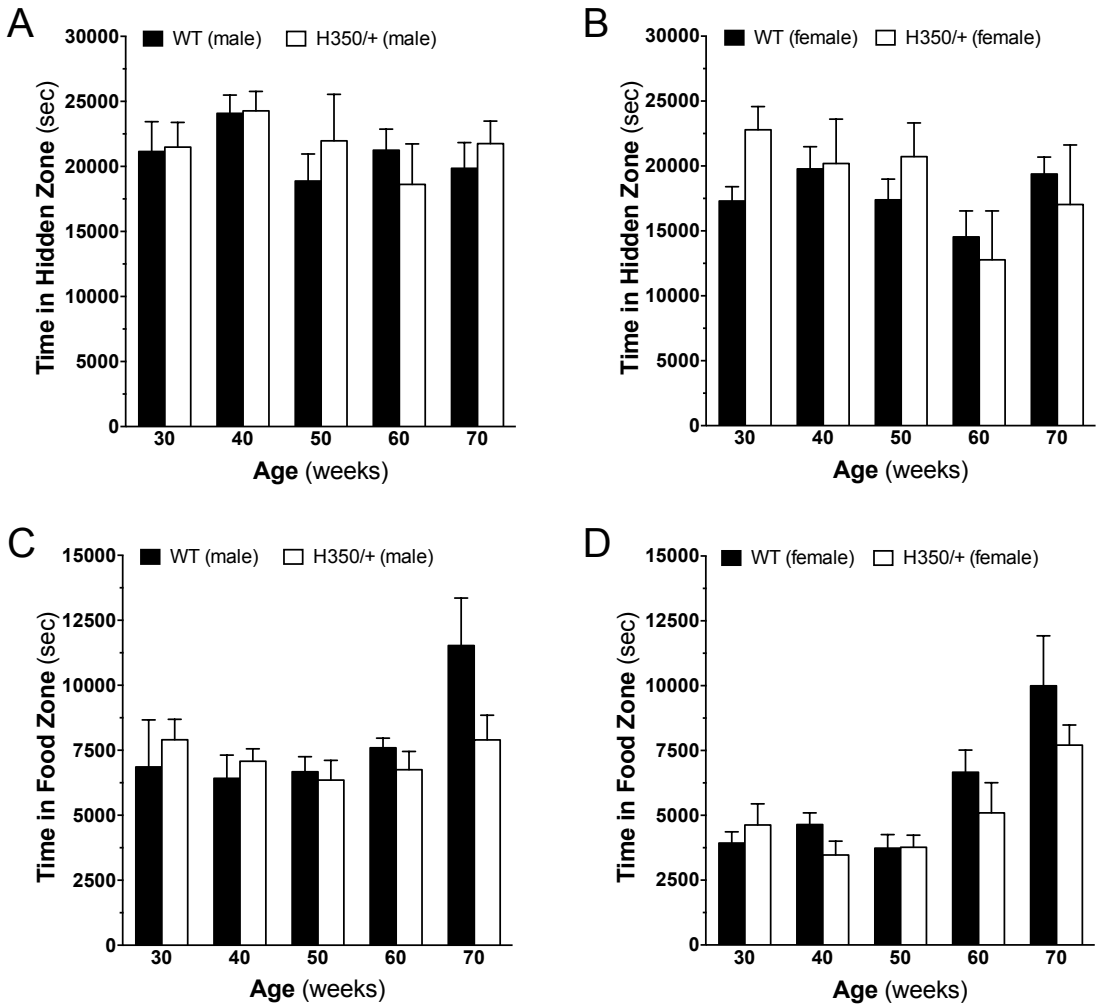

Supplementary Figure 2.1. HdhQ350/+ (A) males and (B) females spent similar amounts of time in the hidden zone compared to their respective wild-type littermates at all time points. HdhQ350/+ (C) males and (D) females spent similar amounts of time in the food zone compared to their respective wild-type littermates. N=7-8 for all groups. Error bars represent S.E.M., with two-way ANOVA with Bonferroni post-hoc test.

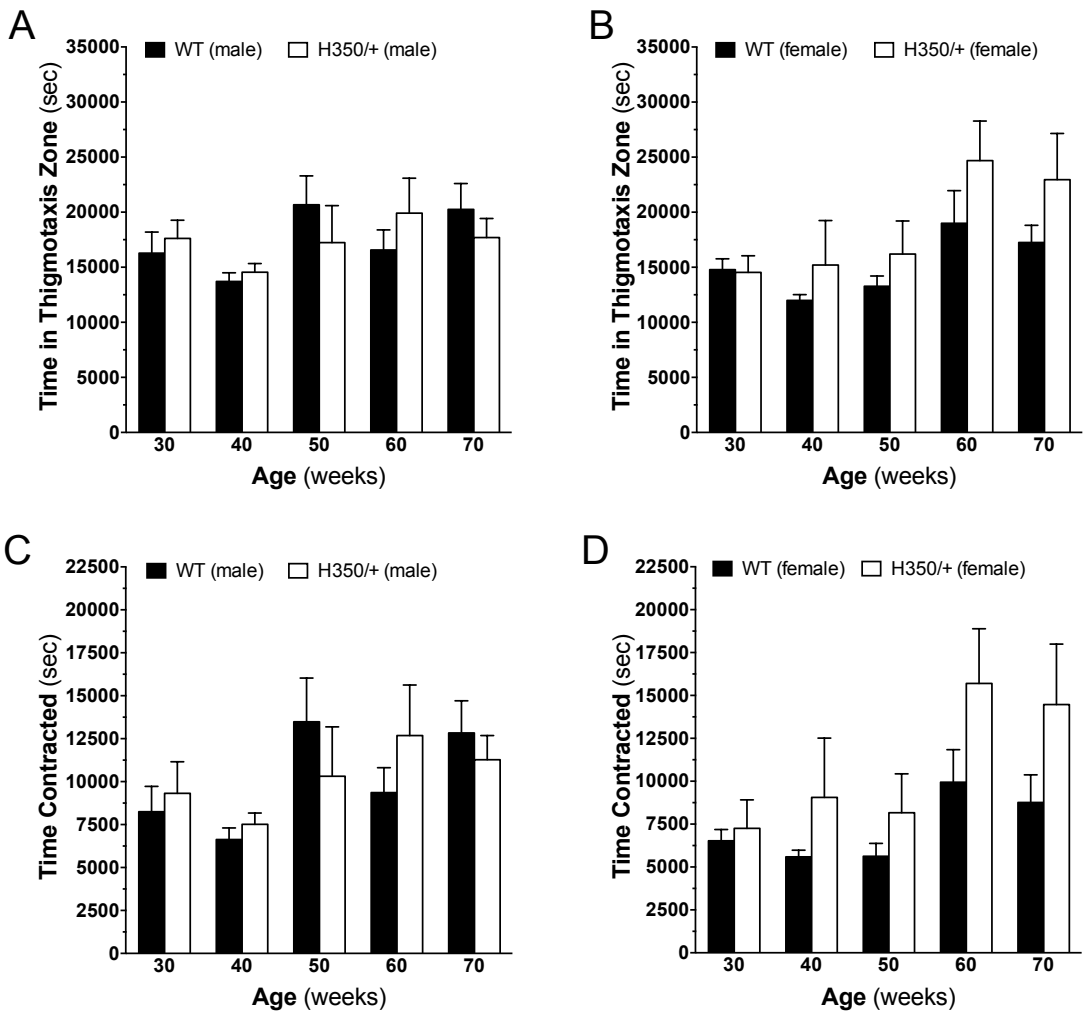

Supplementary Figure 2.2. HdhQ350/+ (A) males and (B) females spent similar amounts of time along the walls of the Phenotyper chamber, compared to their respective wild-type littermates at all time points. (C) Male HdhQ350/+ mice spent similar amounts of time with their bodies contracted than their male wild-type littermates but (D) female HdhQ350/+ mice spent more time contracted than female wild-type littermates. N=7-8 for all groups. Error bars represent S.E.M., with two-way ANOVA with Bonferroni post-hoc test.

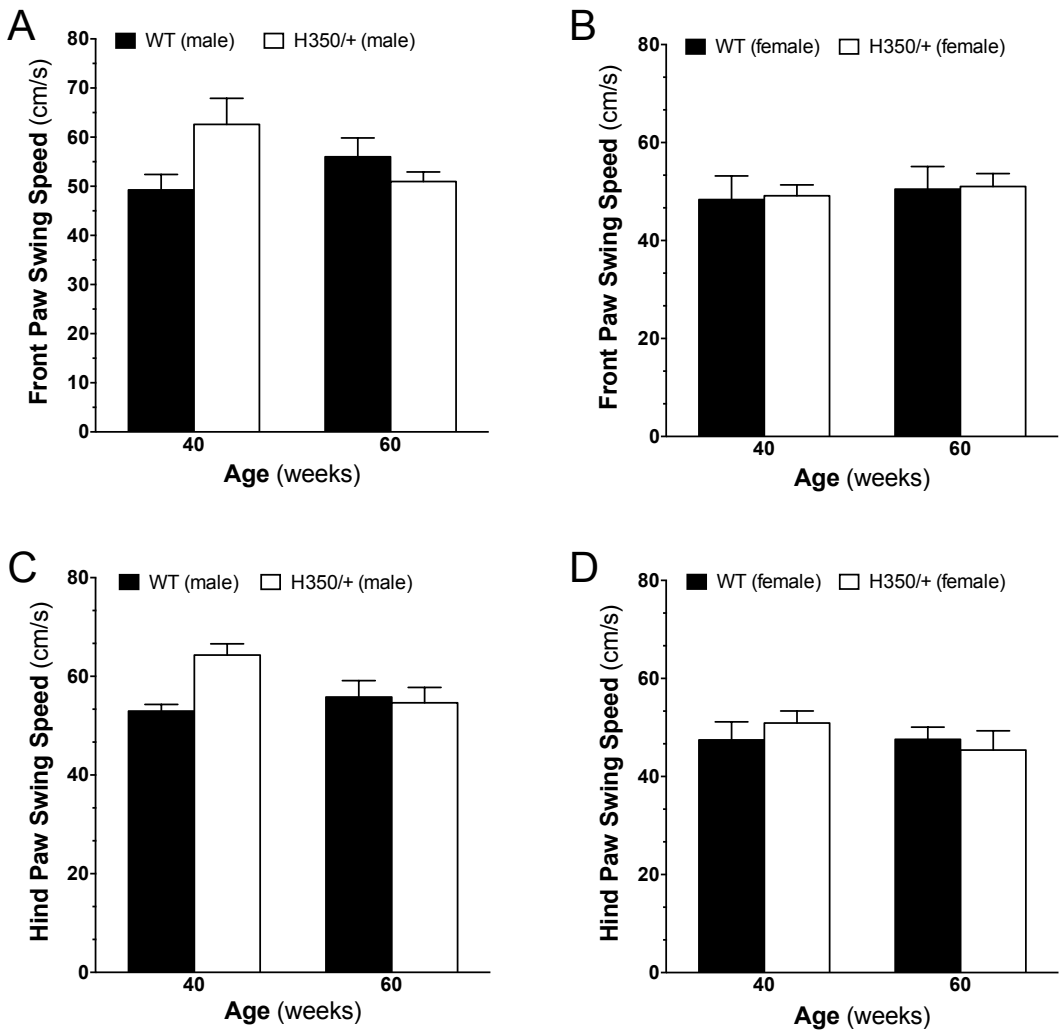

Supplementary Figure 2.3. HdhQ350/+ (A) males and (B) females had similar front paw swing speeds than their respective wild-type littermates at 40 and 60 weeks of age. HdhQ350/+ (C) males and (D) females had similar hind paw swing speeds than their respective wild-type littermates. N=6-8 for all groups. Error bars represent S.E.M., with two-way ANOVA with Bonferroni post-hoc test.

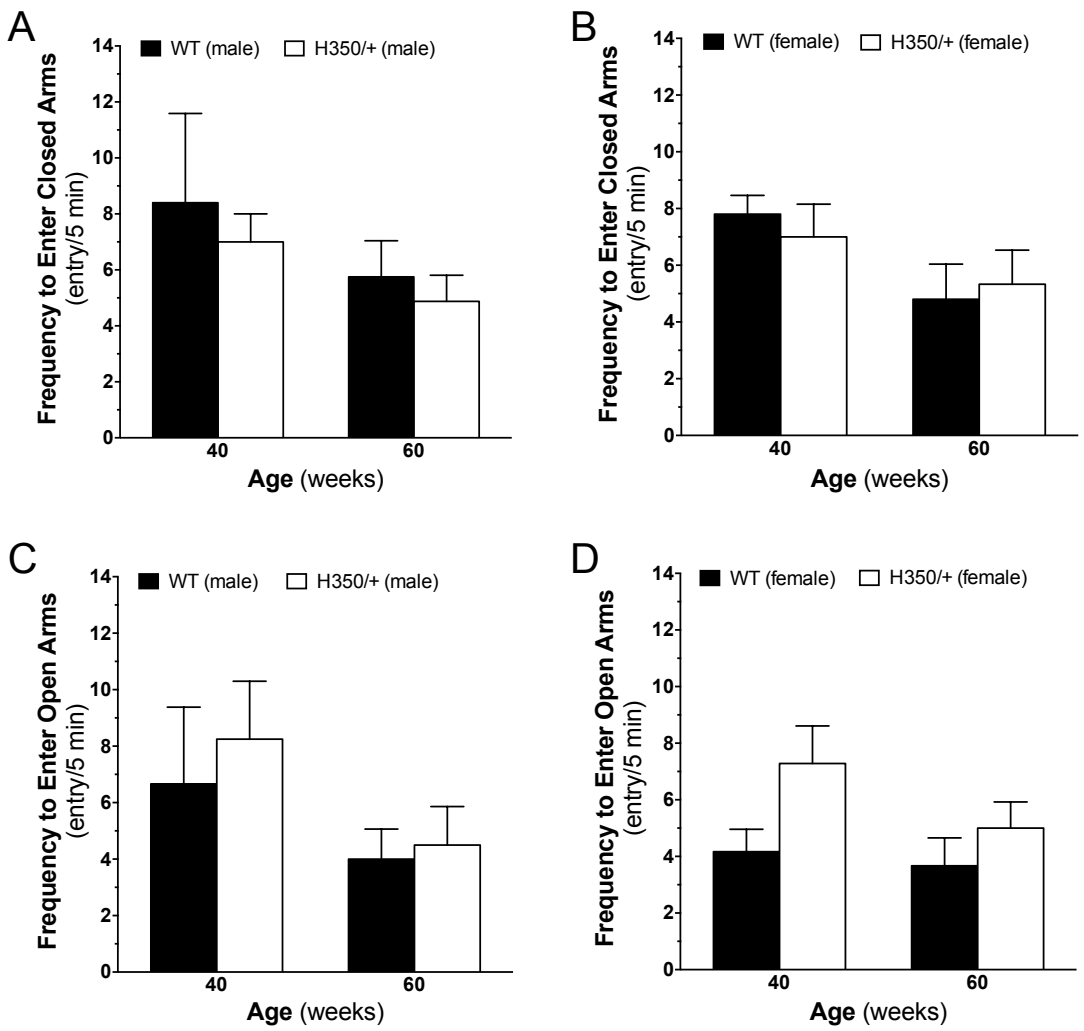

Supplementary Figure 2.4. HdhQ350/+ (A) males and (B) females had similar frequencies to enter the closed arms of the elevated plus maze than their respective wild-type littermates at 40 and 60 weeks of age. HdhQ350/+ (C) males and (D) females had similar frequencies to enter the open arms compared to their respective wild-type littermates. N=7-8 for all groups. Error bars represent S.E.M., with two-way ANOVA with Bonferroni post-hoc test.

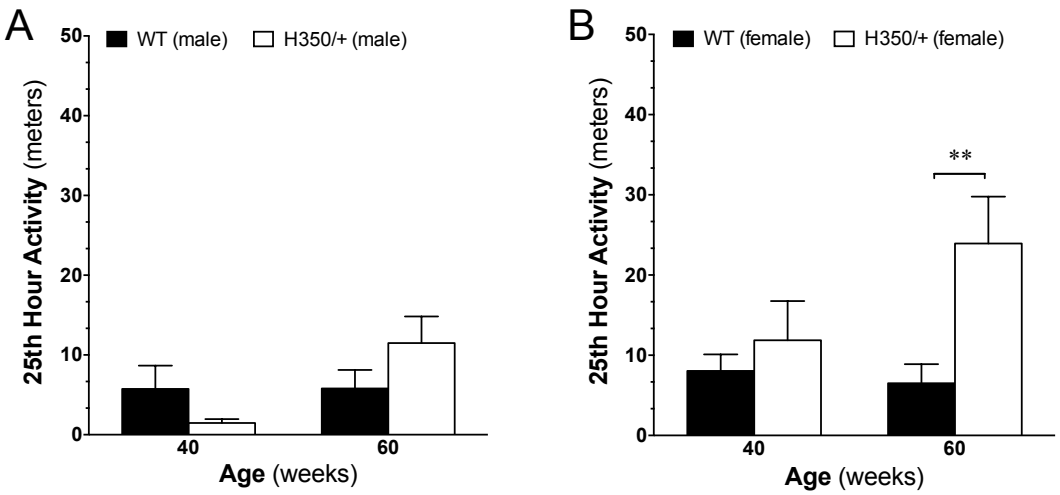

Supplementary Figure 2.5. Locomotor activity was measured at the 25th hour of being placed in the PhenoTyper chamber. (A) HdhQ350/+ male mice covered similar distances compared to male wild-type littermates but (B) female HdhQ350/+ mice covered more distance compared to female wild-type littermates. N=7-8 for all groups. Error bars represent S.E.M. and **p<0.01 with two-way ANOVA with Bonferroni post-hoc test.

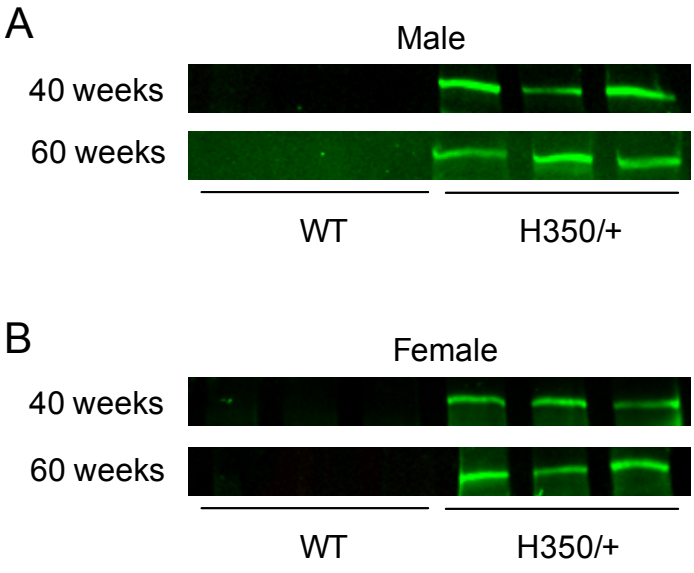

Supplementary Figure 2.6. Western blot of polyglutamine expansion at 40 and 60 weeks of age in (A) male and (B) female HdhQ350/+ mice compared to their respective wild-type littermates.

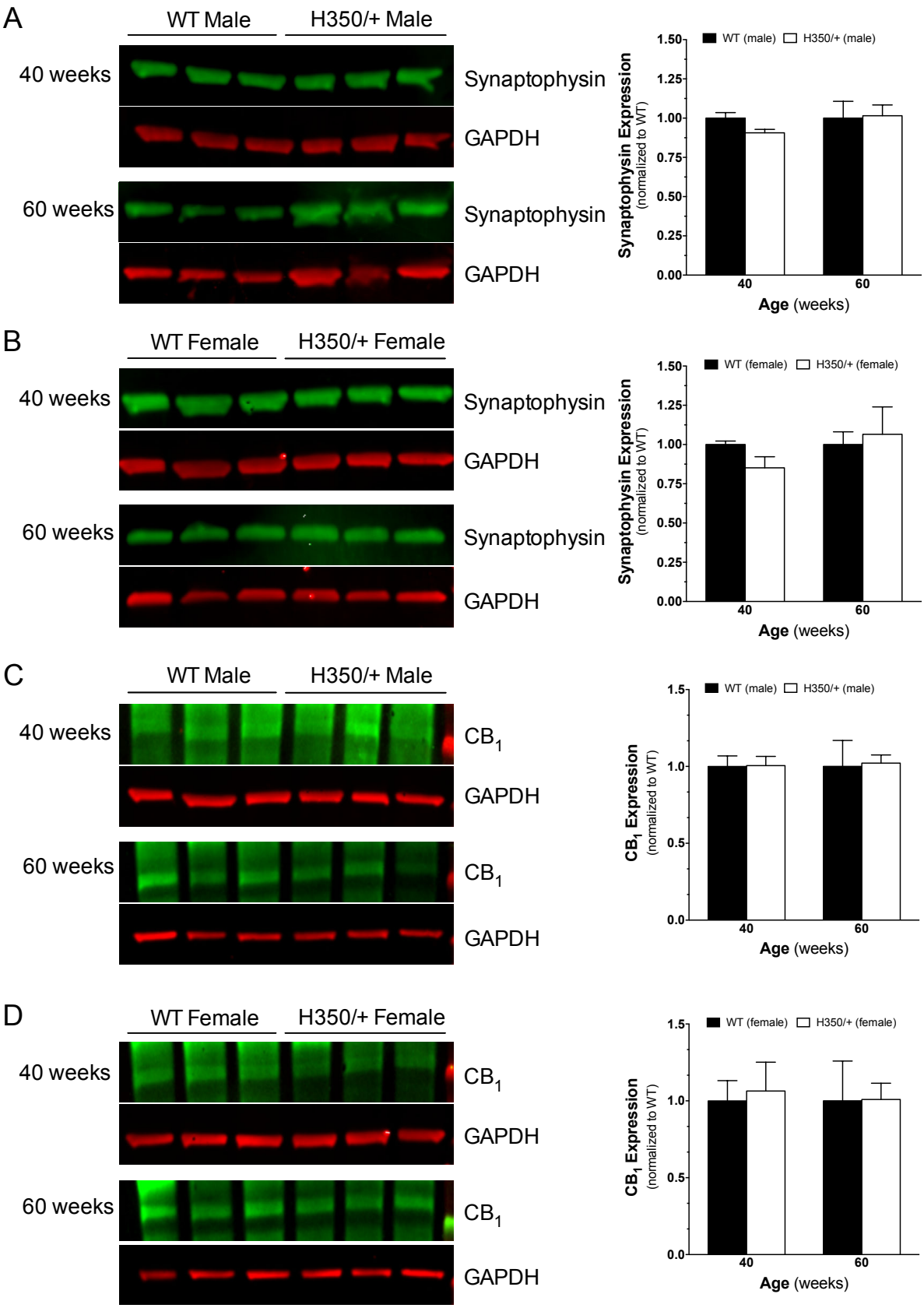
A
WT Male
H350/+ Male
40 weeks
Synaptophysin
GAPDH
60 weeks
Synaptophysin
GAPDH
WT (male)
H350/+ (male)
Synaptophysin Expression
(normalized to WT)
1.50
1.25
1.00
0.75
0.50
0.25
0.00
40
60
Age (weeks)
B
WT Female
H350/+ Female
40 weeks
Synaptophysin
GAPDH
60 weeks
Synaptophysin
GAPDH
WT (female)
H350/+ (female)
Synaptophysin Expression
(normalized to WT)
1.50
1.25
1.00
0.75
0.50
0.25
0.00
40
60
Age (weeks)
C
WT Male
H350/+ Male
40 weeks
CB1
GAPDH
60 weeks
CB1
GAPDH
WT (male)
H350/+ (male)
CB1 Expression
(normalized to WT)
1.5
1.0
0.5
0.0
40
60
Age (weeks)
D
WT Female
H350/+ Female
40 weeks
CB1
GAPDH
60 weeks
CB1
GAPDH
WT (female)
H350/+ (female)
CB1 Expression
(normalized to WT)
1.5
1.0
0.5
0.0
40
60
Age (weeks)

Supplementary Figure 2.7. Striatal western blot analysis of synaptophysin in (A) male and (B) female HdhQ350/+ and respective wild-type littermates at 40 and 60 weeks revealed no change in synaptophysin expression. Striatal western blot analysis of CB_1 in (C) male and (D) female HdhQ350/+ and respective wild-type littermates at 40 and 60 weeks revealed no change in CB_1 expression. Error bars represent S.E.M., with two-way ANOVA with Bonferroni post-hoc test.

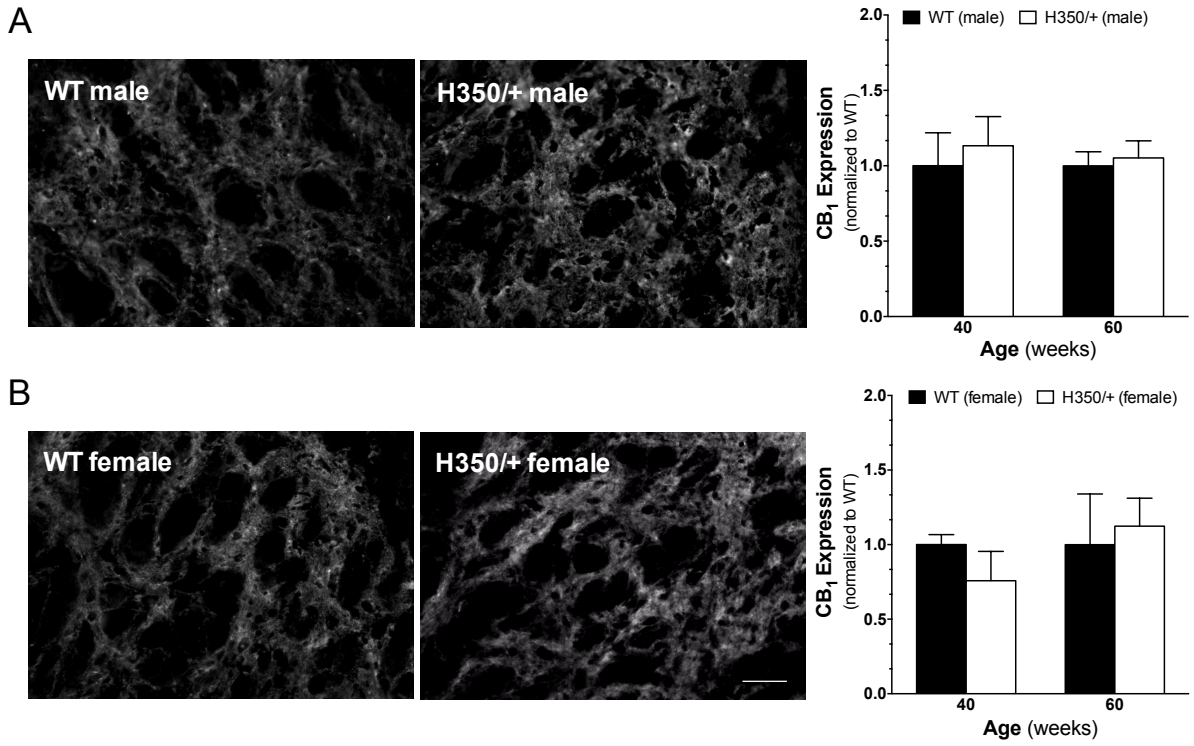

Supplementary Figure 2.8. Representative images of CB_1 immunoreactivity at 60 weeks of age. CB_1 was co-stained with enkephalin to assess for changes on the axon terminals of striatal cells into the globus pallidus. HdhQ350/+ (A) males and (B) females showed similar levels of CB_1 immunoreactivity compared to respective wild-type littermates. Scale bar denotes 50um. N=3 for all groups. Error bars represent S.E.M., with two-way ANOVA with Bonferroni post-hoc test.

Chapter III: Short-term ABHD6 Inhibition in the HdhQ200/200 Mouse Line to Treat Huntington's Disease

3.1 Overview and rationale

Despite the many promising neuroprotective qualities of cannabinoids, studies utilizing cannabinoid drugs, either phyto-derived or synthetic, have yielded ambiguous results in the treatment of HD. An early study in 2010 examined the chronic use of high doses of CB_1 agonists (THC or HU210) or a FAAH inhibitor (URB597) on R6/1 mice (Dowie et al., 2010). After 8 weeks of daily treatment, none of the drugs improved motor impairments. In fact, HU210-treated mice suffered an increase in seizure events and number of ubiquinated aggregates, suggesting a worsened pathology. Moreover, there was no impact on ligand binding of CB_1, D1, D2, serotonin 5HT-2A, or $GABA_A$ receptors. However, a study later in 2010 reported that HD progression was delayed by a chronic low dose of THC on R6/2 mice, rescuing motor impairment, striatal degeneration and aggregation number (Blazquez et al., 2010). THC also rescued neuronal markers GAD67, synaptophysin, PSD-95, and BDNF expression. Another study in 2014 reported that chronic, but not acute, treatment of the synthetic CB_1 agonist, WIN 55,212-2, rescued motor impairment and DARPP-32-positive cell loss in R6/1 mice (Pietropaolo et al., 2014). A more recent study in 2016 found that VCE-003.2, a cannabigerol quinone derivative, was able to rescue the loss of DARPP-32 neurons and reverse the upregulation of proinflammatory markers and microglial activation in toxin-induced mouse models of HD (Díaz-Alonso et al., 2016). VCE-003.2 also improved motor deficits. Taken together, these results demonstrate promising potential of utilizing cannabinoid-based therapeutics in treating HD, but also reveal a delicate treatment window.

ABHD6 is a *bona fide* member of the eCB signaling system and is an enzyme that hydrolyzes approximately 4% of total 2-AG hydrolysis, secondary to the main hydrolyzing enzymes MAGL and ABHD12 (Blankman et al., 2007). Our lab has demonstrated that ABHD6 inhibition protects against pentylenetetrazole-induced generalized tonic-clonic and myoclonic seizures, as well as spontaneous seizures in R6/2 mice through action on $GABA_A$ receptors (Naydenov, Horne, et al., 2014). This study suggests that ABHD6 inhibition indirectly reduces excitatory transmission, and in addition, treatment with ABHD6 inhibitors does not cause tolerance or receptor desensitization, important factors when considering cannabinoid therapeutics (Naydenov, Horne, et al., 2014). In addition, activation of CB_1 receptors via the increase in 2-AG has been shown to up-regulate pro-survival genes, such as BDNF, which is typically lost in HD (Marsicano et al., 2003; Roze et al., 2011). Therefore, we hypothesize that short-term ABHD6 inhibition in a reliable mouse model of HD will result in a delayed onset of select symptoms, through a reduction of excitotoxicity and up-regulation of neuroprotective markers, all factors influenced by cannabinoid signaling.

Although there are numerous mouse models of HD, none reliably replicate human behavioral symptoms and pathology. Key criteria include a mid-to-late age onset of behavioral symptoms, shortened lifespan by approximately 50-75%, measurable progressive motor impairments, preferential early loss of striatal neurons, expression of mHtt aggregates, and brain atrophy. We previously characterized the HdhQ350/+ mouse line, a mouse line that expresses one mutant copy of *Hdh*, the mouse homolog to *HTT,* containing a pathogenic 350 polyQs (Cao, Detloff, Gardner, & Stella, 2017). Because this mouse model genetically mirrors what occurs in HD, we believe that the HdhQ mouse model is a powerful, reliable model to examine effects of polyQ expansions on disease progression. We found that although the HdhQ350/+ mouse line

exhibited several classic symptoms, such as reduced weight, grip strength, motor coordination, and spontaneous locomotor activity, it did not exhibit pronounced neuropathology or a shortened lifespan. The HdhQ200/200 mouse line, a mouse homozygous for the expression of 200 polyQs, remains uncharacterized. We hypothesize that with two mutated copies of *Hdh*, the HdhQ200/200 mouse model will fulfill the criteria to reliably replicate human HD.

In this study, we aim to characterize the HdhQ200/200 mouse line based on criteria from previous HD models. We found significant behavioral and pathological deficits in HdhQ200/200 mice, primarily in female mice and prominently emerging at 10 months of age. We then sought out to explore if short-term ABHD6 inhibition could alleviate symptom severity and pathological development at 10 months of age, uncovering therapeutic potential in treating grip strength, motor coordination and spontaneous dark phase activity in the HdhQ200/200 mouse line.

3.2 Results

3.2.1 General phenotype of HdhQ200/200 mice: Life span, weight, grip strength

HdhQ200/200 mice were generated from breeding HdhQ200/+ by HdhQ200/+ mice, producing an average litter size of 7 pups, with roughly 20% homozygote, 41% heterozygote and 39% wild-type mice. This did not significantly deviate from the expected Mendelian ratio. HdhQ200/200 mice had a reduced life span of approximately 12 months of age; both males and females displayed overt signs of tremor, hunching, unsteady movements, and inactivity. We also observed a vastly significant reduction in weight between HdhQ200/200 mice and respective wild-type littermates at all tested time points (male: $F_{(1, 53)}=36.24$, $p<0.0001$; female: $F_{(1, 51)}=99.91$, $p<0.0001$) (Figure 3.1A, B). Post-hoc analyses revealed significant reduced weight at 12 months of age in male HdhQ200/200 mice and at all tested time points in female

HdhQ200/200 mice when compared to their respective wild-type littermates. Further analysis into a sex-dependent effect of reduced weight showed no difference between male or female HdhQ200/200 mice when weights were normalized to their respective wild-type littermates (Supplementary Figure 3.1A). These results show that both male and female HdhQ200/200 mice were equally affected by the mutation in weight when compared to wild-type littermates.

Mice were then assessed for muscle strength, as muscle atrophy is a common symptom in HD. We measured the latency to fall from an inverted wire cage top as a metric for limb grip strength. Male HdhQ200/200 mice did not have altered grip strength but female HdhQ200/200 mice showed a significant decrease, especially at 10 and 12 months of age ($F_{(1,\ 51)}$=28.71, p<0.0001) (Figure 3.1C, D). It is possible that the lack of body weight may be due to loss in muscle mass and strength, but unlikely since only female HdhQ200/200 mice showed loss of muscle strength while both sexes had reduced weight. Conclusively, these results show that only female HdhQ200/200 mice had an effect of the HdhQ mutation on limb grip strength.

3.2.2 Locomotor activity of HdhQ200/200 mice: Dark and light phase activities, exploration

HD patients often display sleep and circadian disruptions, including abnormal day-night ratios (Morton, 2013). Using the Noldus PhenoTyper, an automated home-cage monitoring system, we were able to measure daily patterns of locomotion over a 72-hour time period and found that both male and female HdhQ200/200 mice exhibited an overall decrease in spontaneous locomotion during the dark phase (when mice are active) (male: $F_{(1,\ 45)}$=15.89, p=0.001; female: $F_{(1,\ 41)}$=11.80, p=0.001) (Figure 3.1E, F). Post-hoc analysis revealed a significant decrease in spontaneous dark phase activity at 8 and 10 months of age in males, and at 6 months in females. When HdhQ200/200 animals were normalized to their respective wild-type littermates to investigate if there was a sex difference in this observation, we found that

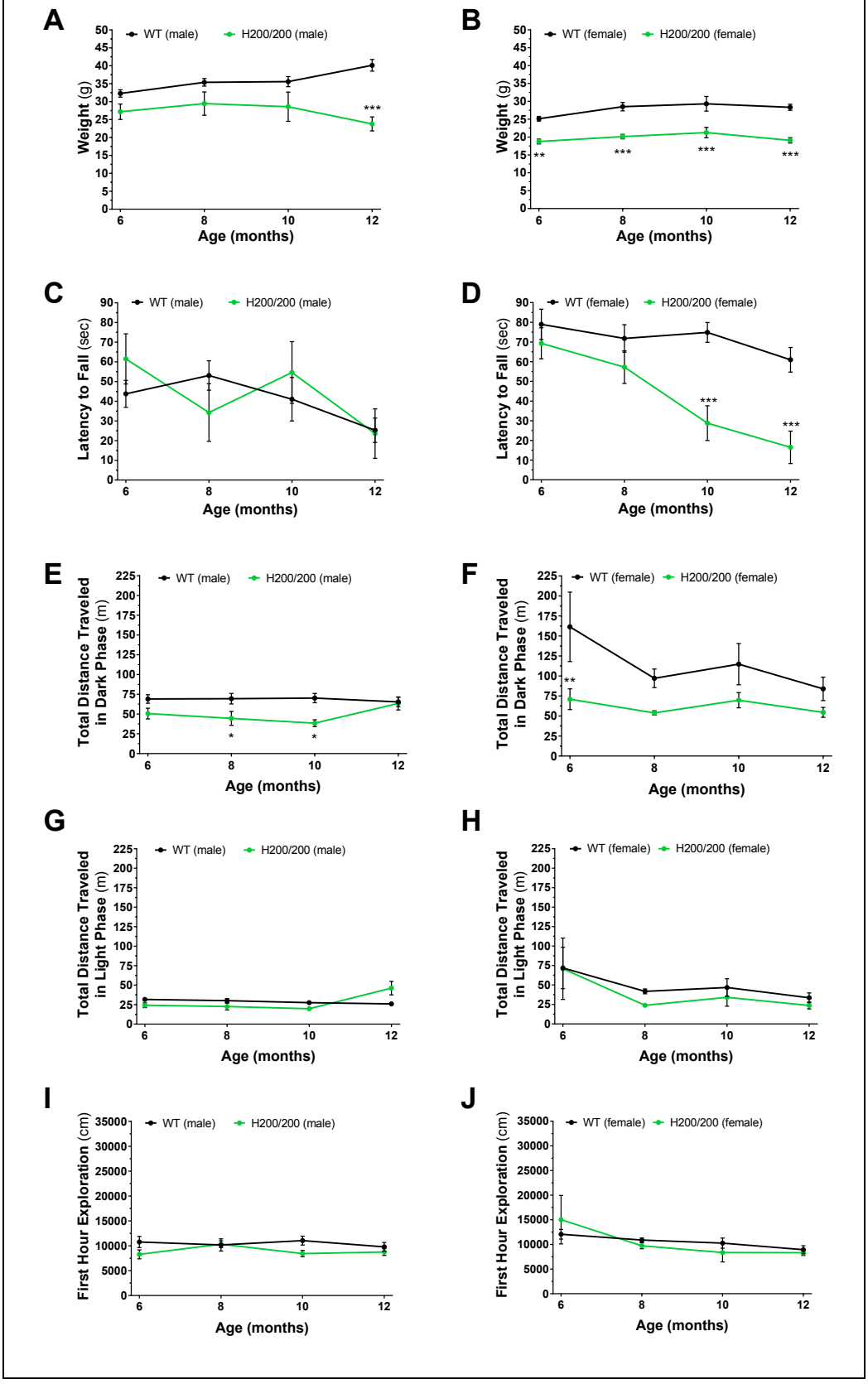
A
WT (male)
H200/200 (male)
Weight (g)
Age (months)
B
WT (female)
H200/200 (female)
Weight (g)
Age (months)
C
WT (male)
H200/200 (male)
Latency to Fall (sec)
Age (months)
D
WT (female)
H200/200 (female)
Latency to Fall (sec)
Age (months)
E
WT (male)
H200/200 (male)
Total Distance Traveled in Dark Phase (m)
Age (months)
F
WT (female)
H200/200 (female)
Total Distance Traveled in Dark Phase (m)
Age (months)
G
WT (male)
H200/200 (male)
Total Distance Traveled in Light Phase (m)
Age (months)
H
WT (female)
H200/200 (female)
Total Distance Traveled in Light Phase (m)
Age (months)
I
WT (male)
H200/200 (male)
First Hour Exploration (cm)
Age (months)
J
WT (female)
H200/200 (female)
First Hour Exploration (cm)
Age (months)

Figure 3.1. General behavioral phenotype of HdhQ200/200 male and female mice when compared to wild-type littermates from 6 to 12 months of age. (A) Male and (B) female HdhQ200/200 mice show reduced weight. (C) Male HdhQ200/200 mice did not show reduced grip strength. (D) Female HdhQ200/200 mice had reduced grip strength compared to female wild-type littermates. Both (E) male and (F) female HdhQ200/200 mice had reduced spontaneous dark phase locomotor activity but neither (G) male nor (H) female HdhQ200/200 mice had altered spontaneous light phase locomotor activity. (I) Male and (J) female HdhQ200/200 mice did not differ from wild-type littermates in exploratory activity. N=5-12 for all groups. Error bars represent S.E.M. and *p<0.05, **p<0.01, ***p<0.001 with two-way ANOVA with Bonferroni post-hoc test.

there was a significant effect between sexes in the loss of dark phase spontaneous locomotor activity, again showing that female HdhQ200/200 mice are more affected by the HdhQ mutation ($F_{(1,\ 41)}$=6.28, p=0.016) (Supplementary Figure 3.1B). Correspondingly, we analyzed the spontaneous locomotor activity during the light phase to see if there were any changes in animals' inactive phase and together with the dark phase results, if overall circadian rhythm was altered. We did not see any significant changes in the distance traveled in the light phase in either male or female HdhQ200/200 mice compared to their respective wild-type littermates at any age, indicating that activity abnormalities were exclusive to the dark phase (Figure 3.1G, H). Taken together, we found that although there were no changes in overall circadian rhythm, HdhQ200/200 animals had reduced spontaneous dark phase locomotor activity, with a more pronounced deficit in female HdhQ200/200 mice.

Locomotor activity in the first hour of being placed into the PhenoTyper chamber was used to assess for exploration and interest of a novel environment. This may allude to cognitive and psychiatric deficits, such as apathy or loss of curiosity. There was an effect of the HdhQ200/200 mutation in male HdhQ200/200 mice, with reduced distance in exploration of an

unfamiliar environment over time ($F_{(1, 43)}$=4.429, p=0.041) (Figure 3.1I). Conversely, female HdhQ200/200 mice did not differ in their exploratory behavior when compared to female wild-type littermates (Figure 3.1J). This data shows that male HdhQ200/200 mice exclusively show apathy and reduced curiosity, indications of psychiatric and cognitive impairments, in exploration of a novel environment.

3.2.3 Motor behavior of HdhQ200/200 mice: Motor coordination

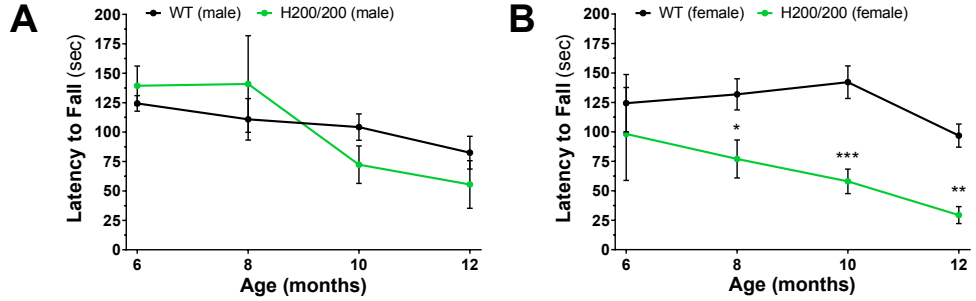

Figure 3.2. Motor coordination is affected in female, but not male, HdhQ200/200 mice. (A) Male HdhQ200/200 mice did not differ from male wild-type littermates in their latency to fall. (B) Female HdhQ200/200 mice had significantly reduced latency to fall. N=4-10 for all groups. Error bars represent S.E.M. and *p<0.05, **p<0.01, ***p<0.001 with two-way ANOVA with Bonferroni post-hoc test.

Impaired motor coordination is a classic symptom in HD patients as well as other HD animal models. Motor coordination was measured on an accelerating rotarod by comparing the daily averages of an animal's latency to fall over 7 trials from 6 to 12 months of age. Male HdhQ200/200 mice did not differ in their average latency to fall when compared to male wild-type littermates by two-way ANOVA analysis, whereas female HdhQ200/200 mice exhibited a significant decrease in motor coordination compared to female wild-type littermates ($F_{(1, 39)}$=26.57, p<0.0001) (Figure 3.2A, B). Post-hoc analysis revealed a significant decrease in motor coordination at 8, 10 and 12 months of age in female HdhQ200/200 mice. These results indicate

that only female, but not male, HdhQ200/200 mice have significantly impaired motor coordination.

3.2.4 Neuropathology of HdhQ200/200 brains: Medium spiny neurons and neuronal markers

We used semi-quantitative immunohistochemistry to investigate the neuropathology of HdhQ200/200 mice and if behavioral impairments correlated with disrupted protein expression of classic neuropathological markers of HD pathogenesis. We focused on 10 months of age, as this was the age where behavioral impairments were most significant across multiple symptoms. We assessed for downregulation of DARPP-32 expression, a dopamine- and cAMP-regulated neuronal phosphoprotein found in MSNs of the striatum. Interestingly, we found a significant decrease in DARPP-32 expression in male, but not female, HdhQ200/200 mice when compared to their respective wild-type littermates (male: p=0.018; female: p=0.083) (Figure 3.3A, B). While we did not uncover any changes in striatal synaptophysin expression (Supplementary Figure 3.2A, B), a key component of presynaptic machinery for neurotransmitter release that is known to be decreased in HD, we found approximately 2x decrease in CB_1 expression in the globus pallidus in female, but not male, HdhQ200/200 mice at 10 months of age (p=0.018) (Figure 3.3C, D) (Goto & Hirano, 1990). We were specifically targeting the CB_1 receptor population located on the axon terminals of MSNs that are part of the indirect pathway and project to the globus pallidus, as these presynaptic G protein-coupled receptors are known to be lost early in HD patients and animal models (Glass et al., 1993; Horne et al., 2012; Naydenov, Sepers, et al., 2014). To identify this population, we co-stained for enkephalin, a marker for the globus pallidus. Interestingly, we also saw an approximate 2x reduction in enkephalin expression in only female, but not male, HdhQ200/200 mice (p=0.019) (Figure 3.3E, F). We next analyzed protein expression of vGLUT2 (vesicular glutamate transporter 2) and vGAT (vesicular GABA

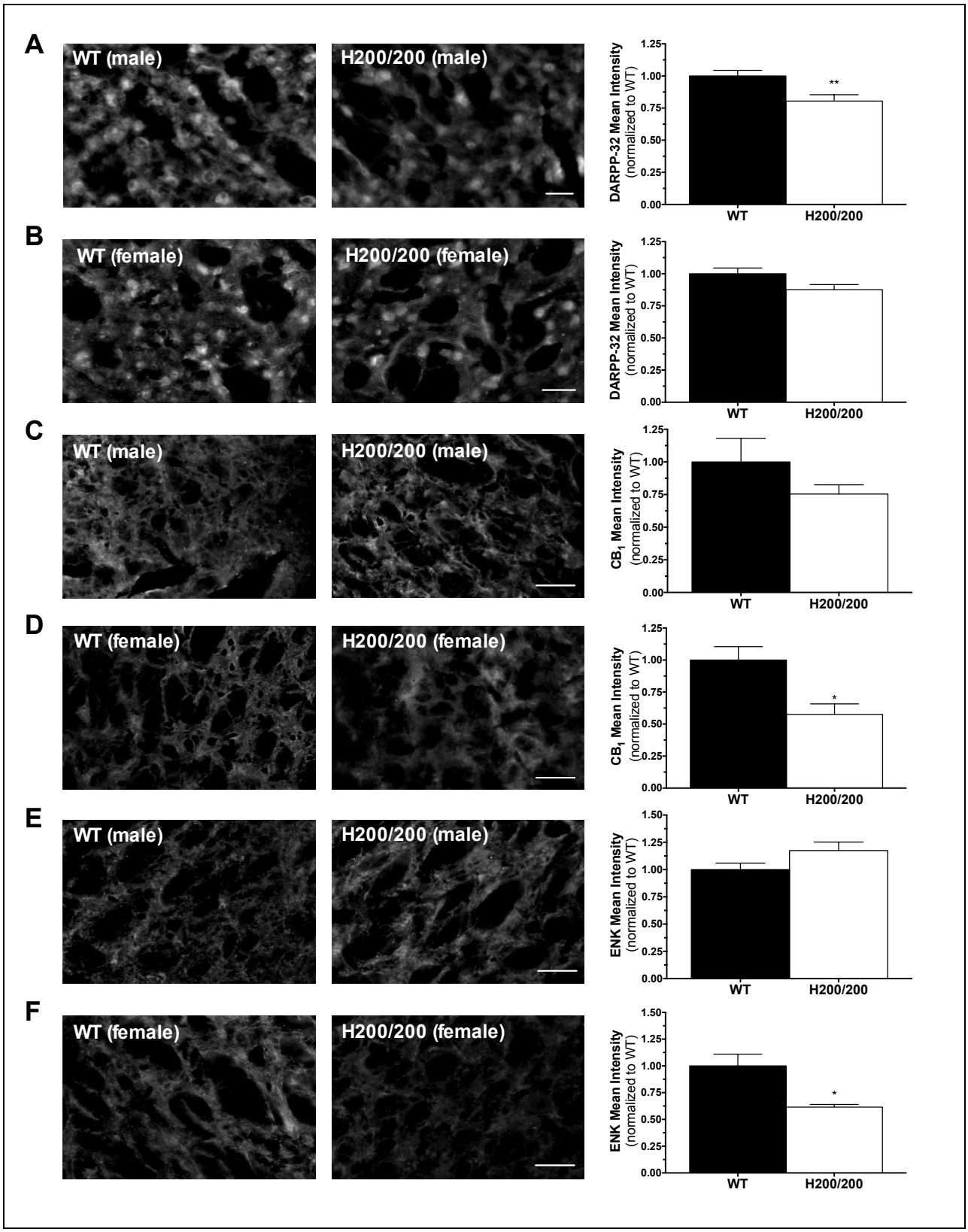
A
WT (male)
H200/200 (male)
DARPP-32 Mean Intensity (normalized to WT)
1.25
1.00
0.75
0.50
0.25
0.00
**
WT
H200/200
B
WT (female)
H200/200 (female)
DARPP-32 Mean Intensity (normalized to WT)
WT
H200/200
C
WT (male)
H200/200 (male)
CB1 Mean Intensity (normalized to WT)
WT
H200/200
D
WT (female)
H200/200 (female)
CB1 Mean Intensity (normalized to WT)
*
WT
H200/200
E
WT (male)
H200/200 (male)
ENK Mean Intensity (normalized to WT)
1.50
1.25
1.00
0.75
0.50
0.25
0.00
WT
H200/200
F
WT (female)
H200/200 (female)
ENK Mean Intensity (normalized to WT)
*
WT
H200/200

Figure 3.3. HdhQ200/200 mice show sex-dependent neuropathology at 10 months of age. (A) Male, but not (B) female, HdhQ200/200 mice had a reduction in DARPP-32 expression in the dorsolateral striatum. Representative images were captured at 40x and scale bar denotes 10um. (C) Male HdhQ200/200 mice did not have a significant change in CB_1 expression on MSN axon terminals. (D) Female HdhQ200/200 mice had a significant reduction in CB_1 expression. While (E) male HdhQ200/200 mice did not have a significant change in enkephalin expression in the globus pallidus, (F) female HdhQ200/200 mice showed a significant reduction. Representative images were captured at 20x and scale bar denotes 50um. N=4-5 for all groups. Error bars represent S.E.M. and *p<0.05, **p<0.01 with Student's T-Test.

transporter), to examine synaptic integrity in the striatum. Curiously, we did not see any significant differences across genotypes in either male or female mice (Supplementary Figure 3.3A-D) but did observe a significant decrease in PSD-95 expression in the dorsolateral striatum in female, but not male, HdhQ200/200 mice (p=0.031) (Figure 3.4A, B), indicating a specific, but not generalized, loss in synaptic protein expression. Taken together, these results show a sex difference in several key protein expressions commonly dysregulated in HD at 10 months of age in the HdhQ200/200 mouse model.

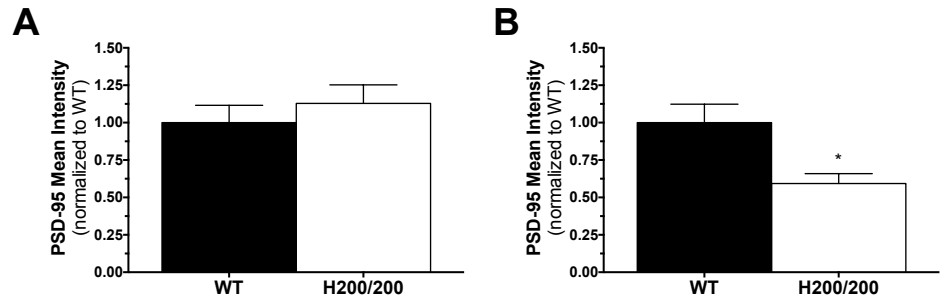

Figure 3.4. Female, but not male, HdhQ200/200 mice have reduced synaptic protein expression in the dorsolateral striatum. (A) Male HdhQ200/200 mice show similar levels of PSD-95 expression. (B) Female HdhQ200/200 mice have reduced expression of PSD-95 at 10 months of age. N=4-5 for all groups. Error bars represent S.E.M. and *p<0.05, with Student's T-Test.

3.2.5 Intracellular calcium dynamics of corticostriatal connection

We next wanted to know if there were physiological, functional abnormalities in corticostriatal connectivity and MSN excitability in the HdhQ200/200 mouse line. Previous work has shown that there is disrupted neuronal activity in multiple HD mouse models, including synaptic dysfunction, altered calcium regulation and MSN hyperexcitability (Miller & Bezprozvanny, 2010; Raymond, 2017). Using *in vivo* electrophysiology and calcium imaging, we aimed to determine if MSN excitability in the HdhQ200/200 mouse line was reflected in alterations of activity-dependent calcium dynamics. This is a novel approach to exploring HD pathogenesis. We used 8-month-old female mice, since female HdhQ200/200 exhibited a more severe phenotype and we wanted to observe physiological changes prior to overt symptom onset. A fiber-optic confocal microscope was used to visualize fluorescence from the genetically-encoded calcium indicator GCaMP6m in the dorsal striatum in response to electrical stimulation

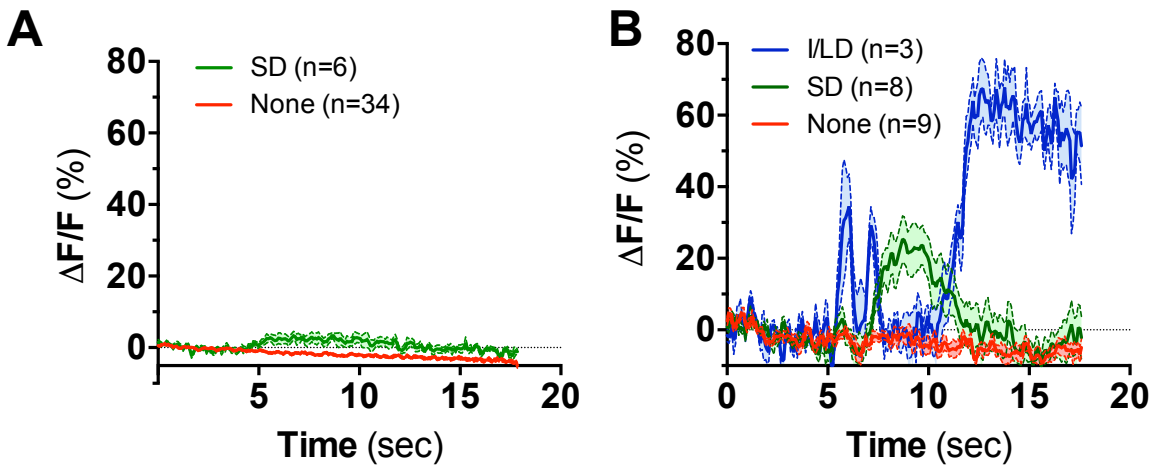

Figure 3.5. HdhQ200/200 mice display abnormal MSN activity in response to cortical stimulation at 8 months of age. Average fluorescence changes (±S.E.M.) in striatal MSNs, reflecting changes in intracellular calcium concentrations, of (A) wild-type or (B) HdhQ200/200 female mice after cortical stimulation at 8 months of age. N=3-4 for all groups.

of the motor cortex in order to study the integrity of the corticostriatal circuit. Fluctuations in fluorescence reflect calcium concentration changes and indicate neuronal activity. Upon stimulation of the motor cortex of 8-month-old wild-type female mice, we observed either no response from MSNs (None, n=34/40) or a short-delayed response (SD, n=6/40) of an increase in 5% calcium fluorescence (Figure 3.5A). This differed greatly from the response we received from HdhQ200/200 female mice. We interestingly observed three distinct response profiles; no response (None, n=9/30), a short-delayed response (SD, n=7/30) or an immediate response followed by a late-delayed response (I/LD, n=3/30) (Figure 3.5B). The SD response in HdhQ200/200 mice was of much greater amplitude compared to wild-type mice, reaching nearly 30% ΔF/F, suggesting hyperexcitability. In addition, the unusual profile of the I/LD response further supports that HdhQ200/200 mice have abnormal calcium dynamics. The response peaks at nearly 70% ΔF/F, again suggesting an augmented response and hyperexcitability. This data suggests that there are severe disturbances, specifically hyperexcitability and abnormal calcium handling, in the corticostriatal connection in HdhQ200/200 mice in as early as 8 months of age, prior to prominent symptom onset.

Based on our behavioral and pathophysiological findings, we established that the HdhQ200/200 mouse line is a reliable model to explore potential therapeutics in treating HD.

3.2.6 Short-term inhibition of ABHD6 in HdhQ200/200 mice at 10 months of age

We next wanted to test if short-term inhibition of the hydrolyzing enzyme ABHD6 could improve behavioral symptoms at 10 months of age in the HdhQ200/200 mouse line. We hypothesized that inhibition of ABHD6 would increase 2-AG levels and increase activation of CB_1 signaling, rescuing behavioral and pathological symptoms we characterized above. Mice were surgically implanted with a miniature osmotic pump containing KT-182, a systemic

irreversible carbamate inhibitor, in the subcutaneous flank (Hsu et al., 2013). KT-182 is able to cross the blood-brain-barrier and administration via osmotic pumps has yet to be done, so we validated our delivery method with activity-based protein profiling (ABPP) with HT-01 and confirmed with fluorophosphonaterhodamine (FP-Rh), which are broad-spectrum and tailored SH activity-based probes previously described (Hsu et al., 2012). Results showed that there was complete ABHD6 activity inhibition in the brain in wild-type mice after 7 days of KT-182 administration via osmotic pumps (Figure 3.6). Inhibition was specific to ABHD6, as activities of other eCB enzymes (DAGLα, DAGLβ and FAAH) were not inhibited. There was also no ABHD6 activity in blood samples (data not shown). In addition, we did not observe any overt physical or behavioral side effects due to KT-182. These results show that we were able to achieve complete inhibition of ABHD6 in the brain through osmotic pump delivery without any psychotropic side effects.

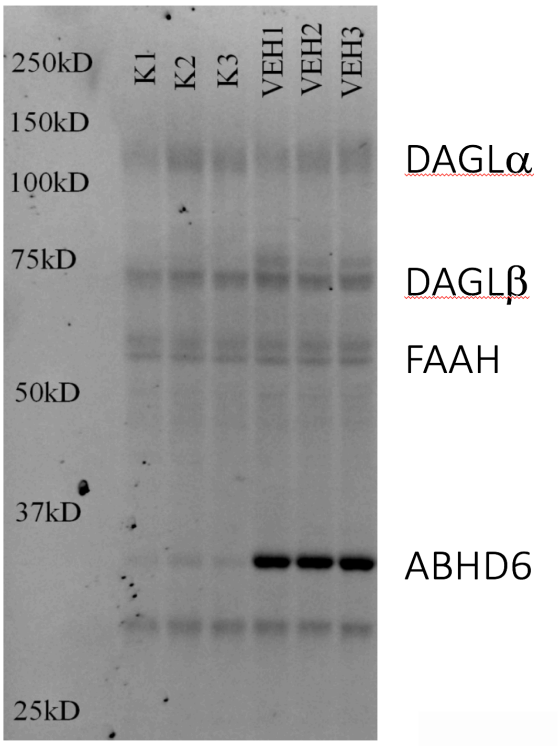

Figure 3.6. ABHD6 is inhibited after one week of treatment. Using ABPP, HT-01 analysis of wild-type mice implanted with osmotic pumps containing KT-182 or vehicle for one week showed inhibition of ABHD6 activity in brain samples. Other eCB enzymes were unaffected by KT-182 treatment.

After validation, we implanted osmotic pumps in male and female HdhQ200/200 mice and wild-type littermates at 10 months of age. After 4 days of continuous administration of 2mg/kg KT-182, mice were placed into PhenoTyper chambers to assess for

spontaneous locomotion, then tested for grip strength and motor coordination. Animals were subsequently sacrificed for neuropathological analysis after a total of 7 days of continuous dosing.

Spontaneous locomotor activity in the PhenoTyper was used to analyze animals' dark and light phase activity and to test if KT-182 treatment is able to alleviate locomotor impairments in the HdhQ200/200 mouse. As expected, KT-182 treatment had no effect on wild-type male or female mice in their dark phase activity at 10 months of age (Figure 3.7A, B). Interestingly, we saw a trend towards decreased locomotor activity in male HdhQ200/200 mice but a trend towards increased locomotor activity in female HdhQ200/200 mice after KT-182 treatment (male: $p=0.324$; female: $p=0.305$) (Figure 3.7A, B). More animals are needed to determine if there is a significant effect of short-term KT-182 treatment and if there is a sex-dependent effect of KT-182 on locomotor activity. While we saw no effect of KT-182 treatment on light phase activity in female wild-type and male and female HdhQ200/200 mice, we curiously saw a significant decrease in wild-type male mice ($p=0.024$).

Locomotor activity in the first hour of being in the PhenoTyper chamber was used as a measurement of exploration of a novel environment. Short-term KT-182 treatment at 10 months of age did not alter exploration in either HdhQ200/200 or wild-type mice of either sex (Figure 3.7E, F). Again, more animals are needed, as the vehicle-treated HdhQ200/200 males and females had higher exploration when compared to the untreated HdhQ200/200 animals in the data previously described (Figure 3.1I, J), suggesting that the animals selected for the vehicle-treated group did not have a pronounced disease phenotype. Taken together, these results suggest that short-term ABHD6 inhibition may alleviate locomotor activity in only female HdhQ200/200 mice but further testing is required.

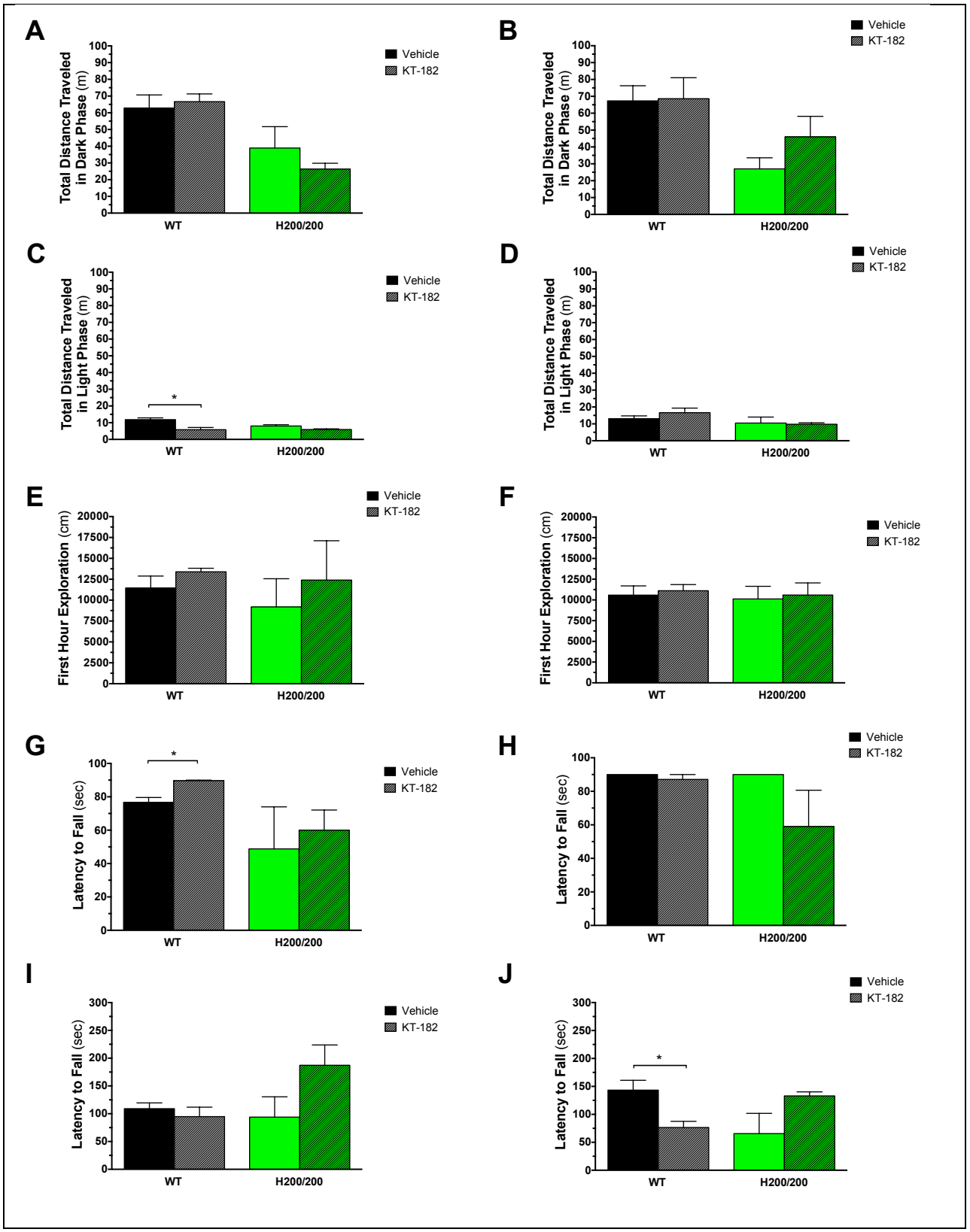
A
Total Distance Traveled in Dark Phase (m)
Vehicle
KT-182
WT
H200/200
B
Total Distance Traveled in Dark Phase (m)
Vehicle
KT-182
WT
H200/200
C
Total Distance Traveled in Light Phase (m)
*
Vehicle
KT-182
WT
H200/200
D
Total Distance Traveled in Light Phase (m)
Vehicle
KT-182
WT
H200/200
E
First Hour Exploration (cm)
Vehicle
KT-182
WT
H200/200
F
First Hour Exploration (cm)
Vehicle
KT-182
WT
H200/200
G
Latency to Fall (sec)
*
Vehicle
KT-182
WT
H200/200
H
Latency to Fall (sec)
Vehicle
KT-182
WT
H200/200
I
Latency to Fall (sec)
Vehicle
KT-182
WT
H200/200
J
Latency to Fall (sec)
*
Vehicle
KT-182
WT
H200/200

Figure 3.7. Short-term ABHD6 inhibition rescues select behavioral impairments in HdhQ200/200 mice at 10 months of age. KT-182 treatment did not increase spontaneous dark phase locomotor activity in (A) male, but did in (B) female HdhQ200/200 mice. Spontaneous light phase locomotor activity was unchanged in (C) male and (D) female wild-type and HdhQ200/200 mice. Exploratory activity was unaffected by KT-182 treatment in both (E) male and (F) female HdhQ200/200 mice. (G) Male, but not (H) female wild-type and HdhQ200/200 mice had increased grip strength when treated with KT-182 over vehicle control groups. KT-182 treatment shows genotype-dependent increase in motor coordination in both (I) male and (J) female HdhQ200/200 mice. N=2-5 for all groups. Error bars represent S.E.M. and *p<0.05 with Student's T-Test.

Preliminary results indicate that short-term KT-182 treatment may have a sex-dependent effect on grip strength. Short-term KT-182 treatment increased the latency to fall in wild-type males over vehicle-treated males (p=0.046) but this trend has yet to be significant in HdhQ200/200 males (p=0.678) (Figure 3.7G). Curiously, we saw a trend towards decreased grip strength due to KT-182 treatment in female HdhQ200/200 mice; however, the vehicle-treated HdhQ200/200 female mice contrasts with the previously described data on HdhQ200/200 females and did not show any grip strength deficits, again suggesting that these control animals did not have the expected disease phenotype (Figure 3.1D, 3.7H). KT-182-treated HdhQ200/200 female mice did have a trend towards an increased score over untreated HdhQ200/200 females as previously described (Figure 3.1D). Wild-type females showed no difference between vehicle- and KT-182-treated groups (Figure 3.7H). These preliminary results suggest some positive effect of KT-182 treatment on grip strength; however, more animals are required for further testing.

Short-term KT-182 treatment may have a genotype-dependent effect on motor coordination, as measured by an accelerating rotarod. Wild-type male mice were unaffected by KT-182 treatment, as they had similar latencies to fall as vehicle-treated wild-type male mice (Figure 3.7I). Male HdhQ200/200 mice treated with KT-182 showed a trend of a 99.2% increase in

latency before falling on the rotarod, however this has yet to reach significance and more animals are needed (p=0.138) (Figure 3.7I). Female wild-type mice, conversely, were significantly affected by KT-182 treatment, with a reduction of 46.6% in motor coordination (p=0.032) (Figure 3.7J). As hypothesized, HdhQ200/200 female mice appear to be positively affected by short-term KT-182 treatment, with an increase of 102.9% in motor coordination over vehicle-treated HdhQ200/200 female and rescued to similar levels as the vehicle-treated wild-type females; however, this has yet to reach significance (p=0.10) (Figure 3.7J). Thus far, these data indicate that short-term ABHD6 inhibition is able to increase motor coordination in male and female HdhQ200/200 mice, with more animals needed in the study.

3.3 Discussion

In the present work, we report a longitudinal description of the HdhQ200/200 mouse line, showing early onset of select behavioral impairments, loss of key neuronal markers and a reduced lifespan. We show that the HdhQ200/200 mouse line reliably replicates HD. Both male and female HdhQ200/200 mice failed to gain as much weight as their respective wild-type littermates, and male and female HdhQ200/200 mice had significantly decreased spontaneous dark phase locomotor activity, with female HdhQ200/200 mice more severely affected. Interestingly, only female HdhQ200/200 mice also had significantly reduced motor coordination and grip strength, and only male HdhQ200/200 mice had reduced exploratory activity. We used sqIHC to examine HD-specific pathology at 10 months of age and found that although only male HdhQ200/200 exhibited DARPP-32 loss, female HdhQ200/200 mice showed significant loss of CB_1 receptors, enkephalin and PSD-95. We then used *in vivo* intracellular calcium imaging to investigate neuronal hyperexcitability in the corticostriatal circuit, a system severely affected in

HD. We found several aberrant neuronal responses, suggesting aberrant MSN calcium handling following cortical stimulation and an impaired corticostriatal connection.

Dissociation between behavioral deficits and pathology is well established in HD animal models; previous work in other mouse models and other HdhQ mouse lines have also revealed this, such as in the HdhQ350/+ model (Cao et al., 2017). In this study, we did not find strong correlations between key behavioral symptoms and pathological abnormalities in the HdhQ200/200 mouse line. We expected to find pathological disease development followed by a decline in behavioral symptoms in both male and female HdhQ200/200 mice. While we found prominent behavioral symptoms in HdhQ200/200 female mice as reviewed above, we only found loss of DARPP-32 expression in male HdhQ200/200 mice at 10 months of age. Although the striatum suffers catastrophic neuronal loss in HD, there is also brain atrophy found in the cerebral cortex, subcortical white matter, thalamus, and hypothalamus in HD patients (Rosenblatt et al., 2006). Brain atrophy in HdhQ200/200 females may be occurring in regions other than the striatum, such as a globus pallidus as evidenced by the decrease in encephalin expression and further studies may support this.

We were able to reveal a functional deficit in corticostriatal connectivity, as evidenced by the *in vivo* intracellular calcium imaging in as early as 8 months old despite not finding widespread changes in synaptic protein expression in HdhQ200/200 mice at 10 months of age. In addition, the lack of cellular loss suggests that behavioral and network abnormalities are due to cellular dysfunction rather than direct atrophy (Figure 3.3B). The diverse and exaggerated responses of MSNs, specifically in the SD and I/LD profiles, after motor cortex stimulation indicate aberrant calcium handling, MSN hyperexcitability and corticostriatal dysfunction in the HdhQ200/200 mouse (Figure 3.5B). This early dysfunction may contribute to the behavioral

deficits seen with the rotarod, as motor control relies heavily on the corticostriatal pathway (Shepherd, 2013). Previous HD mouse models have shown progressive disconnection between the cortex and striatum due to disease progression, such as enhanced glutamate release, and recent work has begun to investigate into the role of calcium in this dysregulation (Cepeda, Wu, André, Cummings, & Levine, 2007; Raymond, 2017). Several lines of evidence point to gain-of-function roles of mHtt; mHtt has been found to directly bind to IP_3R1, the calcium release channel critical in modulating intracellular concentrations of calcium, and augment its activity, leading to glutamate-induced apoptosis in cultured MSNs from YAC128 mice (Miller & Bezprozvanny, 2010). In addition, mHtt increases expression of exNMDA receptors, in which activation of these receptors leads to enhanced cell death pathways (Raymond, 2017). Increased NMDA receptors would increase calcium influx due to activation from elevated glutamate transmission. It would be interesting to examine if the HdhQ200/200 mouse line exhibits increased exNMDA receptors and if that contributes to the aberrant calcium response that we observed. Lastly, mHtt disrupts a cell's homeostatic calcium buffering abilities through alterations of mitochondria function and calcium-binding proteins (Raymond, 2017). Nevertheless, it is clear that the HdhQ200/200 mouse line exhibits calcium dysregulation and that it could play a large role in cellular dysfunction and consequently behavioral impairments in HD.

Preliminary work into the effectiveness of continuous, short-term treatment of the novel ABHD6 inhibitor, KT-182, shows potential in alleviating certain symptoms of HD in the HdhQ200/200 mouse model. Although it would be most beneficial to start treatment prior to symptom onset in patients, we attempted to treat HdhQ200/200 mice at 8 months of age but were unable to establish large enough behavioral deficits between drug- and vehicle-treated groups at

this early stage of disease development. Therefore, we chose 10 months as an age with more pronounced symptoms to study the effectiveness of KT-182. Although we saw conversing trends between male and female HdhQ200/200 mice in regard to dark phase locomotor activity, we saw overall trends in KT-182 treatment increasing exploration, grip strength and motor coordination in HdhQ200/200 male mice over vehicle-treated HdhQ200/200 male mice. KT-182 treatment showed trends of increased dark phase locomotor activity, exploration, and motor coordination in HdhQ200/200 female mice over vehicle-treated HdhQ200/200 female mice. Curiously, we saw an increase in grip strength in vehicle-treated female HdhQ200/200 mice over untreated female HdhQ200/200 mice from the previously described data at 10 months of age (Figure 3.1D, 3.7H), suggesting that animals selected for the vehicle control group had not sufficiently progressed in the disease state. This could confound our results. In addition, osmotic pump implantation may impact overall general activity in mice, as most vehicle-treated groups (including wild-type mice) had overall reduced activity in the PhenoTyper when compared to untreated mice from the previously described data (Figure 3.1E, F, 3.7A, B). More animals with a full disease phenotype will be needed in the vehicle-treated group for accurate conclusions on the effectiveness of short-term KT-182 treatment in HdhQ200/200 mice.

Our results suggest that ABHD6 inhibition may recover several key behavioral deficits in the HdhQ200/200 mouse but it remains unclear what the effect of ABHD6 is on the pathology of HD. ABHD6 inhibition is expected to increase available 2-AG and enhance CB_1 signaling. We hypothesize that this will influence several classical HD markers detailed in this study. Recent work by our lab has shown that rescue of CB_1 receptors in the R6/2 mouse is able to rescue several HD markers (Naydenov, Sepers, et al., 2014). Although DARPP-32, synaptophysin, enkephalin, and PSD-95 are not directly involved with CB_1 signaling, these markers may be

rescued due to other neuroprotective actions mediated by CB_1 and would affect behavioral phenotypes. Additional proteins regulated by CB_1 signaling, such as BDNF, are expected to increase. BDNF is typically lost in HD patients (Roze et al., 2011). It is critical for neuronal support and has also been found to protect against toxic exNMDA receptor signaling by rescuing HD-like mitochondrial dysfunction (Lau, Bengtson, Buchthal, & Bading, 2015; Marsicano et al., 2003). Analysis into the striatal pathological changes induced by ABHD6 inhibition would give us insight into the therapeutic profile of inhibiting this enzyme.

In summary, we show that the HdhQ200/200 mouse line reliably replicates key aspects of HD. Along with behavioral symptoms and pathological development, we also show that the HdhQ200/200 mouse line exhibits disrupted corticostriatal connection with abnormal calcium handling and evidence of MSN hyperexcitability. Using the HdhQ200/200 mouse line as a more accurate model for HD, we explore the potential of utilizing the eCB system for treatment, with preliminary data suggesting great promise in alleviating behavioral symptoms.

3.4 Supplementary figures

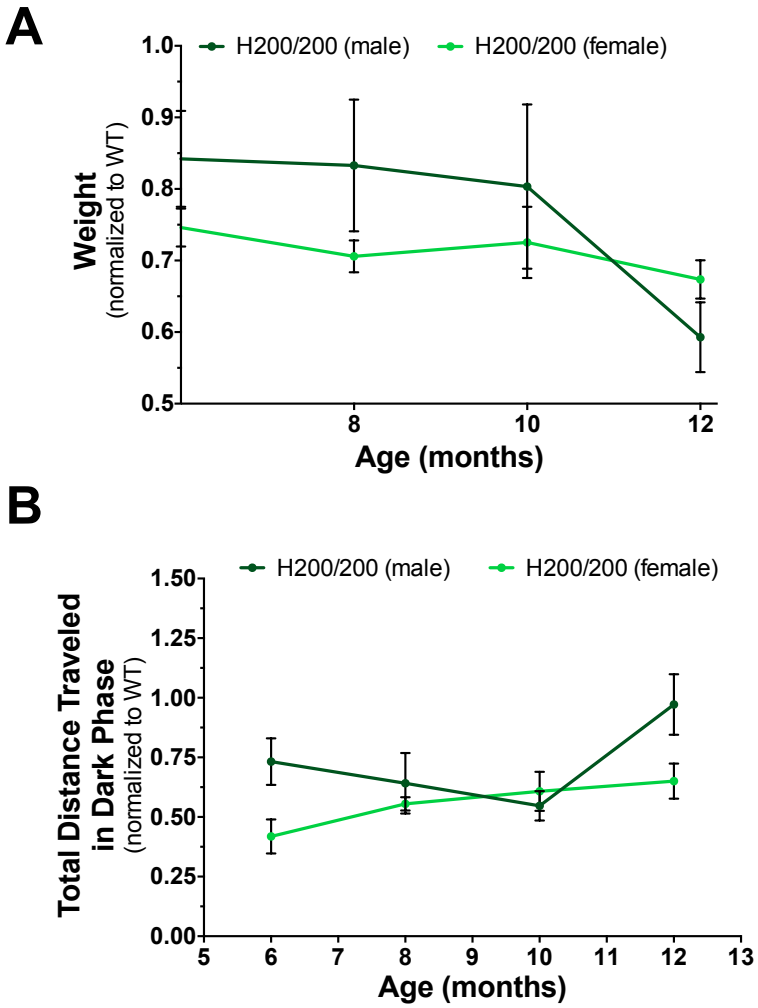

Supplementary Figure 3.1. (A) HdhQ200/200 males and females had similar reduced weight progression when normalized to their respective wild-type littermates. (B) There was no sex-dependent difference in spontaneous dark phase locomotor activity between male and female HdhQ200/200 mice. N=5-12 for all groups. Error bars represent S.E.M. with two-way ANOVA.

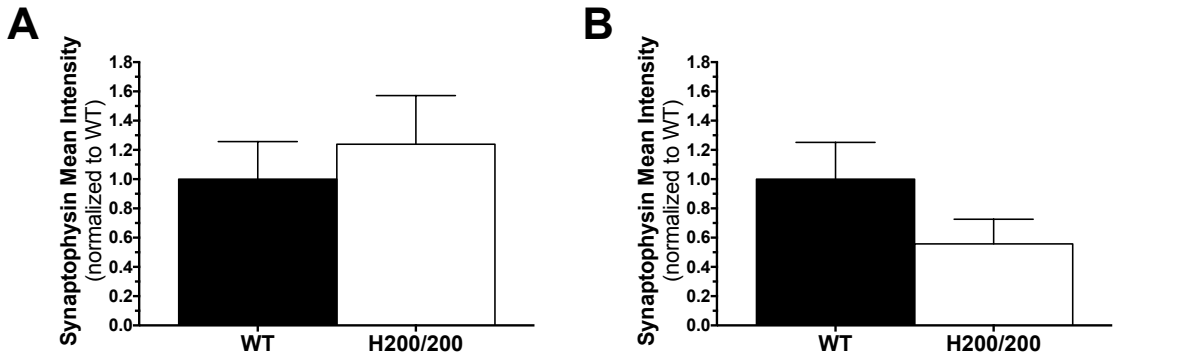

Supplementary Figure 3.2. (A) Male and (B) female HdhQ200/200 mice had no significant differences in synaptophysin expression in the dorsolateral striatum. N=4-5 for all groups. Error bars represent S.E.M. with Student's T-Test.

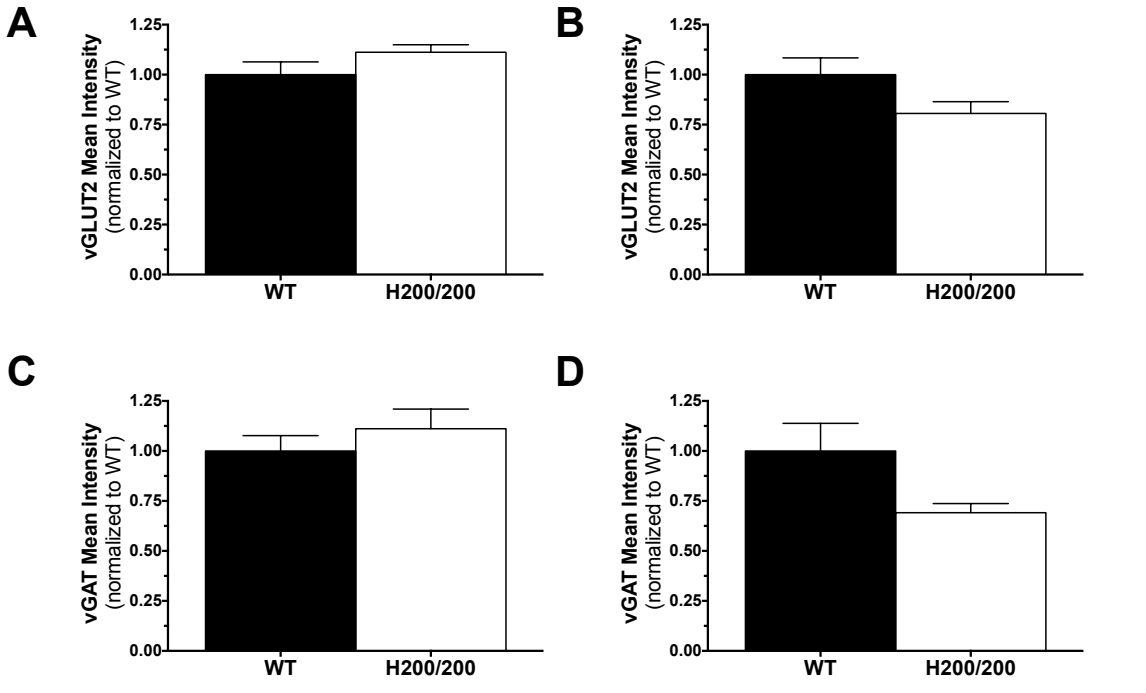

Supplementary Figure 3.3. (A) Male and (B) female HdhQ200/200 mice had no significant differences in vGLUT2 expression in the dorsolateral striatum. Neither (C) male nor (D) female HdhQ200/200 mice differed in vGAT expression in the dorsolateral striatum. N=3-5 for all groups. Error bars represent S.E.M. with Student's T-Test.

Chapter IV: General Discussion

This doctoral thesis examines several novel HD mouse models and the therapeutic potential of the eCB system in these models. Although the gene mutation that causes HD has been known for over 20 years, there lacks a reliable animal model that replicates major behavioral and pathological deficits seen in HD patients. The mouse models created thus far are unable to show a mid-to-late age onset of behavioral symptoms, shortened lifespan, preferential loss of striatal neurons, expression of mHtt aggregates, and brain atrophy. In addition, several eCB therapies have been explored in the treatment of HD but none have successfully used a cannabinoid-based drug that does not have psychotropic side effects and the exact molecular mechanisms of action have yet to be elucidated. The work presented in this doctoral thesis aims to resolve these questions, while also presenting the field with a new understanding into the mechanism and treatment of HD.

4.1 Summary of findings and interpretations

I began this doctoral thesis by first characterizing a novel mouse model of HD. HD research would benefit from an improved mouse model that recapitulates the major behavioral and neuropathological features of HD, and thus enhance the validity of novel therapeutic strategies. In Chapter II, I characterized a novel line of the HdhQ mouse model, the HdhQ350/+ mouse. This line displayed remarkable sex-dependent differences in symptom onset and severity. Both sexes lost weight and grip strength, but HdhQ350/+ males had impaired motor coordination and alterations in gait, while HdhQ350/+ females had reduced dark phase locomotor activity. This study raised new questions into the field of animal models and polyQ effects. My results suggested that expanded polyQ repeats influence disease pathogenesis in a sex-dependent

manner that is not dependent on expression of mHtt, aggregation or expression levels of various HD biomarkers in the striatum. I was intrigued by the strong phenotypic sex differences in this model, and this highlights the importance of including both sexes in HD research. Although I discuss mechanistic possibilities that would contribute to this sex difference in Chapter II, my work is the first to show this occurrence in a mouse model of such high polyQ repeats. It also proposes yet unknown molecular events that may cause high polyQ repeats to differentially impact phenotypes in males and females. Understanding these intricate sex-difference details are critical in designing and developing reliable animal models and understanding not only the HD field, but in translational research as a whole.

However, the lack of shortened lifespan, behavioral severity and neuropathology were limitations to the HdhQ350/+ mouse, possibly due to the heterozygosity of the line, so we explored the novel HdhQ200/200 mouse line. I next characterized behavioral and pathological measures in the HdhQ200/200 mouse line in Chapter III. HdhQ200/200 male and female mice had a reduced lifespan of 12 months and robust behavioral symptoms were prominent at 10 months of age. Both sexes had decreased spontaneous dark phase locomotor activity, whereas only female HdhQ200/200 mice showed significant deficits in grip strength and motor coordination. Male HdhQ200/200 mice had decreased DARPP-32 expression while females had decreased CB_1, enkephalin and PSD-95 expression when compared to their respective wild-type littermates. *In vivo* calcium imaging of the corticostriatal connection revealed aberrant MSN excitability in HdhQ200/200 mice in response to stimulation of the motor cortex in as early as 8 months of age. Taken together, I showed that the HdhQ200/200 mouse line was a dependable model that replicated a number of major HD symptoms and pathology and could reliably be used for mechanistic investigation into novel, more effective therapeutics. Short-term

pharmacological inhibition of ABHD6, the newest discovered eCB enzyme, at 10 months of age showed indications of increasing grip strength, motor coordination and locomotor activity in HdhQ200/200 males and females thus far. My findings indicate that eCB intervention may be sufficiently robust to overcome the numerous molecular and cellular dysfunctions that occur in HD and rescue select behavioral symptoms. Together, these studies highlight the eCB system as a promising pharmacological target to treat HD.

4.2 Future directions

While the findings presented here address unresolved questions in the HD field, they also raise additional research directions to further our understanding of HD and the role of eCBs in the disease.

The newly characterized HdhQ350/+ and HdhQ200/200 mouse lines can help tease apart any apparent sex-differences various polyQ tracts elicit. There is evidence of sex-differences in the HD population; studies have shown that after normalization to polyQ tract lengths, female HD patients had a more severe general phenotype and rate of disease progression than comparable male HD patients (Zielonka et al., 2013). In addition, female HD patients had a significantly altered retinal function in response to light when compared to male HD patients (Pearl et al., 2017). Future studies with the HdhQ mouse models should investigate the effect of large polyQ tracts on sex-specific alterations, beginning with sex hormones. Estrogen has been known to regulate GABA levels, as GABA levels fluctuate across the menstrual cycle (Barth, Villringer, & Sacher, 2015). As MSNs are GABAergic neurons, these changes in GABA levels may influence disease progression particularly in females. In addition, BDNF expression is regulated by estrogen, and thus females may have exceptionally decreased levels of BDNF,

resulting in cellular dysfunction. mHtt has also been found to disrupt the estrous cycle in various rodent models. The first steps would be to investigate levels of estrogen, GABA and BDNF in HdhQ mice. In addition, the various HdhQ mouse lines can be used to investigate if there is a threshold in sex-differential effects due to polyQ length. Sex-differences in HD has only recently come to light and this area still remains largely unknown; further studies using the various HdhQ mouse lines would aid in studying the various effects of polyQ tracts on male and female HD patients.

Further electrophysiological experiments should explore which specific MSN populations are hyperexcitable in the HdhQ200/200 mouse line and the role of eCBs in this dysfunction. Specific emphasis should address whether ABHD6 inhibition reduces this hyperexcitability and assess how it alters synaptic connectivity in the corticostriatal circuit. The effect of the HD mutation can be dissociated between the direct and indirect pathways of the striatum using virally-delivered D1R- or D2R-driven GCaMP6 promoters, respectively. Stimulation of the motor cortex could then tease apart which populations, if not both, are dysfunctional in the HdhQ200/200 mouse line and at what ages. In addition, identification into which cell populations are providing which response profile would provide further insight into the neuronal dysfunction in HD. The eCB contribution to the dysfunction of the corticostriatal circuit can then be investigated, as the eCB system plays an important role in basal ganglia functionality and regulating the numerous neurotransmitters involved. Once the dysfunctional MSN population is identified, the next step should be to test if reinstatement of CB_1 expression in the appropriate population is able to rescue neuronal dysfunction. Generation of mice carrying an additional copy of CB_1 (driven on a promoter that is unaffected by mHtt to avoid downregulation) and expressed in either D1R or D2R neurons would tease apart the role of CB_1 receptors in each

pathway. We have previously shown that rescuing CB_1 expression in all MSNs is able to rescue synaptic function in excitatory synapses in the striatum (Naydenov, Sepers, et al., 2014). These future experiments would extend these results and elucidate if the entire neuronal network is rescued due to rescue of the eCB system in the striatum. This would be an important, novel finding, and would illustrate a broader understanding of the corticostriatal network as well as the role of eCBs. It would also provide insight into the molecular and cellular dysfunctions of the primary target of HD, the striatum.

The exact molecular mechanism by which ABHD6 inhibition influences behavioral and pathological development in the HdhQ200/200 mouse has yet to be clearly established. One crucial component to this project should be to assess that KT-182's therapeutic effects are mediated through 2-AG and CB_1 receptors, as previous work has shown that 2-AG activates various other targets (Bakas et al., 2017; Naydenov, Horne, et al., 2014). Generation of an HdhQ200/200:CB_1-/- mouse would not efficiently answer this question, as a CB_1 knockout on an HD model background already significantly aggravates disease pathology (Blazquez et al., 2010; Mievis et al., 2011). An alternative method would be to utilize cannabinoid pharmacology, specifically with the use of the CB_1-specific antagonist, SR171416. Prolonged treatment of SR171416 alone would be expected to replicate CB_1-knockout mice on an HD background and aggravate disease severity in the HdhQ200/200 mouse. Co-administration of SR171416 and KT-182 would elucidate if the therapeutic benefits of KT-182 treatment are mediated through CB_1 receptors or an alternative molecular target. This experiment could be achieved with daily injections of SR171416 and KT-182 for one week, as co-administration of multiple drugs via osmotic pumps is not yet feasible. If the therapeutic benefits of KT-182 are not blocked by pre-treatment of SR171416 or if it were partially blocked, then I would explore $GABA_A$ receptors or

the COX-2/PGE pathway, which have been found to be involved in other therapeutic effects of ABHD6 inhibitors via reducing excitotoxicity or neuroinflammation (Naydenov, Horne, et al., 2014; Tanaka et al., 2017). If the neuroprotective effects of ABHD6 inhibition are mediated via CB_1 receptors, then I propose that its mechanism of action is a CB_1-mediated reduction in glutamate transmission via inhibition of N-type calcium channels as loss of CB_1 receptors (which is observed in HD) from cortical glutamatergic neurons would remove this inhibition and lead to excitotoxicity (Glass et al., 1993; Marsicano et al., 2003). In support of this, research has shown that R6/2 mice lacking CB_1 receptors on corticostriatal glutamatergic terminals, but not striatal GABAergic neurons, are more susceptible to excitotoxic damage (Chiarlone et al., 2014). Therefore, short-term ABHD6 inhibition should dampen the hyperexcitability observed in HdhQ200/200 mice via increased 2-AG activation of CB_1, resulting in reduced glutamate release

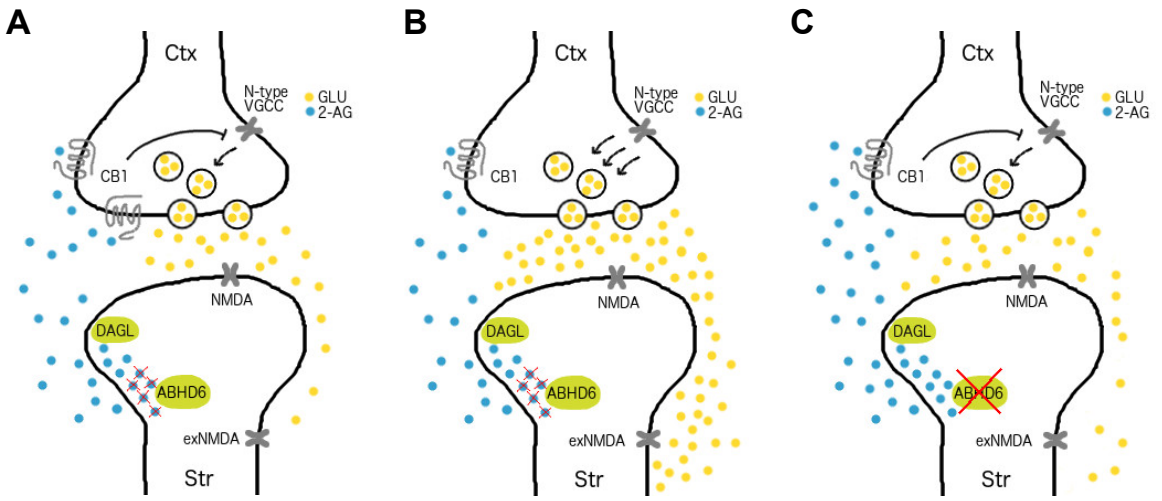

Figure 4.1. Illustration of the effects of 2-AG and CB_1 signaling on glutamate transmission from the cortex (Ctx) to the striatum (Str) in (A) healthy, (B) HD and (C) ABHD6 inhibition in HD brains.

and protecting the striatum against excitotoxicity (Figure 4.1) (Marsicano et al., 2003). In addition, as HdhQ200/200 mice show aberrant calcium handling, CB_1 neuroprotection could also be achieved by reducing NMDA receptor-mediated calcium levels through inhibiting calcium

release from ryanodine-sensitive channels of intracellular stores, preventing NMDA-mediated cell death (Hampson, Miller, Palchik, & Deadwyler, 2011; Liu, Bhat, Bowen, & Cheng, 2009; Zhuang et al., 2005). Results from these experiments would help establish a comprehensive understanding on the effects of ABHD6 inhibition in HD. Together, these experiments would identify the important molecular targets and mechanisms in treating HD for future research to build upon.

To further verify that the HdhQ200/200 mouse line is a reliable model for HD, the neuroinflammatory profile of the HdhQ200/200 mouse should be thoroughly characterized. Neuroinflammation is implicated in HD; elevated levels of astrocytes and activated microglia in the basal ganglia precede behavioral symptom onset in HD patients and other mouse models (Andre, Carty, & Tabrizi, 2015; Ellrichmann, Reick, Saft, & Linker, 2013). Therefore, it would be important to clarify if neuroinflammation is present in the HdhQ200/200 mouse line and if ABHD6 inhibition has an impact, as 2-AG has anti-inflammatory effects in addition to its other neuroprotective traits. HdhQ200/200 mice would be expected to have elevated levels of GFAP and S100β (markers for astrocytes) and IBA-1 (marker for microglia). In addition, micro RNAs (miRNAs) would be used as another indicator of neuroinflammation, as HD cellular models have shown dysregulation of various neuroinflammatory miRNAs. One such miRNA is miRNA-146a, a critical regulator of inflammation in the brain and found to be increased in postmortem HD patients (Martí et al., 2010). After establishing the neuroinflammatory profile of the HdhQ200/200 mouse line, the eCB system can be used as a therapeutic tool in treating HdhQ200/200 mice. CB_2 receptor expression is increased in striatal microglia of R6/2 mice, indicating presence of activated microglia and neuroinflammation, and genetic deletion of CB_2 receptors exacerbates HD pathology through enhanced microglial activation and increased MSN

degeneration, which together reduce the lifespan of R6/2:CB_2-/- mice (Palazuelos et al., 2009). Accordingly, pharmacologically activating CB_2 receptors in R6/2 mice was able to reduce neuroinflammation, brain edema, striatal neuronal loss, and motor symptoms. 2-AG has anti-inflammatory effects through the activation of CB_2 receptors on astrocytes and activated microglia; thus, enhanced activation of CB_2 receptors by elevated 2-AG levels due to ABHD6 inhibition would block microglia activation, prevent cell damage and influence symptom onset (Hollins & Cairns, 2016). In addition, although it has been shown that miRNAs regulate CB_2 expression in diseased states, there has yet to be evidence of CB_2 receptors influencing miRNA expression. Analysis of miRNA changes due to ABHD6 inhibition would therefore be a novel finding (Möhnle et al., 2014). This work would expand on the therapeutic profile of ABHD6 inhibition as a promising treatment for HD and additionally identify the role of CB_2 receptor-mediated signaling in 2-AG's therapeutic benefits in HD.

Finally, an additional experiment to help support the pharmacological results found in Chapter III is to generate HdhQ200/200 mice on an ABHD6-/- background. Although ABHD6-/- mice have yet to be fully characterized, they do not show any major morphological abnormalities, developmental deficits or a reduced lifespan. If HdhQ200/200:ABHD6-/- mice have delayed behavioral and pathological development compared to what I established for HdhQ200/200 mice in Chapter III, this would suggest that decreased ABHD6 and its downstream effects are neuroprotective against mHtt. 2-AG levels would be measured to ensure that there is an increase in 2-AG due to the absence of ABHD6 and that there isn't a compensatory mechanism regulating 2-AG levels in these mice. I would also characterize these mice similarly to the characterization of HdhQ200/200 mice and would expect behavioral and pathological alleviation due to increased CB_1 activation. However, I would not expect these

results to fully replicate the molecular mechanism of pharmacological inhibition of ABHD6 due to the absence of ABHD6 during the pre-diseased state. Because the eCB system is critical in early development, there may be compensatory mechanisms that negate the increase in 2-AG or other molecular, cellular and network rearrangements that alter the course of the disease due to developmental absence of ABHD6 (Elphick, 2012). This limitation could be circumvented with the generation of a tamoxifen-inducible ABHD6-/- mouse. With a tamoxifen-inducible ABHD6-/- mouse, we would be able to induce removal of ABHD6 prior to symptom onset and avoid any major molecular, cellular and network rearrangements. In all, this study would provide valuable insight into the role of ABHD6 and the eCB system in the development of HD.

4.3 Conclusions and general relevance

This doctoral thesis furthers our understanding on the role of eCB signaling in HD across different polyQ mouse lines and highlights the eCB system as a promising target for therapeutic intervention. My work characterizes several genetic mouse lines, establishing one as a reliable model of HD and demonstrates that short-term ABHD6 inhibitions shows promise in rescuing select behavioral impairments associated with HD. HD remains incurable; current treatments only reduce symptom severity and do not target the underlying molecular and cellular dysfunctions. Here, I present a valid mouse model in which to base further studies into potential new therapeutics on the treatment of HD. A solid foundation into the understanding of the molecular mechanisms, pathways and network dysfunctions will lead to new discoveries in the process towards a cure for HD.

Materials and Methods

HdhQ350/+ and HdhQ200/200 mice colony

Mice were housed in a pathogenic-free facility in accordance with the National Institutes of Health; the Institutional Animal Care and Use Committee at the University of Washington approved all experiments. All mice were maintained on a C57BL/6 genetic background. For all HdhQ350/+ experiments, female and male heterozygous HdhQ350 knock-in mice were mated to produce heterozygous and wild-type littermates. For all HdhQ200/200 experiments, female and male heterozygous HdhQ200/+ knock-in mice were mated to produce homozygous, heterozygous and wild-type littermates. Animals were housed in cages grouped by sex and mixed genotype, had *ad libitum* access to food and water and were on a 12-hour light/dark cycle. Genotyping was performed with tail snips using primers "cccattcattgcccttgctg" and "gcggctgaggggggttga" with a SimpliAmp Thermal Cycler (Thermo Fisher Scientific, Bothell, WA).

H350/+ Behavioral studies

Balanced cohorts of males and females were used for behavioral studies. The same individual was analyzed at each time point (every 10 weeks, starting at 30 weeks to 70 weeks of age). All behavioral studies were performed during the light phase of the light/dark cycle, between 9am and 4pm. Cages and equipment were thoroughly cleaned with 70% ethanol and dried with a paper towel between trials. Grip strength was assessed with a grip strength meter (Columbus Instruments, Columbus, OH). With mice grasping a metal grid with their forepaws, continual gentle force was used to pull the mouse slowly away from the grid. A strain gauge recorded the maximum force applied just prior to release. The elevated plus maze was measured with 5-

minute trials using a vertically mounted video camera and analyzed in Ethovision XT 9 (Noldus, Wageningen, The Netherlands). With rodents, increased time spent in closed arms denotes increased anxiety and increased time spend in open arms suggests decreased anxiety and more exploration. Rotarod (Med Associates Inc., St. Albans, VT) testing included 7 consecutive trials, separated by 30-minute resting periods over 3 days. The rotarod rotational speed used for testing trails began at 4 rpm and increased to 40 rpm for a maximum of 5 minutes, with an acceleration of 0.2 rpm per every 4 seconds. Motor learning was divided into "fast" and "slow" learning, as adapted from (Costa et al., 2004). "Fast" motor learning was calculated by the difference between trial 1 and 7 in day 1, and "slow" motor learning was calculated by the difference for all three testing days. Catwalk testing included 3 trials, where animals were placed at one end of the catwalk apparatus (Noldus, Wageningen, The Netherlands), with a vertically mounted camera under the walkway that recorded their movements as they crossed an infrared track. Crossings where the animal stopped, reared or turned around were excluded. The Phenotyper (Noldus, Wageningen, the Netherlands) testing consisted of 72-hour trials where animals were individually housed in 30cm x 30cm Plexiglas cages with access to water, food and housing. A vertically mounted camera continuously tracked animal movement and digital traces were analyzed in Ethovision XT 9.

HdhQ200/200 Behavioral studies

Balanced cohorts of males and females were used for behavioral studies. Naïve mice were used at all time points (6, 8, 10, 12 months) and then sacrificed for immunohistochemistry or immunoblotting. All behavioral studies were performed during the light phase of the light/dark cycle, between 9am and 4pm. Cages and equipment were thoroughly cleaned with 70% ethanol

and dried with a paper towel between trials. Grip strength was measured by recording the latency to fall when animals were placed on a wire cage top and then inverted. A maximum score of 90 seconds was used. Rotarod (Med Associates Inc., St. Albans, VT) testing included 7 consecutive trials, separated by 15-minute resting periods. The rotarod rotational speed used for testing trails began at 4 rpm and increased to 40 rpm for a maximum of 5 minutes, with an acceleration of 0.2 rpm per every 4 seconds. The Phenotyper (Noldus, Wageningen, the Netherlands) testing consisted of 72-hour trial periods where animals were individually housed in 30cm x 30cm Plexiglas cages with access to water, food and housing. A vertically mounted camera continuously tracked animal movement and digital traces were analyzed in Ethovision XT 11.

Miniature osmotic pump surgery

Mice were treated with buprenorphine (0.5mg/kg) and lidocaine (2mg/kg) for systemic and local analgesia. Alzet miniature osmotic pumps (1007D) were filled with either vehicle or KT-182 (dissolved in 1:1:18 ethanol:PEG-40:PBS) and surgically implanted into the subcutaneous lower flank of male and female HdhQ200/200 and wild-type mice 1 week prior to 10 months of age. Drug was administered at a rate of 0.5ul/hour to achieve 2mg/kg/day. Mice were placed under isoflurane anesthesia and allowed ample time in a recovery cage before returning to their homecage. Only mice undergoing surgery were housed together along with supplemental food mash and gel. Mice were checked on daily and after 5 days post-surgery, mice underwent behavioral studies.

ABPP (Activity-Based Protein Profiling)

Mice were euthanized via cervical dislocation, their brains were washed with ice cold lysis buffer (0.25M sucrose, 20mM HEPES, 2mM DTT, in deionized H2O) twice before dounce homogenization. Blood samples and brain tissues were processed using dounce homogenizer and placed in ice for 15 minutes. Tissue homogenates were centrifuged at 800xg for 5 minutes at 4°C. Supernatants were separated to remove debris from unlysed tissue. Supernatants were centrifuged at 100,000xg for 45 minutes at 4°C. Resulting pellet was resuspended in assay buffer (20mM HEPES in deionized H_2O). Proteome concentrations were normalized using Bio-Rad DC protein assay and treated with either HT-01 or FP-Rh at 1uM final concentration for 30 minutes at 37°C. The reaction was quenched using SDS-PAGE loading buffer. After separation by SDS-PAGE (10% acrylamide), samples were visualized by in-gel fluorescence scanning using Chemidoc MP imaging system (Bio-Rad, Hercules, CA).

Immunohistochemistry

Mice were euthanized with ketamine/xylazine and perfused with 20mL PBS, followed by 10mL 4% paraformaldehyde. Brains were extracted and post-fixed in 4% paraformaldehyde overnight at 4°C. Brains were then dehydrated (first in 15% sucrose and then 30% sucrose for 24 hours each) and frozen over dry ice. Coronal sections were cut to a thickness of 30µm using a sliding microtome and placed in cryoprotectant for storage at -20°C. IHC analysis of each time point group was processed and stained in parallel. For staining, 2 slices per animal were removed from cryoprotectant, washed 3xPBS and incubated for 90 minutes at room temperature in blocking buffer (PBS, 5% goat serum, 1% Triton x-100). Slices were then transferred to primary staining solutions (PBS, 2.5% goat serum, 0.5% Triton x-100) for 72 hours at 4°C. Sections were then washed 8xPBS-T and secondary staining was performed using Alexa secondary antibodies at a

dilution of 1:500 (PBS, 2.5% goat serum, 0.5% Triton x-100). Additional slices were stained only with secondary staining solutions to serve as non-specific secondary background staining. After secondary staining, sections were washed 6xPBS-T, 1xPBS, mounted on slides and allowed to dry at room temperature overnight. Coverslips were added and sealed with Fluoromount (Sigma, St. Louis, MO) and nail polish.

Immunoblotting

Mice were euthanized via cervical dislocation, their brains immediately removed and rinsed in ice cold PBS. Striata were dissected and flash frozen in liquid nitrogen. Striatal tissue was then homogenized in RIPA Buffer (Santa Cruz Biotechnology, Dallas, TX) using a dounce homogenizer on ice followed by sonication. Protein levels were measured using a BCA assay. Each time point group was processed and analyzed in parallel. Specifically, 20-25µg of protein was loaded per lane and gels were transferred to PVDF and blocked with Licor Odyssey Blocking Buffer (LI-COR, Lincoln, NE). Blots were stained overnight with primary antibodies prepared in TBS solution containing 5% BSA and 0.02% NaN_3 at 4°C, followed by 3 rinses in TBS-T. Secondary staining was carried out for 2 hours in TBS containing 5% BSA at room temperature. Blots were then rinsed 3xTBS-T, imaged and analyzed with fluorescence. Expression level of target proteins was quantified with ImageLab (LI-COR, Lincoln, NE) and normalized to GAPDH expression. Values were normalized to the corresponding wild-type sex average.

SDDAGE (Semi-Denaturing Detergent Agarose Gel Electrophoresis)

Striatal tissue was prepared as described above and solubilized in SDDAGE lysis buffer (Tris, NaCl, EDTA, 5% glycerol, DTT, 1% NP-40, $MgCl_2$, DNase, PMSF+NEM). Samples were incubated in SDDAGE loading buffer (TAE, 20% glycerol, 8% SDS, 0.01% bromophenol blue) for at least 10 minutes, loaded in a pre-poured gel (TAE, 1.5% agarose, 0.1% SDS) and ran at 34V for 6 hours on ice. Samples were then transferred overnight using a semi-dry capillary apparatus and developed with the western blot protocol described above. Blots were analyzed with HRP.

In Vivo Electrophysiology and Calcium Imaging

Two weeks following viral injection surgery (AAV-CAG-GCaMP6m, $3x10^9$ particles/ ml, 0.5 ml bilateral), HdhQ200/200 and wild-type littermates were deeply anesthetized with urethane (1g/kg, i.p.) and placed in a stereotaxic frame. Fluorescence images were acquired by scanning confocal microscopy coupled to a fiber-optic probe (Mauna Kea Technologies). Spontaneous calcium dynamics were imaged for 5 minutes (12 Hz scan rate) prior to electrical stimulation. To evoke activation of the striatum, antidromic stimulation of direct pathway fibers from the substantia nigra pars reticulata was performed. Images were acquired for 5 seconds to establish baseline fluorescence, followed by electrical stimulation from a bipolar stimulating electrode (200 mA, 0.5 sec) with an additional 15 seconds of imaging. Once striatal neurons were isolated, the motor cortex was stimulated with increasing intensity (ramping from 50 to 400 mA using 50 mA increments every 0.5 seconds). Data was analyzed offline using ImageCell software (Mauna Kea Technologies) and MatLab. The number of spontaneous events was quantified, as well as amplitude and duration of these events, and the amplitude and duration of electrically evoked events.

Antibodies

The following antibodies were used in this study: CB_1 receptor (L15 pAb guinea pig, gift from Ken Mackie); synaptophysin (mouse, Synaptic Systems 101011); DARPP-32 (rabbit, Abcam ab40801); DAPI (Invitrogen D3571); 1C2 (mouse, Millipore MAB1574); GAPDH (mouse, Sigma 1405848; rabbit, Cell Signaling Technology 5174); Alexa Fluor 488/555/647 (goat/donkey, ThermoFisher); IRDye 680/800 (goat, LI-COR Biosciences); HRP-conjugated secondaries (goat, Cell Signaling Technology).

Microscopy

Images were collected on a Marianas microscope (Intelligent Imaging Innovations, Inc. Denver, CO) equipped with either 20x/0.75 NA or 40x/0.75 NA air objective lens with CoolSnap HQ cooled monochrome camera (Photometrics, Tucson, AZ) as Z-stacks of 10 at the NIDCD Research Core Center at the University of Washington. Noise reduction of images was achieved by deconvolution of Nearest Neighbors using SlideBook (Intelligent Imaging Innovations, Inc., Denver, CO). Exposure times were optimized for each antibody to ensure that >99% pixels were within the linear range. Excitation laser of 403nm was used to excite DAPI, FITC to excite Alexa 488, Cy3/TRITC to excite Alexa 555, and FarCy5 to excite Alexa 647.

Semi-quantitative image analysis and statistics

All images were analyzed using ImageJ (National Institutes of Health) with custom written macros. Macros were applied blindly to each batch of images and analyzed as previously reported by our laboratory (Horne et al., 2012). Each z-stack was flattened into one image of

average or maximum pixel intensity and each channel was split into an individual image. The mean intensity and standard deviation of each fluorophore was measured and background signal was removed by thresholding images to mean + standard deviation, corresponding to the top third brightest pixels in the Gaussian distribution. After thresholding, final measurements were made by taking the mean intensity of the remaining pixels or by calculating the average cellular size. Values were normalized to the corresponding wild-type sex average.

Statistical analyses

Statistical analyses and graphs were generated using GraphPad PRISM 6 (San Diego, CA). Grubbs' test was used to detect any outliers. Two-way ANOVA was used to compare measurements with a Bonferroni post-hoc analysis. A repeated two-way ANOVA was used for behaviors with complete data sets when appropriate. Student's T-Test was used for comparing applicable data. A chi-square test was used for Mendelian frequencies. For calcium imaging, area under the curve for evoked events was compared across groups using a repeated two-way ANOVA. Data were considered significant if $p \leq 0.05$.

References

Adjeroud, N., Yagüe, S., Yu-Taeger, L., Bozon, B., Leblanc-Veyrac, P., Riess, O., . . . El Massioui, N. (2015). Reduced impact of emotion on choice behavior in presymptomatic BACHD rats, a transgenic rodent model for Huntington Disease. *Neurobiology of learning and memory*. doi:10.1016/j.nlm.2015.10.003

Alhouayek, M., Masquelier, J., Cani, P. D., Lambert, D. M., & Muccioli, G. G. (2013). Implication of the anti-inflammatory bioactive lipid prostaglandin D2-glycerol ester in the control of macrophage activation and inflammation by ABHD6. *Proceedings of the National Academy of Sciences, 110*(43), 17558-17563. doi:10.1073/pnas.1314017110

Andre, R., Carty, L., & Tabrizi, S. J. (2015). Disruption of immune cell function by mutant huntingtin in Huntington's disease pathogenesis. *Current opinion in pharmacology, 26*, 33-38. doi:10.1016/j.coph.2015.09.008

Andrew, S. E., Goldberg, Y. P., Kremer, B., Telenius, H., Theilmann, J., Adam, S., . . . Kalchman, M. A. (1993). The relationship between trinucleotide (CAG) repeat length and clinical features of Huntington's disease. *Nature genetics, 4*(4), 398-403. doi:10.1038/ng0893-398

Apostol, B. L. (2005). Mutant huntingtin alters MAPK signaling pathways in PC12 and striatal cells: ERK1/2 protects against mutant huntingtin-associated toxicity. *Human molecular genetics, 15*(2), 273-285. doi:10.1093/hmg/ddi443

Baggelaar, M. P., van Esbroeck, A. C. M., van Rooden, E. J., Florea, B. I., Overkleeft, H. S., Marsicano, G., . . . van der Stelt, M. (2017). Chemical Proteomics Maps Brain Region Specific Activity of Endocannabinoid Hydrolases. *ACS chemical biology, 12*(3), 852-861. doi:10.1021/acschembio.6b01052

Bakas, T., van Nieuwenhuijzen, P. S., Devenish, S. O., McGregor, I. S., Arnold, J. C., & Chebib, M. (2017). The direct actions of cannabidiol and 2-arachidonoyl glycerol at GABAA receptors. *Pharmacological research, 119*, 358-370. doi:10.1016/j.phrs.2017.02.022

Barth, C., Villringer, A., & Sacher, J. (2015). Sex hormones affect neurotransmitters and shape the adult female brain during hormonal transition periods. *Frontiers in neuroscience, 9*(6), 37. doi:10.3389/fnins.2015.00037

Bellocchio, L., LafenEtre, P., Cannich, A., Cota, D., Puente, N., Grandes, P., . . . Marsicano, G. (2010). Bimodal control of stimulated food intake by the endocannabinoid system. *Nature Neuroscience, 13*(3), 281-283. doi:10.1038/nn.2494

Bissonnette, S., Vaillancourt, M., Hébert, S. S., Drolet, G., & Samadi, P. (2013). Striatal pre-enkephalin overexpression improves Huntington's disease symptoms in the R6/2 mouse model of Huntington's disease. *PLoS ONE, 8*(9), e75099. doi:10.1371/journal.pone.0075099

Blankman, J. L., Simon, G. M., & Cravatt, B. F. (2007). A Comprehensive Profile of Brain Enzymes that Hydrolyze the Endocannabinoid 2-Arachidonoylglycerol. *Chemistry & Biology, 14*(12), 1347-1356. doi:10.1016/j.chembiol.2007.11.006

Blazquez, C., Chiarlone, A., Sagredo, O., Aguado, T., Pazos, M. R., Resel, E., . . . Guzman, M. (2010). Loss of striatal type 1 cannabinoid receptors is a key pathogenic factor in Huntington's disease. *Brain, 134*(1), 119-136. doi:10.1093/brain/awq278

Bode, F. J., Stephan, M., Suhling, H., Pabst, R., Straub, R. H., Raber, K. A., . . . von Hörsten, S. (2008). Sex differences in a transgenic rat model of Huntington's disease:

decreased 17beta-estradiol levels correlate with reduced numbers of DARPP32+ neurons in males. *Human molecular genetics, 17*(17), 2595-2609. doi:10.1093/hmg/ddn159

Borlongan, C. V., Koutouzis, T. K., & Sanberg, P. R. (1997). 3-Nitropropionic acid animal model and Huntington's disease. *Neuroscience and Biobehavioral Reviews, 21*(3), 289-293.

Bowman, A. L., & Makriyannis, A. (2012). Highly Predictive Ligand-based Pharmacophore and Homology Models of ABHD6. *Chemical Biology & Drug Design, 81*(3), 382-388. doi:10.1111/cbdd.12086

Cao, J. K., Detloff, P. J., Gardner, R. G., & Stella, N. (2017). Sex-Dependent Behavioral Impairments in the HdhQ350/+ Mouse Line. *Behavioural Brain Research, 337*, 34-45. doi:10.1016/j.bbr.2017.09.026

Cepeda, C., Wu, N., André, V. M., Cummings, D. M., & Levine, M. S. (2007). The corticostriatal pathway in Huntington's disease. *Progress in Neurobiology, 81*(5-6), 253-271. doi:10.1016/j.pneurobio.2006.11.001

Cha, J.-H. J. (2000). Transcriptional dysregulation in Huntington's disease. *Trends in neurosciences, 23*(9), 387-392.

Chiarlone, A., Bellocchio, L., Blázquez, C., Resel, E., Soria-Gómez, E., Cannich, A., . . . Guzmán, M. (2014). A restricted population of CB1 cannabinoid receptors with neuroprotective activity. *Proceedings of the National Academy of Sciences, 111*(22), 8257-8262. doi:10.1073/pnas.1400988111

Chiodi, V., Uchigashima, M., Beggiato, S., Ferrante, A., Armida, M., Martire, A., . . . Popoli, P. (2012). Unbalance of CB1 receptors expressed in GABAergic and glutamatergic neurons in a transgenic mouse model of Huntington's disease. *Neurobiology of Disease, 45*(3), 983-991. doi:10.1016/j.nbd.2011.12.017

Ciamei, A., Detloff, P. J., & Morton, A. J. (2015). Progression of behavioural despair in R6/2 and Hdh knock-in mouse models recapitulates depression in Huntington's disease. *Behavioural Brain Research*, 1-7. doi:10.1016/j.bbr.2015.05.010

Costa, R. M., Cohen, D., & Nicolelis, M. A. L. (2004). Differential Corticostriatal Plasticity during Fast and Slow Motor Skill Learning in Mice. *Current Biology, 14*(13), 1124-1134. doi:10.1016/j.cub.2004.06.053

Coyle, J. T., & Schwarcz, R. (1976). Lesion of striatal neurones with kainic acid provides a model for Huntington's chorea. *Nature, 263*(5574), 244-246.

Denovan-Wright, E. M., & Robertson, H. A. (2000). Cannabinoid receptor messenger RNA levels decrease in a subset of neurons of the lateral striatum, cortex and hippocampus of transgenic Huntington's disease mice. *NSC, 98*(4), 705-713.

Díaz-Alonso, J., Paraíso-Luna, J., Navarrete, C., del Río, C., Cantarero, I., Palomares, B., . . . Muñoz, E. (2016). VCE-003.2, a novel cannabigerol derivative, enhances neuronal progenitor cell survival and alleviates symptomatology in murine models of Huntington's disease. *Nature Publishing Group, 6*, 29789. doi:10.1038/srep29789

Dowie, M. J., Bradshaw, H. B., Howard, M. L., Nicholson, L. F. B., Faull, R. L. M., Hannan, A. J., & Glass, M. (2009). Altered CB1 receptor and endocannabinoid levels precede motor symptom onset in a transgenic mouse model of Huntington's disease. *NSC, 163*(1), 456-465. doi:10.1016/j.neuroscience.2009.06.014

Dowie, M. J., Howard, M. L., Nicholson, L. F. B., Faull, R. L. M., Hannan, A. J., & Glass, M. (2010). Behavioural and molecular consequences of chronic cannabinoid treatment in

Huntington's disease transgenic mice. *NSC, 170*(1), 324-336. doi:10.1016/j.neuroscience.2010.06.056

Dragatsis, I., Efstratiadis, A., & Zeitlin, S. (1998). Mouse mutant embryos lacking huntingtin are rescued from lethality by wild-type extraembryonic tissues. *Development (Cambridge, England), 125*(8), 1529-1539.

Du, X., Leang, L., Mustafa, T., Renoir, T., Pang, T. Y., & Hannan, A. J. (2012). Environmental enrichment rescues female-specific hyperactivity of the hypothalamic-pituitary-adrenal axis in a model of Huntington's disease. *Translational psychiatry, 2*(7), e133. doi:10.1038/tp.2012.58

Duyao, M. P., Auerbach, A. B., Ryan, A., Persichetti, F., Barnes, G. T., McNeil, S. M., . . . Joyner, A. L. (1995). Inactivation of the mouse Huntington's disease gene homolog Hdh. *Science, 269*(5222), 407-410.

Duzdevich, D., Li, J., Whang, J., Takahashi, H., Takeyasu, K., Dryden, D. T. F., . . . Edwardson, J. M. (2011). Unusual structures are present in DNA fragments containing super-long Huntingtin CAG repeats. *PLoS ONE, 6*(2), e17119. doi:10.1371/journal.pone.0017119

Ehrlich, M. E. (2012). Huntington's Disease and the Striatal Medium Spiny Neuron: Cell-Autonomous and Non-Cell-Autonomous Mechanisms of Disease. *Neurotherapeutics, 9*(2), 270-284. doi:10.1007/s13311-012-0112-2

Ellrichmann, G., Reick, C., Saft, C., & Linker, R. A. (2013). The Role of the Immune System in Huntington's Disease. *Clinical and Developmental Immunology, 2013*(2), 1-11. doi:10.1155/2013/541259

Elphick, M. R. (2012). The evolution and comparative neurobiology of endocannabinoid signalling. *Philosophical transactions of the Royal Society of London. Series B, Biological sciences, 367*(1607), 3201-3215. doi:10.1098/rstb.2011.0394

Ferrante, R. J. (2009). Mouse models of Huntington's disease and methodological considerations for therapeutic trials. *Biochimica et biophysica acta, 1792*(6), 506-520. doi:10.1016/j.bbadis.2009.04.001

Fisette, A., Tobin, S., Décarie-Spain, L., Bouyakdan, K., Peyot, M.-L., Madiraju, S. R. M., . . . Alquier, T. (2016). α/β-Hydrolase Domain 6 in the Ventromedial Hypothalamus Controls Energy Metabolism Flexibility. *CellReports, 17*(5), 1217-1226. doi:10.1016/j.celrep.2016.10.004

Glass, M., Faull, R. L., & Dragunow, M. (1993). Loss of cannabinoid receptors in the substantia nigra in Huntington's disease. *NSC, 56*(3), 523-527.

Goto, S., & Hirano, A. (1990). Synaptophysin expression in the striatum in Huntington's disease. *Acta neuropathologica, 80*(1), 88-91.

Gouix, E., Léveillé, F., Nicole, O., Cellular, C. M. M. a., & 2009. Reverse glial glutamate uptake triggers neuronal cell death through extrasynaptic NMDA receptor activation. *Elsevier*. doi:10.1016/j.mcn.2009.01.002

Graham, R. K., Deng, Y., Slow, E. J., Haigh, B., Bissada, N., Lu, G., . . . Hayden, M. R. (2006). Cleavage at the Caspase-6 Site Is Required for Neuronal Dysfunction and Degeneration Due to Mutant Huntingtin. *Cell, 125*(6), 1179-1191. doi:10.1016/j.cell.2006.04.026

Grima, J. C., Daigle, J. G., Arbez, N., Cunningham, K. C., Zhang, K., Ochaba, J., . . . Rothstein, J. D. (2017). Mutant Huntingtin Disrupts the Nuclear Pore Complex. *Neuron, 94*(1), 93-107.e106. doi:10.1016/j.neuron.2017.03.023

Halfmann, R., & Lindquist, S. (2008). Screening for amyloid aggregation by Semi-Denaturing Detergent-Agarose Gel Electrophoresis. *Journal of visualized experiments : JoVE*(17). doi:10.3791/838

Hampson, R. E., Miller, F., Palchik, G., & Deadwyler, S. A. (2011). Cannabinoid receptor activation modifies NMDA receptor mediated release of intracellular calcium: implications for endocannabinoid control of hippocampal neural plasticity. *Neuropharmacology, 60*(6), 944-952. doi:10.1016/j.neuropharm.2011.01.039

Hardingham, G. E., Fukunaga, Y., & Bading, H. (2002). Extrasynaptic NMDARs oppose synaptic NMDARs by triggering CREB shut-off and cell death pathways. *Nature Neuroscience, 5*(5), 405-414. doi:10.1038/nn835

Heng, M. Y., Detloff, P. J., & Albin, R. L. (2008). Rodent genetic models of Huntington disease. *Neurobiology of Disease, 32*(1), 1-9. doi:10.1016/j.nbd.2008.06.005

Heng, M. Y., Duong, D. K., Albin, R. L., Tallaksen-Greene, S. J., Hunter, J. M., Lesort, M. J., . . . Detloff, P. J. (2010). Early autophagic response in a novel knock-in model of Huntington disease. *Human molecular genetics, 19*(19), 3702-3720. doi:10.1093/hmg/ddq285

Heng, M. Y., Tallaksen-Greene, S. J., Detloff, P. J., & Albin, R. L. (2007). Longitudinal Evaluation of the Hdh(CAG)150 Knock-In Murine Model of Huntington's Disease. *Journal of Neuroscience, 27*(34), 8989-8998. doi:10.1523/JNEUROSCI.1830-07.2007

Hodgson, J. G., Agopyan, N., Gutekunst, C. A., Leavitt, B. R., LePiane, F., Singaraja, R., . . . Hayden, M. R. (1999). A YAC mouse model for Huntington's disease with full-length mutant huntingtin, cytoplasmic toxicity, and selective striatal neurodegeneration. *Neuron, 23*(1), 181-192.

Hollins, S. L., & Cairns, M. J. (2016). MicroRNA: Small RNA mediators of the brains genomic response to environmental stress. *Progress in Neurobiology, 143*, 61-81. doi:10.1016/j.pneurobio.2016.06.005

Holzmann, C., Schmidt, T., Thiel, G., brain, J. E. M., & 2001. (2001). Functional characterization of the human Huntington's disease gene promoter. *Elsevier, 92*(1-2), 85-97. doi:10.1016/S0169-328X(01)00149-8

Hong, Y., Zhao, T., Li, X.-J., & Li, S. (2016). Mutant Huntingtin Impairs BDNF Release from Astrocytes by Disrupting Conversion of Rab3a-GTP into Rab3a-GDP. *The Journal of neuroscience : the official journal of the Society for Neuroscience, 36*(34), 8790-8801. doi:10.1523/JNEUROSCI.0168-16.2016

Horn, C. C., Henry, S., Meyers, K., & Magnusson, M. S. (2011). Behavioral patterns associated with chemotherapy-induced emesis: a potential signature for nausea in musk shrews. *Frontiers in neuroscience, 5*, 88. doi:10.3389/fnins.2011.00088

Horne, E. A., Coy, J., Swinney, K., Fung, S., Cherry, A. E. T., Marrs, W. R., . . . Stella, N. (2012). Downregulation of cannabinoid receptor 1 from neuropeptide Y interneurons in the basal ganglia of patients with Huntington's disease and mouse models. *European Journal of Neuroscience, 37*(3), 429-440. doi:10.1111/ejn.12045

Hsu, K.-L., Tsuboi, K., Adibekian, A., Pugh, H., Masuda, K., & Cravatt, B. F. (2012). DAGLβ inhibition perturbs a lipid network involved in macrophage inflammatory responses. *Nature Chemical Biology, 8*(12), 999-1007. doi:10.1038/nchembio.1105

Hsu, K.-L., Tsuboi, K., Chang, J. W., Whitby, L. R., Speers, A. E., Pugh, H., & Cravatt, B. F. (2013). Discovery and Optimization of Piperidyl-1,2,3-Triazole Ureas as Potent, Selective, and in Vivo-Active Inhibitors of α/β-Hydrolase Domain Containing 6 (ABHD6). *Journal of Medicinal Chemistry, 56*(21), 8270-8279. doi:10.1021/jm400899c

Huntington, G. (2003). On chorea. *The Journal of neuropsychiatry and clinical …*.

Kaczocha, M., Glaser, S. T., & Deutsch, D. G. (2009). Identification of intracellular carriers for the endocannabinoid anandamide. *Proceedings of the National Academy of Sciences, 106*(15), 6375-6380. doi:10.1073/pnas.0901515106

Kalonia, H., Kumar, P., & Kumar, A. (2010). Targeting oxidative stress attenuates malonic acid induced Huntington like behavioral and mitochondrial alterations in rats. *European journal of pharmacology, 634*(1-3), 46-52. doi:10.1016/j.ejphar.2010.02.031

Kaufman, A. M., Milnerwood, A. J., Sepers, M. D., Coquinco, A., She, K., Wang, L., . . . Raymond, L. A. (2012). Opposing roles of synaptic and extrasynaptic NMDA receptor signaling in cocultured striatal and cortical neurons. *The Journal of neuroscience : the official journal of the Society for Neuroscience, 32*(12), 3992-4003. doi:10.1523/JNEUROSCI.4129-11.2012

Kuljis, D. A., Gad, L., Loh, D. H., MacDowell Kaswan, Z., Hitchcock, O. N., Ghiani, C. A., & Colwell, C. S. (2016). Sex Differences in Circadian Dysfunction in the BACHD Mouse Model of Huntington's Disease. *PLoS ONE, 11*(2), e0147583. doi:10.1371/journal.pone.0147583

Kumar, A., Zhang, J., Tallaksen-Greene, S., Crowley, M. R., Crossman, D. K., Morton, A. J., . . . Detloff, P. J. (2016). Allelic series of Huntington's disease knock-in mice reveals expression discorrelates. *Human molecular genetics, 25*(8), 1619-1636. doi:10.1093/hmg/ddw040

Labbadia, J., & Morimoto, R. I. (2013). Huntington's disease: underlying molecular mechanisms and emerging concepts. *Trends in biochemical sciences, 38*(8), 378-385. doi:10.1016/j.tibs.2013.05.003

Landles, C., & Bates, G. P. (2004). Huntingtin and the molecular pathogenesis of Huntington's disease. *EMBO reports, 5*(10), 958-963. doi:10.1038/sj.embor.7400250

Lau, D., Bengtson, C. P., Buchthal, B., & Bading, H. (2015). BDNF Reduces Toxic Extrasynaptic NMDA Receptor Signaling via Synaptic NMDA Receptors and Nuclear-Calcium-Induced Transcription of inhba/Activin A. *CellReports, 12*(8), 1353-1366. doi:10.1016/j.celrep.2015.07.038

Léveillé, F., Papadia, S., Fricker, M., Bell, K. F. S., Soriano, F. X., Martel, M.-A., . . . Hardingham, G. E. (2010). Suppression of the intrinsic apoptosis pathway by synaptic activity. *The Journal of neuroscience : the official journal of the Society for Neuroscience, 30*(7), 2623-2635. doi:10.1523/JNEUROSCI.5115-09.2010

Li, F., Fei, X., Xu, J., & Ji, C. (2008). An unannotated α/β hydrolase superfamily member, ABHD6 differentially expressed among cancer cell lines. *Molecular Biology Reports, 36*(4), 691-696. doi:10.1007/s11033-008-9230-7

Lin, C.-H., Tallaksen-Greene, S., Chien, W.-M., Cearley, J. A., Jackson, W. S., Crouse, A. B., . . . Detloff, P. J. (2001). Neurological abnormalities in a knock-in mouse model of Huntington's disease. *Human molecular genetics, 10*(2), 137-144.

Little, P. J., Compton, D. R., Johnson, M. R., & Melvin, L. S. (1988). Pharmacology and stereoselectivity of structurally novel cannabinoids in mice. *The Journal of Pharmacology and Experimental Therapeutics, 247*, 1047-1051.

Liu, Q., Bhat, M., Bowen, W. D., & Cheng, J. (2009). Signaling pathways from cannabinoid receptor-1 activation to inhibition of N-methyl-D-aspartic acid mediated calcium influx and neurotoxicity in dorsal root ganglion neurons. *The Journal of Pharmacology and Experimental Therapeutics, 331*(3), 1062-1070. doi:10.1124/jpet.109.156216

Luthi-Carter, R., & Cha, J.-H. J. (2003). Mechanisms of transcriptional dysregulation in Huntington's disease. *Clinical Neuroscience Research, 3*(3), 165-177. doi:10.1016/S1566-2772(03)00059-8

MacDonald, M. E., Ambrose, C. M., Duyao, M. P., Myers, R. H., Lin, C., Srinidhi, L., . . . Grote. (1993). A novel gene containing a trinucleotide repeat that is expanded and unstable on Huntington's disease chromosomes. *Cell, 72*(6), 971-983.

Mackie, K., & Stella, N. (2006). Cannabinoid receptors and endocannabinoids: evidence for new players. *The AAPS journal, 8*(2), E298-306. doi:10.1208/aapsj080234

Mangiarini, L., Sathasivam, K., Seller, M., Cozens, B., Harper, A., Hetherington, C., . . . Bates, G. P. (1996). Exon 1 of the HD gene with an expanded CAG repeat is sufficient to cause a progressive neurological phenotype in transgenic mice. *Cell, 87*(3), 493-506.

Marrs, W. R., Blankman, J. L., Horne, E. A., Thomazeau, A., Lin, Y. H., Coy, J., . . . Stella, N. (2010). The serine hydrolase ABHD6 controls the accumulation and efficacy of 2-AG at cannabinoid receptors. *Nature Publishing Group, 13*(8), 951-957. doi:10.1038/nn.2601

Marrs, W. R., Horne, E. A., Ortega-Gutierrez, S., Cisneros, J. A., Xu, C., Lin, Y. H., . . . Stella, N. (2011). Dual inhibition of alpha/beta-hydrolase domain 6 and fatty acid amide hydrolase increases endocannabinoid levels in neurons. *The Journal of biological chemistry, 286*(33), 28723-28728. doi:10.1074/jbc.M110.202853

Marsicano, G., Goodenough, S., Monory, K., Hermann, H., Eder, M., Cannich, A., . . . Lutz, B. (2003). CB1 cannabinoid receptors and on-demand defense against excitotoxicity. *Science, 302*(5642), 84-88. doi:10.1126/science.1088208

Martí, E., Pantano, L., Bañez-Coronel, M., Llorens, F., Miñones-Moyano, E., Porta, S., . . . Estivill, X. (2010). A myriad of miRNA variants in control and Huntington's disease brain regions detected by massively parallel sequencing. *Nucleic Acids Research, 38*(20), 7219-7235. doi:10.1093/nar/gkq575

Matsuda, L. A., Lolait, S. J., Brownstein, M. J., Young, A. C., & Bonner, T. I. (1990). Structure of a cannabinoid receptor and functional expression of the cloned cDNA. *Nature, 346*(6284), 561-564. doi:10.1038/346561a0

Max, D., Hesse, M., Volkmer, I., & Staege, M. S. (2009). High expression of the evolutionarily conserved alpha/beta hydrolase domain containing 6 (ABHD6) in Ewing tumors. *Cancer science, 100*(12), 2383-2389. doi:10.1111/j.1349-7006.2009.01347.x

McCaw, E. A., Hu, H., Gomez, G. T., Hebb, A. L. O., Kelly, M. E. M., & Denovan-Wright, E. M. (2004). Structure, expression and regulation of the cannabinoid receptor gene (CB1) in Huntington's disease transgenic mice. *European Journal of Biochemistry, 271*(23-24), 4909-4920. doi:10.1111/j.1432-1033.2004.04460.x

Menalled, L., & Brunner, D. (2014). Animal models of Huntington's disease for translation to the clinic: Best practices. *Movement Disorders, 29*(11), 1375-1390. doi:10.1002/mds.26006

Mievis, S., Blum, D., & Ledent, C. (2011). Worsening of Huntington disease phenotype in CB1 receptor knockout mice. *Neurobiology of Disease, 42*(3), 524-529. doi:10.1016/j.nbd.2011.03.006

Miller, B. R., & Bezprozvanny, I. (2010). Corticostriatal circuit dysfunction in Huntington's disease: intersection of glutamate, dopamine and calcium. *Future neurology, 5*(5), 735-756. doi:10.2217/fnl.10.41

Mo, C., Renoir, T., Pang, T. Y. C., & Hannan, A. J. (2013). Short-term memory acquisition in female Huntington's disease mice is vulnerable to acute stress. *Behavioural Brain Research, 253*, 318-322. doi:10.1016/j.bbr.2013.07.041

Möhnle, P., Schütz, S. V., Schmidt, M., Hinske, C., Hübner, M., Heyn, J., . . . Kreth, S. (2014). MicroRNA-665 is involved in the regulation of the expression of the cardioprotective cannabinoid receptor CB2 in patients with severe heart failure. *Biochemical and biophysical research communications, 451*(4), 516-521. doi:10.1016/j.bbrc.2014.08.008

Morton, A. J. (2013). Circadian and sleep disorder in Huntington's disease. *Experimental Neurology, 243*(C), 34-44. doi:10.1016/j.expneurol.2012.10.014

Morton, A. J., Glynn, D., Leavens, W., Zheng, Z., Faull, R. L. M., Skepper, J. N., & Wight, J. M. (2009). Paradoxical delay in the onset of disease caused by super-long CAG repeat expansions in R6/2 mice. *Neurobiology of Disease, 33*(3), 331-341. doi:10.1016/j.nbd.2008.11.015

Morton, A. J., Wood, N. I., Hastings, M. H., Hurelbrink, C., Barker, R. A., & Maywood, E. S. (2005). Disintegration of the sleep-wake cycle and circadian timing in Huntington's disease. *Journal of Neuroscience, 25*(1), 157-163. doi:10.1523/JNEUROSCI.3842-04.2005

Munro, S., Thomas, K. L., & Abu-Shaar, M. (1993). Molecular characterization of a peripheral receptor for cannabinoids. *Nature, 365*(6441), 61-65. doi:10.1038/365061a0

Nasir, J., Floresco, S. B., O'Kusky, J. R., Diewert, V. M., Richman, J. M., Zeisler, J., . . . Hayden, M. R. (1995). Targeted disruption of the Huntington's disease gene results in embryonic lethality and behavioral and morphological changes in heterozygotes. *Cell, 81*(5), 811-823. doi:10.1016/0092-8674(95)90542-1

Navia-Paldanius, D., Savinainen, J. R., & Laitinen, J. T. (2012). Biochemical and pharmacological characterization of human α/β-hydrolase domain containing 6 (ABHD6) and 12 (ABHD12). *Journal of lipid research, 53*(11), 2413-2424. doi:10.1194/jlr.M030411

Naydenov, A. V., Horne, E. A., Cheah, C. S., Swinney, K., Hsu, K.-L., Cao, J. K., . . . Stella, N. (2014). ABHD6 Blockade Exerts Antiepileptic Activity in PTZ-Induced Seizures and in Spontaneous Seizures in R6/2 Mice. *Neuron, 83*(2), 361-371. doi:10.1016/j.neuron.2014.06.030

Naydenov, A. V., Sepers, M. D., Swinney, K., Raymond, L. A., Palmiter, R. D., & Stella, N. (2014). Genetic rescue of CB1 receptors on medium spiny neurons prevents loss of excitatory striatal synapses but not motor impairment in HD mice. *Neurobiology of Disease, 71*, 140-150. doi:10.1016/j.nbd.2014.08.009

Nussbaum-Krammer, C. I., & Morimoto, R. I. (2014). Caenorhabditis elegans as a model system for studying non-cell-autonomous mechanisms in protein-misfolding diseases. *Disease models & mechanisms, 7*(1), 31-39. doi:10.1242/dmm.013011

Oparina, N. Y., Delgado-Vega, A. M., Martinez-Bueno, M., Magro-Checa, C., Fernandez, C., Castro, R. O., . . . Kozyrev, S. V. (2014). PXK locus in systemic lupus erythematosus:

fine mapping and functional analysis reveals novel susceptibility gene ABHD6. *Annals of the Rheumatic Diseases*. doi:10.1136/annrheumdis-2013-204909

Palazuelos, J., Aguado, T., Pazos, M. R., Julien, B., Carrasco, C., Resel, E., . . . Galve-Roperh, I. (2009). Microglial CB2 cannabinoid receptors are neuroprotective in Huntington's disease excitotoxicity. *Brain, 132*(11), 3152-3164. doi:10.1093/brain/awp239

Papouin, T., & Oliet, S. H. R. (2014). Organization, control and function of extrasynaptic NMDA receptors. *Philosophical transactions of the Royal Society of London. Series B, Biological sciences, 369*(1654), 20130601. doi:10.1098/rstb.2013.0601

Pearl, J. R., Heath, L. M., Bergey, D. E., Kelly, J. P., Smith, C., Laurino, M. Y., . . . Jayadev, S. (2017). Enhanced retinal responses in Huntington's disease patients. *Journal of Huntington's disease, 6*(3), 237-247. doi:10.3233/JHD-170255

Peavy, G. M., Jacobson, M. W., Goldstein, J. L., Hamilton, J. M., Kane, A., Gamst, A. C., . . . Corey-Bloom, J. (2010). Cognitive and functional decline in Huntington's disease: Dementia criteria revisited. *Movement Disorders, 25*(9), 1163-1169. doi:10.1002/mds.22953

Peng, Q., Wu, B., Jiang, M., Jin, J., Hou, Z., Zheng, J., . . . Duan, W. (2016). Characterization of Behavioral, Neuropathological, Brain Metabolic and Key Molecular Changes in zQ175 Knock-In Mouse Model of Huntington's Disease. *PLoS ONE, 11*(2), e0148839. doi:10.1371/journal.pone.0148839

Pietropaolo, S., Bellocchio, L., Ruiz-Calvo, A., Cabanas, M., Du, Z., Guzmán, M., . . . Cho, Y. H. (2014). Chronic cannabinoid receptor stimulation selectively prevents motor impairments in a mouse model of Huntington's disease. *Neuropharmacology*, 1-7. doi:10.1016/j.neuropharm.2014.07.021

Pouladi, M. A., Morton, A. J., & Hayden, M. R. (2013). Choosing an animal model for the study of Huntington's disease. *Nature Reviews Neuroscience, 14*(10), 708-721. doi:10.1038/nrn3570

Pouladi, M. A., Stanek, L. M., Xie, Y., Franciosi, S., Southwell, A. L., Deng, Y., . . . Hayden, M. R. (2012). Marked differences in neurochemistry and aggregates despite similar behavioural and neuropathological features of Huntington disease in the full-length BACHD and YAC128 mice. *Human molecular genetics, 21*(10), 2219-2232. doi:10.1093/hmg/dds037

Pribasnig, M. A., Mrak, I., Grabner, G. F., Taschler, U., Knittelfelder, O., Scherz, B., . . . Zimmermann, R. (2015). α/β Hydrolase Domain-containing 6 (ABHD6) Degrades the Late Endosomal/Lysosomal Lipid Bis(monoacylglycero)phosphate. *The Journal of biological chemistry, 290*(50), 29869-29881. doi:10.1074/jbc.M115.669168

Raymond, L. A. (2017). Striatal synaptic dysfunction and altered calcium regulation in Huntington disease. *Biochemical and biophysical research communications, 483*(4), 1051-1062. doi:10.1016/j.bbrc.2016.07.058

Rey, A. A., Purrio, M., Viveros, M.-P., & Lutz, B. (2012). Biphasic effects of cannabinoids in anxiety responses: CB1 and GABA(B) receptors in the balance of GABAergic and glutamatergic neurotransmission. *Neuropsychopharmacology, 37*(12), 2624-2634. doi:10.1038/npp.2012.123

Roos, R. A. (2010). Huntington's disease: a clinical review. *Orphanet journal of rare diseases, 5*(1), 40. doi:10.1186/1750-1172-5-40

Rosenblatt, A., Liang, K. Y., Zhou, H., Abbott, M. H., Gourley, L. M., Margolis, R. L., . . . Ross, C. A. (2006). The association of CAG repeat length with clinical progression in

Huntington disease. *Neurology, 66*(7), 1016-1020. doi:10.1212/01.wnl.0000204230.16619.d9

Ross, C. A., & Tabrizi, S. J. (2011). Huntington's disease: from molecular pathogenesis to clinical treatment. *The Lancet Neurology, 10*(1), 83-98. doi:10.1016/S1474-4422(10)70245-3

Roze, E., Cahill, E., Martin, E., Bonnet, C., Vanhoutte, P., Betuing, S., & Caboche, J. (2011). Huntington's disease and striatal signaling. *Frontiers in neuroanatomy, 5*. doi:10.3389/fnana.2011.00055/abstract

Sanberg, P. R., Calderon, S. F., Giordano, M., & Tew, J. M. (1989). The quinolinic acid model of Huntington's disease: locomotor abnormalities. *Experimental ….*

Schilling, G., Klevytska, A., Tebbenkamp, A. T. N., Juenemann, K., Cooper, J., Gonzales, V., . . . Borchelt, D. R. (2007). Characterization of huntingtin pathologic fragments in human Huntington disease, transgenic mice, and cell models. *Journal of neuropathology and experimental neurology, 66*(4), 313-320. doi:10.1097/nen.0b013e318040b2c8

Schipper-Krom, S., Juenemann, K., & Reits, E. A. J. (2012). The Ubiquitin-Proteasome System in Huntington's Disease: Are Proteasomes Impaired, Initiators of Disease, or Coming to the Rescue? *Biochemistry Research International, 2012*(3), 1-12. doi:10.1038/ng864

Shepherd, G. M. G. (2013). Corticostriatal connectivity and its role in disease. 1-14. doi:10.1038/nrn3469

Stella, N. (2004). Cannabinoid signaling in glial cells. *Glia, 48*(4), 267-277. doi:10.1002/glia.20084

Straiker, A., Hu, S. S. J., Long, J. Z., Arnold, A., Wager-Miller, J., Cravatt, B. F., & Mackie, K. (2009). Monoacylglycerol Lipase Limits the Duration of Endocannabinoid-Mediated Depolarization-Induced Suppression of Excitation in Autaptic Hippocampal Neurons. *Molecular Pharmacology, 76*(6), 1220-1227. doi:10.1124/mol.109.059030

Suzuki, M., Nagai, Y., Wada, K., & Koike, T. (2012). Calcium leak through ryanodine receptor is involved in neuronal death induced by mutant huntingtin. *Biochemical and biophysical research communications, 429*(1-2), 18-23. doi:10.1016/j.bbrc.2012.10.107

Swayne, L. A., Chen, L., Hameed, S., Barr, W., Charlesworth, E., Colicos, M. A., . . . Braun, J. E. A. (2005). Crosstalk between huntingtin and syntaxin 1A regulates N-type calcium channels. *Molecular and cellular neurosciences, 30*(3), 339-351. doi:10.1016/j.mcn.2005.07.016

Tanaka, M., Moran, S., Wen, J., Affram, K., Chen, T., Symes, A. J., & Zhang, Y. (2017). WWL70 attenuates PGE 2 production derived from 2-arachidonoylglycerol in microglia by ABHD6-independent mechanism. *Journal of Neuroinflammation, 14*(1), 7. doi:10.1186/s12974-016-0783-4

Tang, T.-S., Tu, H., Chan, E. Y. W., Maximov, A., Wang, Z., Wellington, C. L., . . . Bezprozvanny, I. (2003). Huntingtin and huntingtin-associated protein 1 influence neuronal calcium signaling mediated by inositol-(1,4,5) triphosphate receptor type 1. *Neuron, 39*(2), 227-239. doi:10.1016/S0896-6273(03)00366-0

Tchantchou, F., & Zhang, Y. (2013). Selective Inhibition of Alpha/Beta-Hydrolase Domain 6 Attenuates Neurodegeneration, Alleviates Blood Brain Barrier Breakdown, and Improves Functional Recovery in a Mouse Model of Traumatic Brain Injury. *Journal of Neurotrauma, 30*(7), 565-579. doi:10.1089/neu.2012.2647

Thomas, G., Betters, J. L., Lord, C. C., Brown, A. L., Marshall, S., Ferguson, D., . . . Brown, J. M. (2013). The Serine Hydrolase ABHD6 Is a Critical Regulator of the Metabolic Syndrome. *CellReports, 5*(2), 508-520. doi:10.1016/j.celrep.2013.08.047

Tong, Y., Ha, T. J., Liu, L., Nishimoto, A., Reiner, A., & Goldowitz, D. (2011). Spatial and temporal requirements for huntingtin (Htt) in neuronal migration and survival during brain development. *The Journal of neuroscience : the official journal of the Society for Neuroscience, 31*(41), 14794-14799. doi:10.1523/JNEUROSCI.2774-11.2011

Trottier, Y., Lutz, Y., Stevanin, G., Imbert, G., Devys, D., Cancel, G., . . . Tora, L. (1995). Polyglutamine expansion as a pathological epitope in Huntington's disease and four dominant cerebellar ataxias. *Nature, 378*(6555), 403-406. doi:10.1038/378403a0

Turu, G., & Hunyady, L. (2010). Signal transduction of the CB1 cannabinoid receptor. *Journal of Molecular Endocrinology, 44*(2), 75-85. doi:10.1677/JME-08-0190

Van Dellen, A., Welch, J., Dixon, R. M., Cordery, P., York, D., Styles, P., . . . Hannan, A. J. (2000). N-Acetylaspartate and DARPP-32 levels decrease in the corpus striatum of Huntington's disease mice. *Neuroreport, 11*(17), 3751-3757.

Van Laere, K., Casteels, C., Dhollander, I., Goffin, K., Grachev, I., Bormans, G., & Vandenberghe, W. (2010). Widespread Decrease of Type 1 Cannabinoid Receptor Availability in Huntington Disease In Vivo. *Journal of Nuclear Medicine, 51*(9), 1413-1417. doi:10.2967/jnumed.110.077156

Walker, F. O. (2007). Huntington's disease. *Lancet (London, England), 369*(9557), 218-228. doi:10.1016/S0140-6736(07)60111-1

Wei, M., Jia, M., Zhang, J., Yu, L., Zhao, Y., Chen, Y., . . . Zhang, C. (2017). The Inhibitory Effect of α/β-Hydrolase Domain-Containing 6 (ABHD6) on the Surface Targeting of GluA2- and GluA3-Containing AMPA Receptors. *Frontiers in molecular neuroscience, 10*, 55. doi:10.3389/fnmol.2017.00055

Wei, M., Zhang, J., Jia, M., Yang, C., Pan, Y., Li, S., . . . Zhang, C. (2016). α/β-Hydrolase domain-containing 6 (ABHD6) negatively regulates the surface delivery and synaptic function of AMPA receptors. *Proceedings of the National Academy of Sciences, 113*(19), E2695-2704. doi:10.1073/pnas.1524589113

Wen, J., Jones, M., Tanaka, M., Selvaraj, P., Symes, A. J., Cox, B., & Zhang, Y. (2018). WWL70 protects against chronic constriction injury-induced neuropathic pain in mice by cannabinoid receptor-independent mechanisms. *Journal of Neuroinflammation, 15*(1), 9. doi:10.1186/s12974-017-1045-9

Wen, J., Ribeiro, R., Tanaka, M., & Zhang, Y. (2015). Activation of CB2 receptor is required for the therapeutic effect of ABHD6 inhibition in experimental autoimmune encephalomyelitis. *Neuropharmacology, 99*, 196-209. doi:10.1016/j.neuropharm.2015.07.010

Woodman, B., Butler, R., Landles, C., Lupton, M. K., Tse, J., Hockly, E., . . . Bates, G. P. (2007). The HdhQ150/Q150 knock-in mouse model of HD and the R6/2 exon 1 model develop comparable and widespread molecular phenotypes. *Brain Research Bulletin, 72*(2-3), 83-97. doi:10.1016/j.brainresbull.2006.11.004

Yu-Taeger, L., Petrasch-Parwez, E., Osmand, A. P., Redensek, A., Metzger, S., Clemens, L. E., . . . Nguyen, H. P. (2012). A novel BACHD transgenic rat exhibits characteristic neuropathological features of Huntington disease. *The Journal of neuroscience : the official journal of the Society for Neuroscience, 32*(44), 15426-15438. doi:10.1523/JNEUROSCI.1148-12.2012

Zajac, M. S., Pang, T. Y. C., Wong, N., Weinrich, B., Leang, L. S. K., Craig, J. M., . . . Hannan, A. J. (2010). Wheel running and environmental enrichment differentially modify exon-specific BDNF expression in the hippocampus of wild-type and pre-motor symptomatic male and female Huntington's disease mice. *Hippocampus, 20*(5), 621-636. doi:10.1002/hipo.20658

Zarringhalam, K., Ka, M., Kook, Y.-H., Terranova, J. I., Suh, Y., King, O. D., & Um, M. (2012). An open system for automatic home-cage behavioral analysis and its application to male and female mouse models of Huntington's disease. *Behavioural Brain Research, 229*(1), 216-225. doi:10.1016/j.bbr.2012.01.015

Zeitlin, S., Liu, J.-P., Chapman, D. L., Papaioannou, V. E., & Efstratiadis, A. (1995). Increased apoptosis and early embryonic lethality in mice nullizygous for the Huntington's disease gene homologue. *Nature genetics, 11*(2), 155-163. doi:10.1038/ng1095-155

Zhao, S., Mugabo, Y., Ballentine, G., Attane, C., Iglesias, J., Poursharifi, P., . . . Prentki, M. (2016). α/β-Hydrolase Domain 6 Deletion Induces Adipose Browning and Prevents Obesity and Type 2 Diabetes. *CellReports, 14*(12), 2872-2888. doi:10.1016/j.celrep.2016.02.076

Zhao, S., Poursharifi, P., Mugabo, Y., Levens, E. J., Vivot, K., Attane, C., . . . Prentki, M. (2015). α/β-Hydrolase domain-6 and saturated long chain monoacylglycerol regulate insulin secretion promoted by both fuel and non-fuel stimuli. *Molecular metabolism, 4*(12), 940-950. doi:10.1016/j.molmet.2015.09.012

Zhuang, S.-Y., Bridges, D., Grigorenko, E., McCloud, S., Boon, A., Hampson, R. E., & Deadwyler, S. A. (2005). Cannabinoids produce neuroprotection by reducing intracellular calcium release from ryanodine-sensitive stores. *Neuropharmacology, 48*(8), 1086-1096. doi:10.1016/j.neuropharm.2005.01.005

Zielonka, D., Marinus, J., Roos, R. A. C., De Michele, G., Di Donato, S., Putter, H., . . . Landwehrmeyer, G. B. (2013). The influence of gender on phenotype and disease progression in patients with Huntington's disease. *Parkinsonism & related disorders, 19*(2), 192-197. doi:10.1016/j.parkreldis.2012.09.012

Zuccato, C., Valenza, M., & Cattaneo, E. (2010). Molecular Mechanisms and Potential Therapeutical Targets in Huntington's Disease. *Physiological Reviews, 90*(3), 905-981. doi:10.1152/physrev.00041.2009